Evaluation of the EOR Potential in Shale Oil Reservoirs by Cyclic Gas Injection

A THESIS

BY

Tao Wan B.S.

Submitted to the Office of Graduate Studies of Texas Tech

University in partial fulfillment of the

requirements for the degree of

MASTER OF SCIENCE

IN

PETROLEUM ENGINEERING

Approved

by

Dr. James Sheng

Chair of Committee

Dr. M.Rafiqul Awal

Dr. Marshall Watson

Dominick Casadonte

Dean of the Graduate School

May, 2013

Acknowledgements

I would like to begin by expressing sincere gratitude to the members of my committee, Dr. James Sheng, Dr. M.Rafiqul Awal and Dr. Marshall Watson for their constructive criticism and invaluable advice. I should give strong appreciation to Dr. Sheng for working with me patiently and directing me throughout this expedited process. I was grateful he allowed me the privilege to work with him. A sincere thank you extends to the Texas Tech University Petroleum Engineering department for allowing me the opportunity to obtain a degree from a distinguished institution.

I express my gratitude and appreciation to the Petroleum Engineering Department for financial support in the form of assistantships. Also I would like to express my heartfelt gratitude to my family who has encouraged me through every day of this journey.

Table of Contents

List of Tables

List of Figures

Abstract

The current available technique to produce shale oil is through primary depletion using horizontal wells with multiple transverse fractures. The oil recovery factor is only a few percent. There is a big prize to be claimed in terms of enhanced oil recovery (EOR).

Well productivity in shale oil and gas reservoirs comes from the horizontal wells with transverse fractures that connect natural fracture complexity. The natural fracture complexity provides a network for injected fluids to contact matrix material. However, in such a system, flooding may not sufficiently enhance oil recovery because the injected fluids may break through to production wells via the fracture network. A cyclic injection scheme is one way to solve this problem. Considering that the matrix permeability is ultra-low, we propose cyclic gas injection in this paper.

We used a simulation approach having evaluated the EOR potential from cyclic gas injection. Our simulation results indicate that oil recovery can be increased up to 29% by using cyclic gas injection in a hydraulically fractured shale reservoir for 60 cycles, compared with the original 6.5% recovery from the primary depletion. If high pressure is used to reach miscibility and more cycles are employed, more than 40% oil recovery can be achieved.

In this thesis, we also a performed detailed evaluation of gas injection in general. We have evaluated the oil recovery potentials of different scenarios, from primary depletion, immiscible gas injection, to gas injection with different degrees of miscibility. Different EOR mechanisms are discussed and quantified as well. The results of this paper bring a new prospect to enhance oil recovery in shale oil reservoirs.

Nomenclature

B_o=Oil formation volume factor, bbl/STB

B_g=Gas formation volume factor, bbl/scf

B_{oi}=Initial oil formation volume factor

C_w=Water compressibility, psi^{-1}

C_f=Formation compressibility, psi^{-1}

FOE=Field oil recovery factor

FGIR=Field gas injection rate

FGIT=Field gas injection total

FPR=Field average reservoir pressure

FOPT=Field oil production total

FGOR=Field gas oil ratio

G_{inj}=Cumulative gas injection, scf

Kx=Permeability in x direction

Ky=Permeability in y direction

Kz=permeability in z direction

m=Ratio of initial gas-cap-gas reservoir volume to initial reservoir volume

N=Initial oil in place, STB

N_p=Cumulative oil produced, STB

R_{si}=Initial gas solubility, scf/STB

R_s=Gas solubility, scf/STB

R_p=Cumulative gas oil ratio, scf/STB

S_{wi}=Initial water saturation

W_e=Cumulative water influx, bbl

W_{inj}=Cumulative water injected, bbl

W_p=Cumulative water produced, bbl

ω=Mixing parameter for different degree of miscibility

Chapter 1

Introduction

1.1 Statement of the problem

Unconventional reservoirs are being currently aggressively explored and developed in North America with the advent of new technologies such as multi-stage fractured horizontal wells. Since the success achieved in Barnett Shale by using horizontal wells with multistage fracturing techniques, industry initiated the new era of improving the productivity in shale reservoirs. It is known that unconventional shale gas reservoirs exist over large quantities in the United States. It is essential to select the proper completion approaches for horizontal wells considering the ultralow permeability of shale formation. The tight and shale oil reservoirs are still poorly understood.

However, historically, primary production from shale oil reservoirs even applied with hydraulic fracturing techniques was 5-10% OOIP or less. The initial oil rate is high because initial reservoir pressure is high and hydraulic fractures provide highly conductive paths between the reservoir and the wellbore. Oil rate declines as the oil near the fractured area has been produced and after that the oil rate is controlled primarily by the flow resistance from the matrix to the fractures. There is not too much work that has been done in the areas of improving oil recovery in shale oil reservoirs.

Unlike conventional reservoirs, the well productivity in shale reservoirs drops very quickly which makes it very challenging to further improve it and water flooding may have its low injectivity issue. Recent studies have shown that gas injection may be a good choice. The reasons for us initiating these studies include shortage of efficient and economic techniques for improving oil recovery in shale oil reservoirs, inefficiency of conventional methodologies such as waterflooding and the unique nature of unconventional reservoirs like ultra-low porosity and permeability. There are potential difficulties for gas injection applied in conventional well patterns such as bypassing oil and disconnected oil zones caused by massive viscous fingering and channeling by high

pressures, combined with poor mobility ratios and channeling through high permeability streaks.

In our work on the cyclic gas injection project, we only drill a horizontal well that acts both as production well as well as injection well, at the same time implementing fracturing treatment to obtain certain numbers of hydraulic fractures for efficient production from shale oil reservoirs. In this case, the viscous fingering and early breakthrough of injected gas would not occur by using this technique because production and injection are separated.

1.2 Objectives

The goal of this work is to propose a new method for enhancing oil recovery in shale oil reservoirs. We will compare the primary recovery with the EOR implementing the new technique. We will also investigate the effects of different well operating schedules (injection time and production time in each cycle) on the ultimate oil recovery. The purpose for this work is to evaluate the potential EOR that can be achieved by using this technique developed by us.

In this work, we will use a black-oil model to analyze the whole gas injection project without going into the complexity by using a compositional model because of the shortage of reservoir fluid compositional data. In the future work, we will use the compositional model by taking into account of the thermal effects of injected gas on the viscosity reduction.

With the increasing competiveness of global energy demand, gas injection may be a good method which will provide huge benefits for exploring unconventional reservoirs. The modeling work we did in this work will present the physical significance of underlying cyclic gas injection, whose role is predominating when applied with fracture stimulation treatments.

Chapter 2

Literature Review

Our approach has been to determine the effect of gas injection on the recovery of shale oil reservoirs by using a simulator, ECLIPSE and CMG. Provided the presence of horizontal wells with multi-fractures in shale oil reservoirs, we compare the results of primary recovery and incremental oil recovery by miscible cyclic gas injection. The literature search focused on the physics and stimulation of tight gas, shale gas reservoirs and shale oil reservoirs.

2.1 Unconventional resources introduction

As the oil and gas industrial techniques mature, ongoing targets move towards more challenging prospects commonly exhibiting low permeability and often low pressure. Unconventional reservoirs exhibit several challenges which are not commonly found in traditional reservoirs. Unconventional gas reservoirs normally include tight gas sands, geo-pressured zones, deep gas, methane hydrates, coalbed methane, and shale gas. The emergency of new technology, government deregulation, increasing stability of natural gas prices, and the demand for energy provided the opportunity for energy companies to invest on producing and replenishing reserves.

Figure 2.1 Gas shales distribution in the United States

The shale gas production that has received great popularity was the result of government incentives and tax credit. However when the tax credit expired in 1992 many operators that had found success continued to expand drilling and completion programs targeting gas shale reservoirs, indicating that the financial incentives provided by the government have been successful.

2.2 Shale reservoir characteristics

Shales are fine-grained rocks that form from the compaction of silt and clay sized particles. Shales are differentiated from other claystones and mudstones in that they are laminated, finely layered and fissile, which means they can be broken along their laminations(Tom Alexander, 2011). Shales can have complex mixtures of minerals, and the relative connections of the constituents have the potential to make or break a potential resource play. Core samples can provide a wealth of information about the geochemistry and mineralogy, but are limited to the specific location where the sample was retrieved.

To indentify shales that have production potential, geologists look for specific geochemical properties, which are typically derived from core data. Geochemical properties needed to adequately characterize shale resources include total organic carbon (TOC), gas volume and capacity, thermal maturity. Shale oil and shale gas are present in organic rich rocks, which may act both as the source and the cap rock and maybe mixed with clay minerals. Organic materials preserved in rocks came from the decay of plants and animals. The sediments can retain much of their original organic material in anoxic environment where there is less consumers to consume organic matter. As more material accumulates and underlying ooze becomes compacted, the sediments are buried deeper and subjected to heat and pressure. The organic material slowly and partially cooks and is transformed into kerogen. Depending on the time and temperature at which these materials were cooked. The transformation of living organisms through diagenesis into kerogen, kerogen will break down to form hydrocarbons through a chemical process called catagenesis.

Table 2.1 Source rock evaluation criteria. (Courtesy by Schlumberger)

Source rock quality	TOC, %	Pyrolysis S2	Hydrocarbon, ppm
None	<0.5	<2	<200
Poor	0.5 to 1	2 to 3	200 to 500
Fair	1 to 2	3 to 5	500 to 800
Good	2 to 5	5 to 10	>1200
Very good	>5	>10	

Production from unconventional reservoir requires stimulation and fracture treatment that would not be necessary in a conventional high porosity and high permeability reservoir.

2.2.1 Pyrolysis

Pyrolysis is a powerful tool that can be used to assess the quantity, type and thermal

maturity of the whole-rock and kerogen samples. As temperatures rise, the kerogen releases CO2 in addition to hydrocarbons (Richard M.Bateman, 2011). The first peak S1 corresponds to free oil and gas that evolve from the rock sample without cracking the kerogen during the first stage of heating. These hydrocarbon were generated in the subsurface but will be distilled out the sample upon the heating of the sample at 350 ˚C. The second peak S2 indicates that the hydrocarbons that evolve from the sample result from the cracking of heavy hydrocarbons and from the thermal breakdown of kerogen. Thus S2 is an indication of the potential quantity of hydrocarbons that the source rock might still produce if thermal maturation continues. The S3 peak corresponds to CO2 that is evolved from thermal cracking of the kerogen during pyrolysis, expressed in milligrams per gram of rock. A good understanding of the amount heat necessary to create various chemical compounds in the rock can help geochemists understand the history of the rock and the extent of thermal maturation it has already undergone(Kevin McCarthy, 2011).

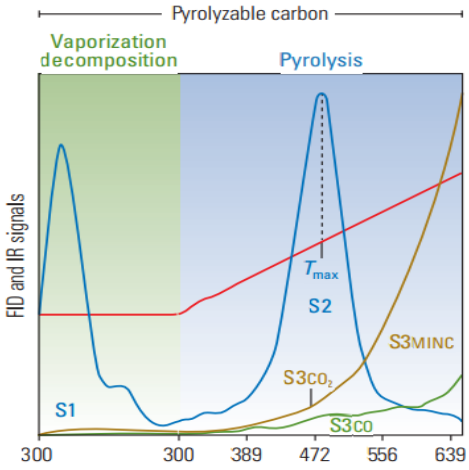

Figure 2.2 Pyrolysis results. Free hydrocarbons are measured by the S1 peak, and the residual hydrocarbons are measured by the S2 peak. (Courtesy by Schlumberger Geochemistry manual)

2.2.2Vitrinite Reflectance

Vitrinite reflectance is normally used as a maturation indicator. Thermal maturity is a function of depositional history. As kerogen is exposed to progressively higher

temperatures over time, vitrinite-cell-wall material and woody plant tissue preserved in the rock that undergoes irreversible alternation and develops increased reflectance. The measurement of vitrinite reflectance (Ro) was originally developed for determination of rank coal maturity. A reflectance value below 0.6% is indicative of kerogen that is immature, not having been exposed to sufficient thermal conditions over adequate time for conversion of the organic material to hydrocarbons. Ro ranges from 0.6% to 0.8% indicate oil and ranges of 0.8% to 1.1% indicate wet gas. As coal rank increases, vitrinite becomes more reflective.

2.3 Horizontal well technique

In the last decades, the applications of horizontal well technology have been widely facilitated by the surging of unconventional reservoirs. At a low drawdown, a horizontal well can have a larger productivity in comparison with vertical wells. The major advantage of horizontal well technology is to enhance the contact area with the formation.

Now it is well understood that horizontal well is one of the greatest improvements in economically developing oil shale reservoirs. The increasing oil price along with the advancements in horizontal drilling and hydraulic fracturing technologies have allowed industries to meet the future energy demand although in the facing of rapid decline in tradition hydrocarbon reserves. The advantages of horizontal well can be considered as followings:

1. Larger flow area
2. Reduce possibility of water or gas cresting
3. Use in enhanced recovery applications
4. Created multiple small fractures
5. Cross several interested pay zones

Since the success achieved in Barnett Shale using horizontal well with multistage

fracturing techniques, industries initiated the new era of horizontal drilling and completion designs to improve the productivity of gas shale well. Now it is well understood that horizontal well is one of the greatest improvements in economically developing gas shale reservoirs. The increasing gas price along with the advancements in horizontal drilling and hydraulic fracturing technologies have allowed industries to meet the future energy demand although in the facing of rapid decline in tradition hydrocarbon reserves. It is known that unconventional shale gas reservoirs exist over large quantities in the United States. There are many shale gas basins remained to be explored and developed. It is essential to select the proper completion approaches for horizontal wells considering the ultralow permeability of shale formation. A lot of literatures can be found regarding completion technique optimizations that are suitable for shale formation.

2.4 Hydraulic Fracturing Application

Hydraulic fracturing has received great recognition for one of the most effective techniques for improving the productivity of unconventional reservoirs. Hydraulic fractures are used to eliminate formation damage and to increase the conductivity of flow path of fluid to the wellbore. Kroemeretc showed that non-Darcy effects are minimized and the well will suffer less productivity reduction once condensate blocking occurs.

Hydraulic fracturing has evolved into a technique suitable to stimulate most wells under extremely varying circumstances. Originally suggested for low-permeability gas, it still plays a crucial role in developing low-permeability formations, and is increasingly used to produce from shales, and coal seams (Economides, 2007). Generally, a vertical well drilled and completed in a tight gas reservoir must be successfully stimulated to produce at commercial gas-flow rates and produce commercial gas volumes. Although in some naturally fractured tight gas reservoirs horizontal wells are successful, often they also need fracture stimulation.

2.5 Horizontal well with multi-stage hydraulic fracturing

Multi-stage fracturing treatment has become a successful means to produce gas from ultralow permeability shale reservoirs. A large volume of fracturing fluid injected in order

to create multiple fractures so that the contact area of the wellbore with reservoir can be significantly improved. Unlike explosives which lasts short momentum is not a good approach. As fluid is pumped into the permeable formation, a pressure differential between the wellbore pressure and the original reservoir pressure is generated. Along with the rate increases, the pressure difference differential also increases. Eventually this pressure differential will cause stress that will exceed the stress needed to break the rock apart forming a fracture.

To create more fracture stage density, multiple perforation clusters appear to be a good way to add fracture density stage. There is an attempt to create more perforation clusters utilizing limited entry, but study indicated that this effectiveness for improving production proved disappointing. Baihly (Baihly, 2010) in his paper argued that only 30% of the perforation intervals contributing showed based on production logging data. Conventional technique of utilization of cemented liners with plug and perf technique has a big disadvantage. Creating more stages is proportional to more fracture trucks, more pumping frac fluid, crews. Furthermore, technically speaking, it is difficult to use cemented liners and bridge plugs to create high stage numbers which also is a time consuming job as stated above.

With techniques advancements, StackFRAC HD application seems to be an efficient and technically feasible way for taking stages count 30 or higher. The process uses a graduated ball drop system at the toe of the well to create upwards 20 or more stages. The system comprises ported sleeves installed between isolation packers on a single liner string. When the ball dropped at the toe of the wellbore, it isolates the circulation of the wellbore resulting the pressure buildup inside the tubing. This process intends the isolation packer to expand to isolate the horizontal wellbore into stages. After that, a ball dropped again into the fluid and pumped down the string will seat in the mechanical sleeve. This action will open the sleeve exposing the ports and diverting the fluid to the formation, which created a hydraulic fracture within the isolated zone.

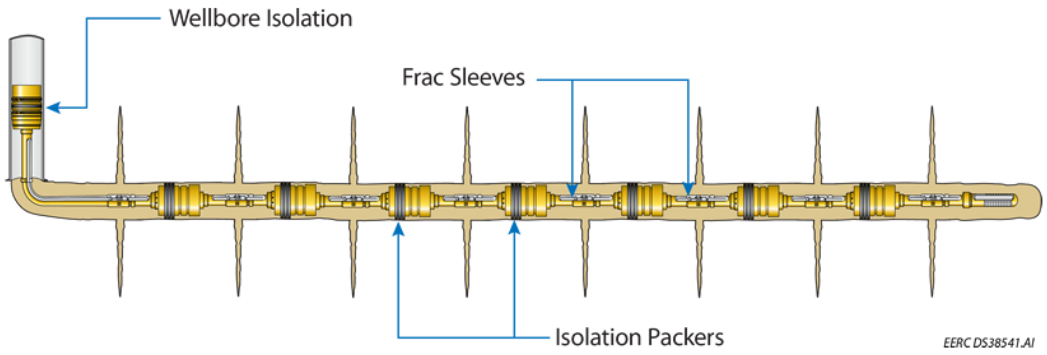

Figure 2.3StackFRAC® HD™ Multi-Stage Fracturing (Courtesy by Packers Plus)

2.6 Cyclic steam Stimulation used for heavy oil production introduction

Cyclic steam stimulation was discovered by accident in the Mene Grande field in Venezuela in 1959 when Shell Oil Company was testing a steam and steam broke out behind casing in a steam injection well. Cyclic steam stimulation was originally used for the development of heavy oil and it was discovered that steam injection into a heavy-oil reservoir could increase production rate by factors of 5 to 10. Thermal recovery processes are the most advanced EOR processes and contribute significant amounts of oil to daily production (Green, 1998). Most of the oil is the result of cyclic steam injection and stream drive. Prior to the advent of thermal recovery techniques, primary production from heavy oil reservoirs was 5% OOIP or less. Production rate was low, declining with time as the reservoir energy depleted. Thermal techniques aim to reduce oil viscosity in order to increase its mobility through the injection of steam that brings heat. In cyclic steam stimulation, steam is injected into a well at a high rate and high pressure for short time (10 days to a month). The well may be shut in for a few days called “soaking period” for heat distribution. The initial oil rate is high because of the reduced oil viscosity at the increased reservoir temperature and under the benefit from accelerating of reservoir pressure by gas injection near the wellbore. Oil rate declines with the decreasing of heated zone temperature results from heat removed with the produced fluids and heat loss.

However, there are some technical failure cases for cyclic steam injection including geological complexity and thermodynamic inefficiencies. Potential difficulties such as

high pressures in injection cycles, combined with poor mobility ratios and high permeability streaks, lead to massive viscous fingering and channeling (Dusseault, 2002). Well problems and surface problems that arise because of cyclic high-pressure steam injection include accelerated corrosion of steel goods, leading to breaching of the casing, occurs relatively commonly.

These potential difficulties combine with the high cost of generating heat and other costs which make the economic viability of such projects problematic. But in our work, we don't care about the thermal effect like the temperature influence of injected fluid which is not steam stimulation, so we used a black-oil model for simplicity. What we mainly evaluated is the viscosity reduction and relative permeability changes of the system caused by miscibility with injected gas. There are also some accelerations of recovery by the increasing reservoir pressure by virtue of injected gas near the fractured area.

The technique we developed is illustrated in Fig 2.4 and 2.5 which shows cyclic gas stimulation is applied in horizontal well with multi-stage hydraulic fractures. Cyclic gas stimulation as a secondary recovery technique is applied after primary production. Different well schedules for cycle variations (Injection time and production time schedule in each cycle) were investigated in our work and it was discovered that there is significant contribution to incremental oil recovery amount to nearly 22%. Historically, primary production from shale oil reservoirs even applied with hydraulic fracturing techniques was 5-10% OOIP or less. We believe the development of this technique will further promote the booming of development of shale oil reservoirs, especially under current lower price of gas period. Without incentives from gas price, the industry inclines to concentrate on the surging development of unconventional reservoirs such as shale oil reservoirs. This thesis is dedicated to study how to improve the recovery in shale oil reservoirs because of no other techniques available at this time.

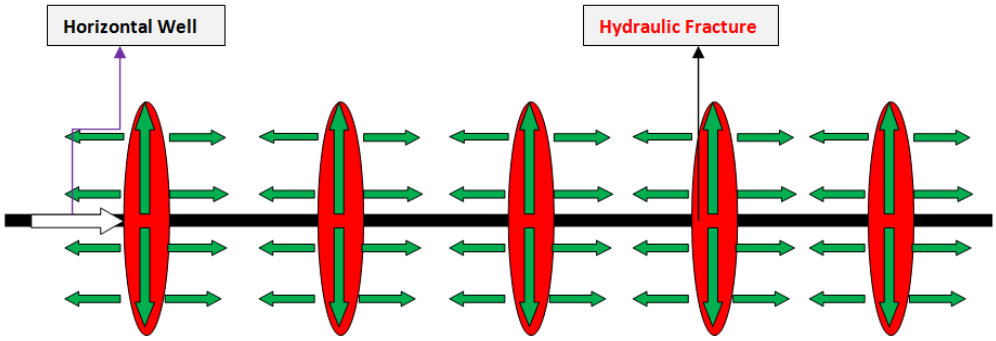

Figure 2.4 Cyclic gas injection applied in horizontal well with multi-hydraulic fractures (Gas injection schematic diagram, horizontal well is used as injection well)

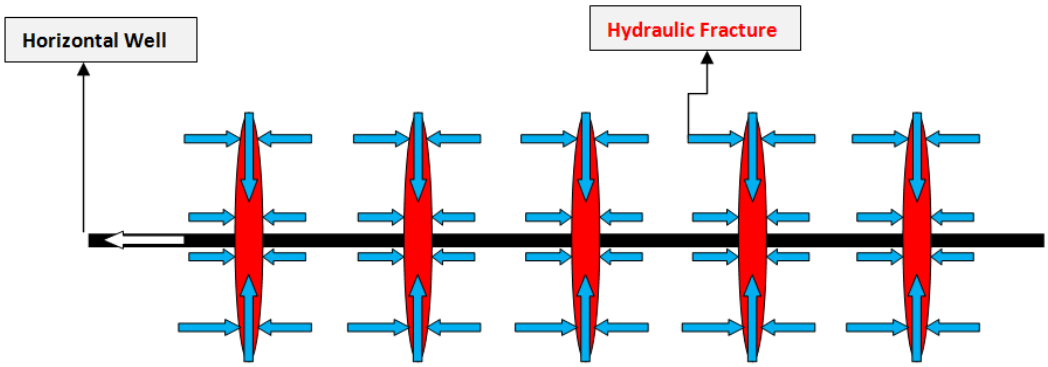

Figure 2.5 Cyclic gas injection applied in horizontal well with multi-hydraulic fractures (Well production schematic diagram, horizontal well is used as production well)

2.7 Recovery Mechanisms

The overall driving mechanisms that provide the natural energy necessary for oil recovery can be categorized as rock and liquid expansion drive, depletion drive, gas cap drive, water drive, gravity drainage drive and combination drive. Oil expansion is a very important part among those mechanisms if without availability of other artificial introduced energy. The rock and fluids expand due to their individual compressibilities. As the expansion of fluids and reduction in the pore volume occur with the decreasing reservoir pressure, the crude oil and water will be forced out of the pore space to the wellbore(Ahmed, 2010). As the pressure drops in the fracture system, oil flows from the

matrix to equilibrate the matrix pressure with the surrounding fracture pressure. This production mechanism can be thought of as expansion of the oil within the matrix block, either above the bubble point or by solution gas drive below the bubble point.

In shale oil reservoirs the majority of the oil is contained in the matrix system, but the production of oil to the wells is through the high permeability fracture system. In such a system an injected fluid does not sweep out oil from the matrix block. Production from the matrix blocks can be associated with various physical mechanisms including: The mechanisms behind gas cyclic injection for increasing shale oil recovery include:

1. The injected gas helps to provide energy for the reservoir.
2. The injected gas dissolves in the crude oil by decreasing oil viscosity and oil expansion.
3. Gas miscible flooding helps reduce gas and oil capillary pressure.

Chapter 3

Hydraulically Fractured Wells Characterizations

Hydraulic fracturing is an essential well completion technology for the development of unconventional resources, such as low-permeability reservoirs, shale reservoirs and coalbed methane. Without application of hydraulic fracturing technique in unconventional resources, making a project to be commercially viable might be problematic. Interpreting the pressure transient data in hydraulically fractured wells is important in evaluating the success of fracture treatment and for predicting fracture performance of fractured wells.

3.1 Flow Patterns in Hydraulically Fractured Wells

Five distinct flow patterns occur in the fracture and formation around a hydraulically fractured well. Successive flow patterns often are separated by transition periods including fracture linear, bilinear, formation linear, elliptical, and pseudoradial flow(Lee, Pressure Transient Testing, 2003). But the fracture linear flow period which lasts very short time and may be masked by wellbore storage effects. In the linear flow, most of the flow liquid comes from the expansion of liquid in the fracture which is similar to the flow occurring in wellbore storage. The duration of fracture linear flow period is estimated by[9,11]

$$t_{fD} = \frac{0.1C_{rD}^2}{\eta_{fD}^2}$$

Where t_{fD} is the dimensionless time in the fracture half-length.

$$t_{fD} = \frac{0.0002637kt}{\phi\mu C_t L_f^2}$$

The dimensionless fracture conductivity is

$$C_{rD} = \frac{k_f w}{\pi k L_f}$$

Nowadays people commonly use $C_{fD} = \frac{k_f w}{k L_f}$

And η_{fD} is dimensionless hydraulic diffusivity defined by

$$\eta_{fD} = \frac{k_f \phi C_t}{k \phi_f C_f}$$

3.2 Pseudoradial Flow Analysis

The pseudoradial flow regime occurs in high permeability formation with a short, highly conductive fracture being created. If a low conductivity fracture is created in a low-permeability reservoir, it will take a long time to reach pseudoradial flow regime which is unlikely to analyze. The time to achieve pseudoradial flow for infinitely conductivity fracture given by:

$$t_{fD} = \frac{0.0002637kt}{\phi \mu C_t L_f^2} \approx 3$$

The characterization of pesudoradial flow is shown on a log-log plot by a flattening of the pressure derivative. For infinite conductivity fracture, skin factor can be correlated with effective wellbore diameter,

$$L_f = 2r_w e^{-s}$$

$$r_w' = r_w e^{-s} = \frac{L_f}{2}$$

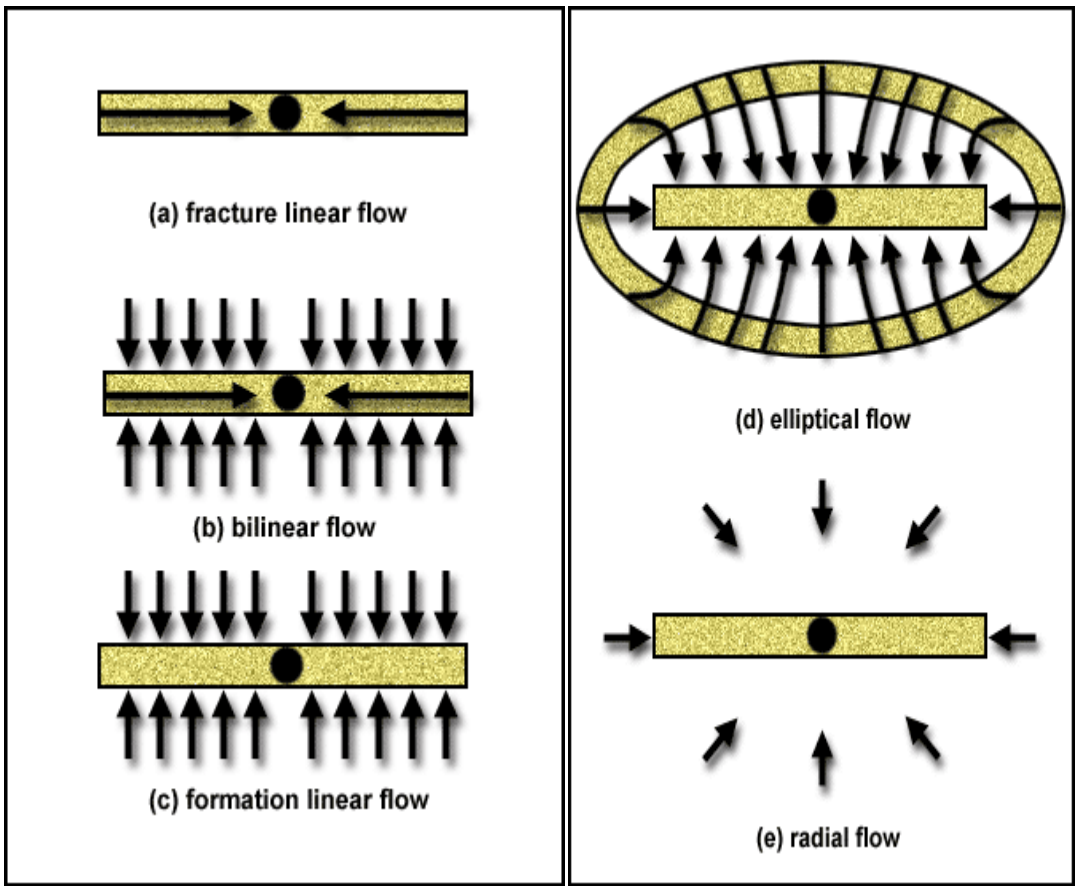

Figure 3.1Different Flow Regimes in the Hydraulic Fractures

3.3 Bilinear Flow Method

The indication of bilinear flow is a quarter slope 1/4 on a log-log graph of p_i-p_{wf} versus t for a constant rate flow. During bilinear flow,

$$P_D = \frac{1.38}{\sqrt{C_{rD}}} t_{fD}^{1/4}$$

$$t_{fD} \frac{dP_D}{dt_{fD}} = \frac{0.345}{\sqrt{C_{rD}}} t_{fD}^{1/4}$$

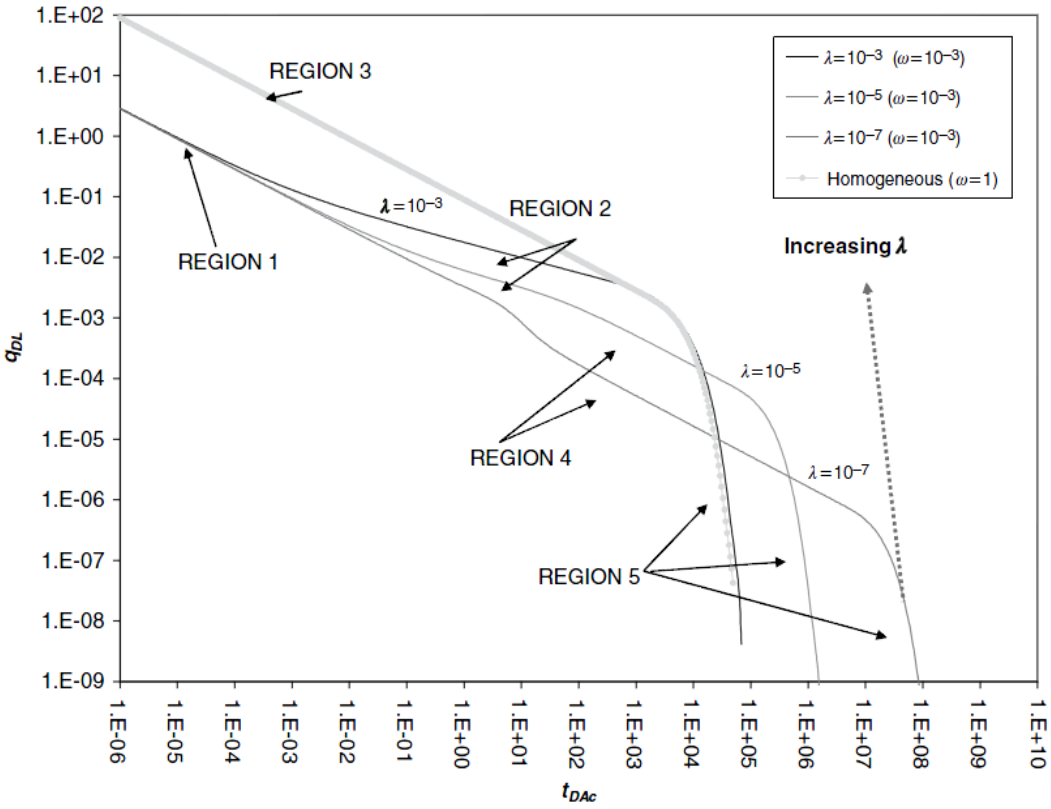

Figure 3.2Illustration of five flow regimes (Courtesy by SPE 114591)

Dr.Soliman Proposed (Soliman, 2005) the after closure analysis to determine some important parameters based on MiniFrac test. A minifrac test is an injection-falloff diagnostic test performed without proppant before a main fracture stimulation treatment. The intent is to break down the formation to create a short fracture during the injection period, and then to observe closure of the fracture system during the ensuing falloff period.

Bilinear Flow Regime:

$$P_{fo} - P_i = 264.6\frac{V}{h}\mu^{0.75}\left(\frac{1}{\phi C_t k}\right)^{0.25}\frac{1}{\sqrt{k_f w_f}}\left(\frac{1}{t_p + \Delta t}\right)^{0.75}$$

$$\log(P_{fo} - P_i) = \log\left(264.6\frac{V}{h}\mu^{0.75}\left(\frac{1}{\phi C_t k}\right)^{0.25}\frac{1}{\sqrt{k_f w_f}}\right) - 0.75\log(t_p + \Delta t)$$

$$\log\left(-t\frac{\partial P_{fo}}{\partial t}\right) = \log\left(198.45\frac{V}{h}\mu^{0.75}\left(\frac{1}{\phi C_t k}\right)^{0.25}\frac{1}{\sqrt{k_f w_f}}\right) - 0.75\log(t_p + \Delta t)$$

The indication for bilinear flow regime is on the log-log graph whose slope is -3/4. For the derivative part, it will show the same -3/4 slope which is independent of the initial reservoir pressure.

3.4 Linear Flow Regime

$$P_{fo} - P_i = 31.05\frac{V}{4h}\left(\frac{\mu}{\phi C_t k L_f^2}\right)^{0.5}\left(\frac{1}{t_p + \Delta t}\right)^{0.5}$$

$$\log(P_{fo} - P_i) = \log\left(31.05\frac{V}{4h}\left(\frac{\mu}{\phi C_t k L_f^2}\right)^{0.5}\right) - 0.5\log(t_p + \Delta t)$$

$$\log\left(-t\frac{\partial P_{fo}}{\partial t}\right) = \log\left(15.52\frac{V}{4h}\left(\frac{\mu}{\phi C_t k L_f^2}\right)^{0.5}\right) - 0.5\log(t_p + \Delta t)$$

The indication for linear flow regime is on the log-log graph whose slope is -1/2. For the derivative part, it will show the same -1/2 slope which is independent of the initial reservoir pressure.

Pseudo-radial Flow Regime

$$P_{fo} - P_i = \frac{1694.4V\mu}{kh}\frac{1}{t_p + \Delta t}$$

$$\log(P_{fo} - P_i) = \log\left(\frac{1694.4V\mu}{kh}\right) - \log(t_p + \Delta t)$$

$$\log\left(-t\frac{\partial P_{fo}}{\partial t}\right) = \log\left(\frac{1694.4V\mu}{kh}\right) - \log(t_p + \Delta t)$$

The indication for pseudo-radial flow regime is on the log-log graph whose slope is -1. For the derivative part, it will show the same -1 slope which is independent of the initial

reservoir pressure.

3.5 Modeling Non Darcy Flow in Hydraulic Fractures Accurately

Given the complex nature of propagation of hydraulic fracture and the unique characterization of shale-gas reservoirs, reservoir simulation may become the better and economic way to predict and evaluate well performance. However, semi-analytical solutions for hydraulically fractured horizontal wells in fractured reservoirs have been published by Medeiros et al. 2007. Analytical solutions for fluid flow in naturally fractured reservoirs were published by Warren and Root (1963) and Kazemi; However, analytical solutions to fluid flow in naturally fractured reservoirs can't fully explain the transient behavior that happened in the matrix blocks in shale reservoirs. Techniques have been developed to model the transient behavior of matrix blocks in reservoir simulators, but many of these techniques still rely on analytical approximations that are utilized within the numerical model to reduce the run time. The most rigorous method to model shale-gas reservoirs is to discretely make grids for the entire reservoir, including the network fractures, hydraulic fracture, matrix blocks, and un-stimulated areas.

The presence of naturally fractures and induced fractures make the analysis in shale oil reservoir become complicated. Shale reservoirs often have a matrix porosity system where the transient behavior in the matrix becomes important. J.L. Miskimins and H.D. Lopez-Hernandez concluded that non-Darcy flow effect have an impact on the performance of a hydraulically fractured well even at low flow rate. In hydraulically fracture stimulation, non-Darcy flow can have a major impact on the reduction of a propped half-length, thus lowering the well's productive capability and overall recovery.

At high gas velocities, non-Darcy flow has to be considered that often happens in high conductive fractures. Darcy showed that the pressure drop through porous media is proportional to the fluid velocity:

$$\frac{\Delta P}{L} = \frac{\mu v}{k}$$

Which$\Delta P/L$ is the pressure drop per length of proppant pack.

At turbulent rates, the pressure gradients become proportional to the square of the velocity as represented by Forcheimer's equation:

$$\frac{\Delta P}{L} = \frac{\mu v}{k} + \beta \rho v^2$$

The non-Darcy feature we consider here is the Forchheimer correction; which takes into accountthe inertia effects due to high velocity that may occur in high permeability regions, such asfractures. Some literature description also prefer another way(Dake, 1978),

$$\frac{dP}{dx} = \left(\frac{\mu}{Kk_r A}\right) q + \beta \rho \left(\frac{q}{A}\right)^2$$

where:

q =the volumetric flow rate

K= the rock permeability

k_r =the relative permeability

A= the area through which flow occurs

μ =the fluid viscosity

ρ =the fluid density

β =the Forchheimer parameter

dp/dx= the pressure gradient normal to the area

As the Forchheimer correction is expected to be significant only in regions of high

velocity, it is assumed that those regions have a constant rock permeability and constant porosity(ECLIPSE Technical Description).

In the above discussion the Forchheimer parameterβ is a constant supplied by the user using the keywords VDFLOW or VDFLOWR.

Chapter 4

Basic Reservoir Model Simulation

4.1 Eagle Ford Shale introduction

The Eagle Ford Shale play began with the horizontal discovery well, STS #1, in October 2008. The play has since expanded from the discovery well located in southwest La Salle Count, Texas, to the Mexican border and northeast to the eastern border of Gonzales and Lavaca Counties (Martin, 2011). Conoco drilled first well in Sugarkane Filed in 2006, however, early production was more Austin Chalk than Eagle Ford. Early development was in more gas rich areas, but recent activity is almost entirely in liquids rich areas.

The Eagle Ford Formation is a sedimentary rock formation from the late Cretaceous age underlying much of South and East Texas. The Eagle Ford shale is the source rock for oil and gas in the Austin Chalk. The upper Cretaceous Austin Chalk was deposited in Texas in a shallow marine setting in water depths that ranged from 30 ft or shallower to 300 ft. The Upper Eagle Ford has higher carbonate and lower clay content. The lower Eagle Ford has higher clay and total organic content. The characteristics of the Eagle Ford change substantially across the south-west-to-northeast strike of the play. Shale thickness ranges from 45 feet in the Austin area to more than 500 feet in the dark shales that outcrop in Dallas county. The Eagle Ford is mainly a clay-rich limestone with low quartz content which makes it less brittle and has a low Young's modulus (1-3 million psi YM) (Borstmayer, 2011). The total organic content (TOC) in Eagle Ford ranges from 3-7%. Porosity varies from 6% to 11%. Depth of wells (TVD) varies from 4,500 ft to 11,500 ft.

Eagle Ford Shale completions are almost exclusively horizontal wells with multiple fracture stages. Even though the Eagle Ford play is quite new, more than 3000 horizontal wells have been drilled and all have been hydraulically fractured. These wells were mostly openhole or slotted liner laterals running from 500 to 4,500 ft in length. The fracture fluid typically used is hybrid which consists of primary a large slug of slick water, followed by linear or XL gel. Stimulation treatments contained up to 20,000 lbm

of proppant or no proppant and up to 120,000 gal of fluid (Hollabaugh, 1993).

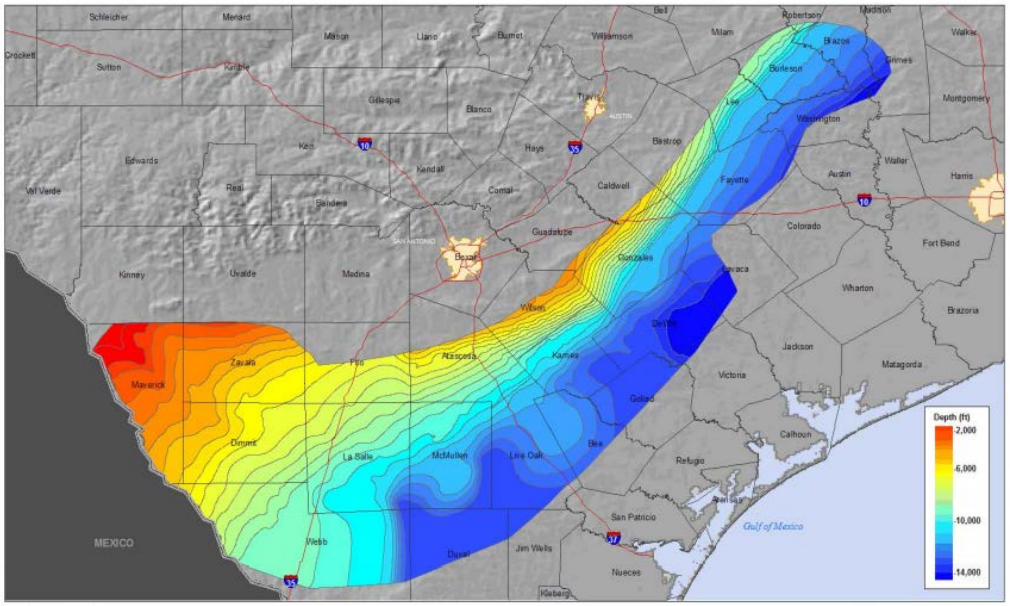

Figure 4.1 Eagle Ford Structure Map

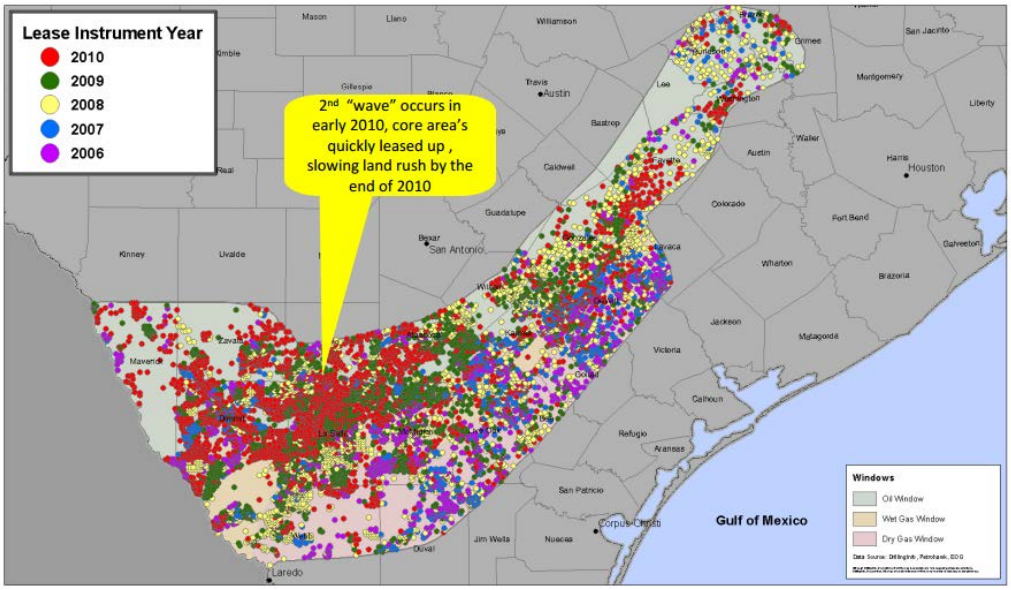

Figure 4.2 Eagle Ford Leasing-Movement into oil window

4.2 Basic Model Description (Horizontal drilling with multi-hydraulic fractures model for Primary Production)

Unconventional reservoirs exhibit many challenges which are not commonly found in traditional reservoirs. The characteristics of low-permeability, fast reservoir pressure depletion make it hard to produce the unconventional reservoirs economically as conventional reservoirs without stimulation techniques. In shale reservoirs, there is almost no oil producing if we don't implement any kinds of stimulations and most of the reservoir energy is consuming on transporting the fluids through tiny pores and throats in the tight formations which possess a higher capillary pressure than conventional reservoirs. In this case, stimulated reservoir volume (SRV) plays a key role in communicating the fluid flow through matrix to fractures that creates highly conductive flow paths for fluid flowing into the wellbore. Hydraulic fracturing is well recognized as one of the most effective stimulation techniques for enhancing the productivity in unconventional reservoirs. Horizontal wells also have the advantages of improving contact area with the formation and were widely facilitated by the surging exploitation of unconventional reservoirs. Horizontal well with multi-stage hydraulic fracturing technique has become a successful and standardized way to commercially produce oil or gas from these shale reservoirs.

Unconventional shale oil/gas reservoirs require some certain stimulated reservoir volume in order to be economically and practically producible. Conventional methods for simulating the fluid flow in fractures is by explicitly using 0.001 ft wide grid cells as fractures, ended up by using tremendous numbers of grid cells to simulate the whole reservoir whose size increases logarithmically away from the fractures as shown in Fig 4.3. As we are always looking for some kinds of efficient and fast computation methods that can save us a lot of time and we are more interested in the area of dramatic pressure drop happening near the fracture, it would be wise to set up fined grid-blocks near the fractures to simulate the large pressure drop happening between fracture and matrix. The physical flow simulation in multi-stage hydraulic fractured reservoirs can be very tedious by using these fine gridblocks to represent a 0.001-ft fracture (approximately total 5-10

million cells for a field simulation). Some studies investigated using 2-ft wide fracture to represent the 0.001 ft wide fracture to model gas production in unconventional shale gas reservoirs. Work by Barry Rubin (2010) is a good example. Their work shows excellent matching results between the 2-ft coarse model and the 0.001-ft realistic reference model. In this case, it can save us lots of gridblocks and computation complexity and time without sacrificing the computing accuracy if we are faced with a project of complex fracture networks. In our work, we will similarly use the 2-ft wide grid cells to simulate the physical fracture flow and make a comparison of production results with the reference solutions from the actual 0.001-ft fracture(Rubin, 2010).

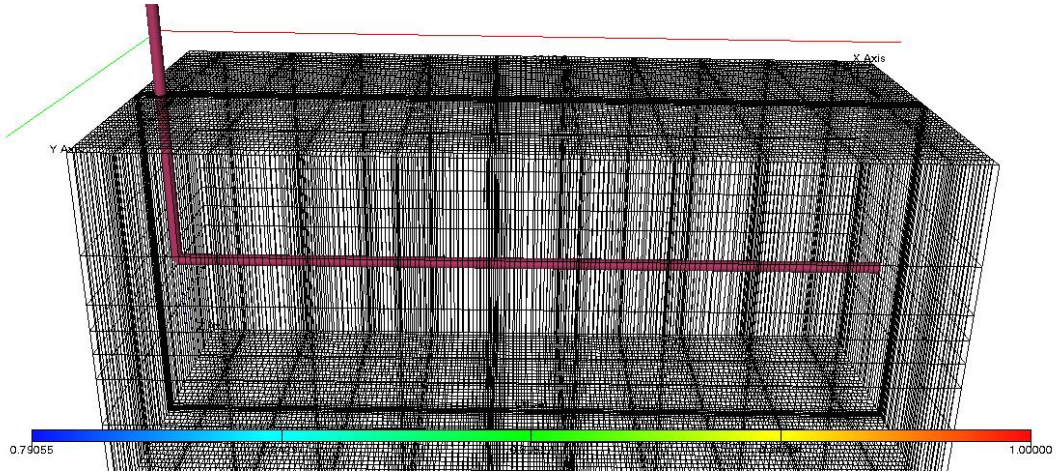

Figure 4.3 Horizontal well with 10 hydraulic fractures model (210×55×7)

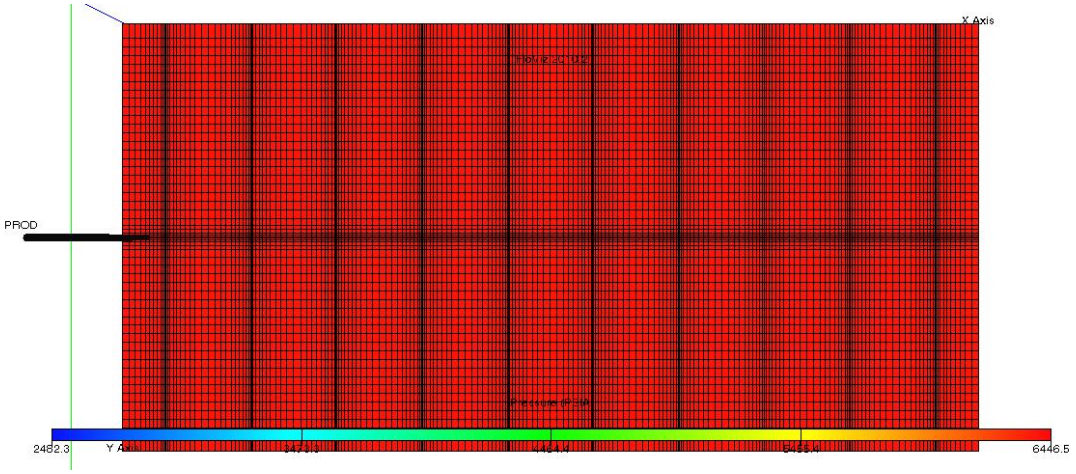

Figure 4.4 Original pressure distributionin a horizontal well

The shale oil reservoir model we used assumed to be 2000 ft long×1000ft wide×200 ft thick. We develop this field with a horizontal well and 10 transverse fractures each placed 200 ft apart. E.Mendoza et al. (2011) presented a case study of optimizing horizontal well hydraulic-fracture spacing in the Eagle Ford reservoir (Mendoza, 2011). They studied a numerical analysis for optimizing the number of hydraulic fracture stages, minimizing the stages' interference and maximizing the expected net present value (NPV). They investigated a 3800-ft long and 425-ft wide well simulation model with a horizontal well drilling. They performed an evaluation by changing the number of fractures and including the production forecast. From their NPV analysis, it was concluded that 20 stages should be considered the recommended scenario. In other words, 200-ft hydraulic-fracture spacing should be a reasonable value.

Fig 4.4 is the graph for illustrating of initial reservoir pressure distribution of the whole reservoir. The reservoir properties data we used in this model is from published data in Eagle Ford shale (Table 4.1) (Bazan,2010).The initial reservoir pressure for this field is 6,425 psi. The permeability for this shale reservoir is ultra-tight about 100 nano-Darcy. The implicit assumption we made is that the investigated Eagle Ford field is homogeneous and isotropic. We assume the modeled Eagle Ford Shale play matrix has the same permeability of 100 nano-Darcy and 6% porosity in each point and in every direction. We will model 10 transverse hydraulic fractures each 500 ft (1/2 length) in a 10E-4 mD shale reservoir (as shown in Fig 4.4). The fracture is assumed to extend from the top to the bottom of the pay (200-ft height). The hydraulic fracture conductivity assumed to be 83.3 md-ft. The fracture $K_f \times A$ should be identical in the simulation model using a 2-ft wide fracture to the simulation model using a 0.001-ft wide fracture. Thus the fracture permeability should be 41.65 md for 2-ft wide fracture.

We use total 80850 (210×55×7) grid-cells to model this whole reservoir in which 2-ft wide with 83.3 md-ft conductivity cells were used to simulate the physical flow in hydraulic fracture. This method was proved to be useful and accurate by lots of studies that were well-documented in the literatures as we discussed above. There are 3850 (10*55*7) cells set up for the ten fractures simulation (each fracture consists of 1*55*7

cells) and the rest are made up of 77000 cells for shale matrix simulation. The grid-block sizes were logarithmically spaced increasing away from each fracture. We use a fine gird surrounding the fracture in order to be able to get adequate representation of flow around the fracture. The purpose for doing this is that it would be accurate to capture the pressure variations and fluid flow from the shale matrix to the fracture and within the fracture. As the majority of the oil is contained in the matrix system, but the production of oil to the wells is through the high permeability fracture system. Fracture system is an important conductive communication between the matrix and the wellbore that deserves our special attention for delineating their flow patterns, pressure variation etc.

Anish Singh Chaudhary et al. (2011) investigated some production behaviors under different permeability, BHP etc by using the data from Eagle Ford Shale. However, they did not propose any sorts of new techniques regarding how to improve the oil recovery in shale oil reservoir. What they did was that they focused on simulating the primary production performance of shale oil reservoirs and did some sensitivity studies of shale oil production performance. The goal of our work is not only to extend some work done by Rubin and Anish Singh Chaudhary but propose a new technique for improving oil recovery in shale oil reservoirs for the first time. The work we completed might encourage a new boom in unconventional reservoirs development because of the huge potential for incremental oil recovery proposed by this paper and current depressed gas price.

Table 4.1 Reservoir properties for Eagle Ford shale

Initial Reservoir Pressure	6,425 psi
Net pay	200 ft
Porosity of Shale matrix	0.06
Compressibility of Shale	$0.5*10^{-5}$ psi^{-1}
Shale Matrix Permeability	0.0001 md
Oil API	42
Reservoir temperature	255 F
Gas Specific Gravity	0.8

Table 4.2 Designed Hydraulic Fractures Properties

Fracture Conductivity	83.3 md-ft
Fracture half length	500 ft
Fracture height	200 ft
Fracture permeability	41.65 (for 2-ft wide fracture)

Fig 4.5 and Fig 4.6 are the matrix relative permeability curves that we used in our model. In hydraulic fracturing rock type we use two straight lines to represent the relative permeability curves, which is accepted in the reservoir simulation (Fig 4.7 and Fig 4.8).

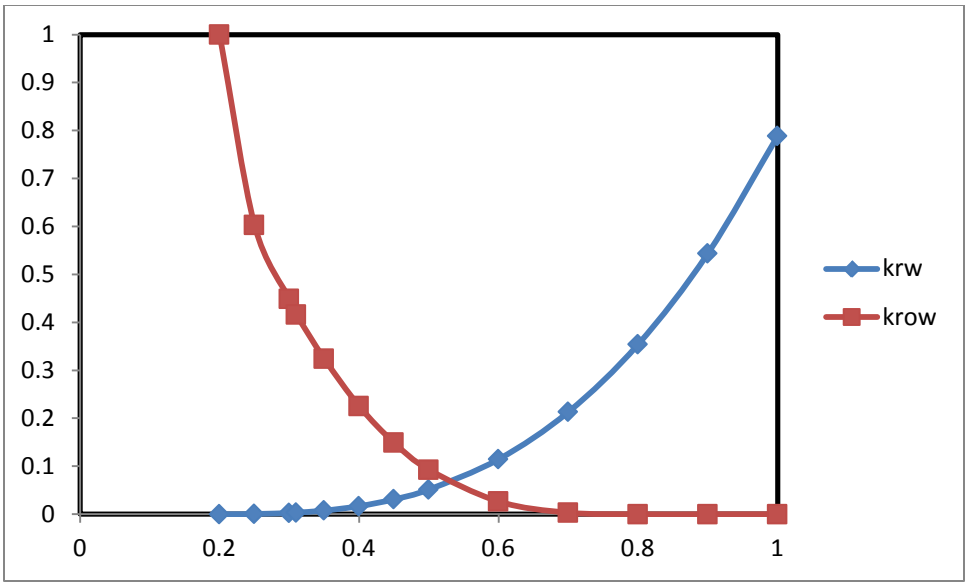

Figure 4.5 Matrix oil and water relative permeability curves

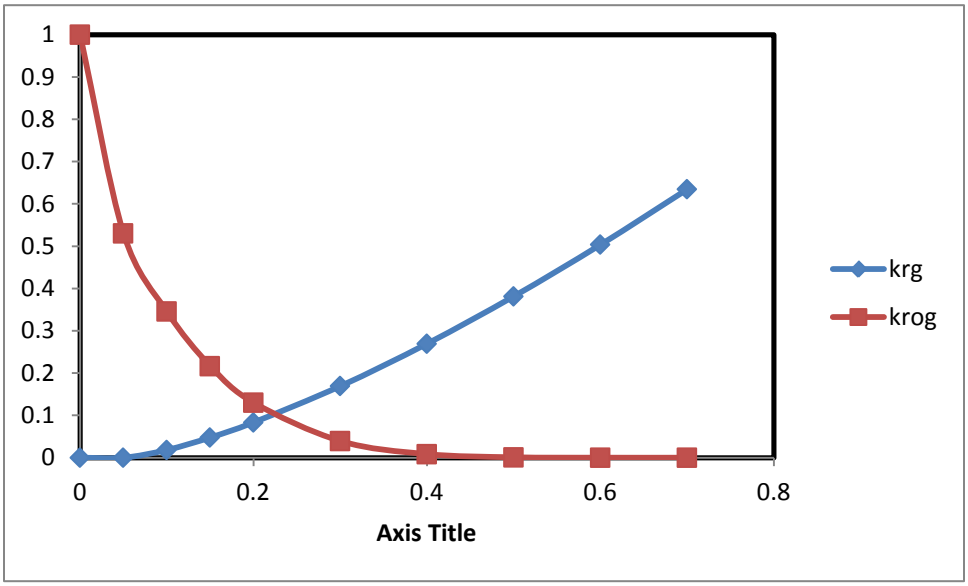

Figure 4.6 Matrix oil and gas relative permeability curves

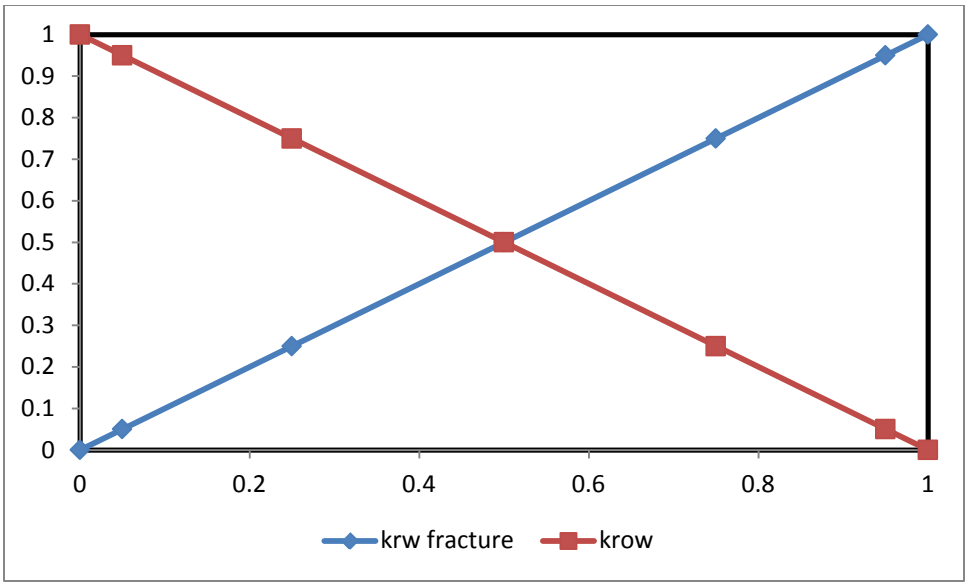

Figure 4.7 Fracture relative permeability curves ofoil and water

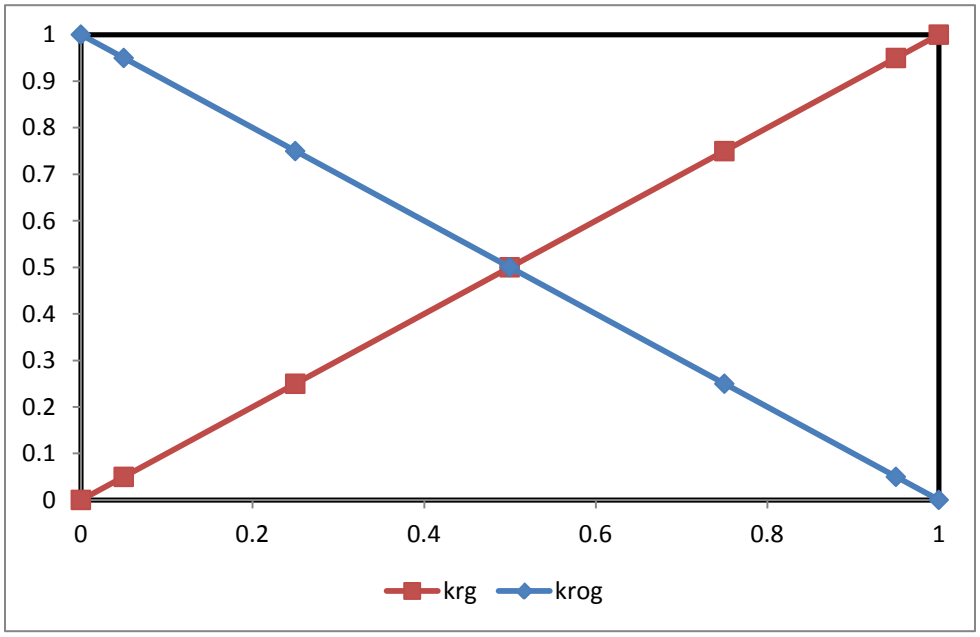

Figure 4.8 Fracture relative permeability curves of oil and gas

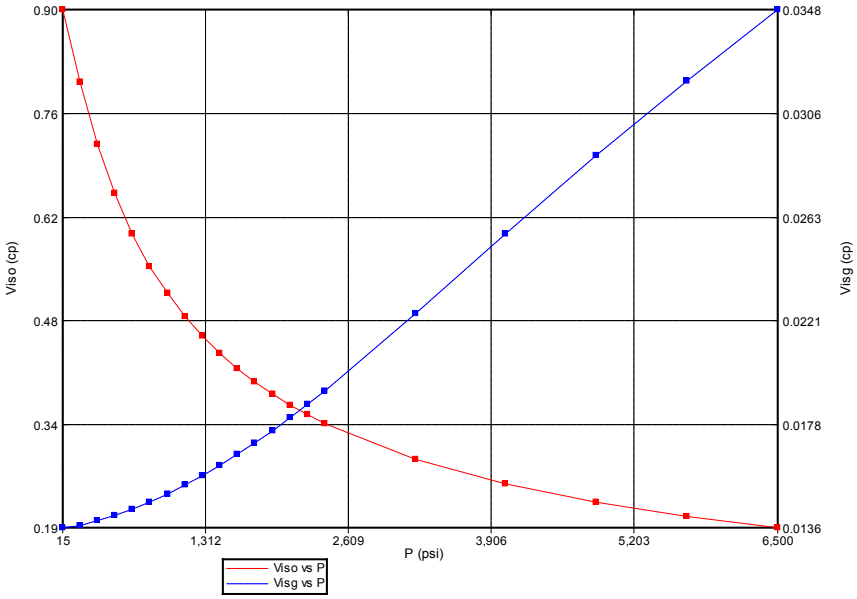

Figure 4.9 Oil and gas viscosity vs. pressure

Fig 4.9 shows the oil and gas viscosity properties changing with pressure.

Table 4.3 Oil and gas PVT data input

P	Rs(ft^3/bbl)	Bo	Eg	Viso	Visg
14.696	4.68138	1.09917	4.10159	0.902644	0.013601
173.583	32.1923	1.11173	49.1225	0.803844	0.013724
332.47	65.2796	1.12711	95.3676	0.719427	0.013905
491.357	101.621	1.1443	142.801	0.651788	0.014127
650.244	140.36	1.16295	191.364	0.59727	0.014385
809.131	181.027	1.18287	240.971	0.552597	0.014677
968.018	223.32	1.20393	291.506	0.515357	0.015001
1126.9	267.027	1.22604	342.824	0.483819	0.015357
1285.79	311.989	1.24913	394.75	0.45674	0.015745
1444.68	358.084	1.27314	447.084	0.433209	0.016164
1603.57	405.212	1.29803	499.604	0.412545	0.016612
1762.45	453.293	1.32376	552.077	0.394234	0.017088
1921.34	502.257	1.3503	604.264	0.377877	0.01759
2080.23	552.048	1.3776	655.935	0.363163	0.018116
2239.11	602.616	1.40566	706.874	0.349843	0.018664
2398	653.915	1.43443	756.888	0.337718	0.019232
3218.4	929.142	1.59372	995.379	0.288941	0.022371
4038.8	1219.15	1.76935	1195.74	0.255067	0.025643
4859.2	1521.47	1.95964	1360.49	0.229917	0.028854
5679.6	1834.43	2.16332	1496.29	0.21036	0.031914
6500	2193.143	2.37939	1609.67	0.19463	0.034795

After we finish the introduction of basic reservoir data, rock and fluid properties and initial reservoir data, it is necessary to initiate the modeling work for examining the accuracy and correctness of the simplified model by simulating only one fractured volume. Simulating the whole Eagle Ford play may contain tremendous number of grid blocks, and it is an intimidating job to model the complex fracture networks if we incorporate the nature fractures. We propose to use a simplified model of simulating just one of these fracture stimulated volumes instead of investigating the whole reservoir.

There are some good reasons for focusing on just one facture stimulated reservoir volume including computing simplicity and work efficiency. The implicit assumption we made here is that each fracture has the same drainage area, the same geometric shape and the same conductivity. As shown in Fig 4.10, bilinear flow occurs in the finite conductive fracture and formation around a hydraulically fractured well. During the bilinear-flow period, bottomhole pressure (BHP) is a linear function of $t^{1/4}$ on Cartesian coordinate paper. The physical flow in each fracture is the same and symmetric on the basis of the assumptions made above, as shown in Fig 4.10. It is well documented that it is valid to simulate only one fractured volume and the ensuing numerical simulations will also validate this. Fractures conductivity we used (C_{fD}=83.3 md-ft) here can be considerate as finite conductive.

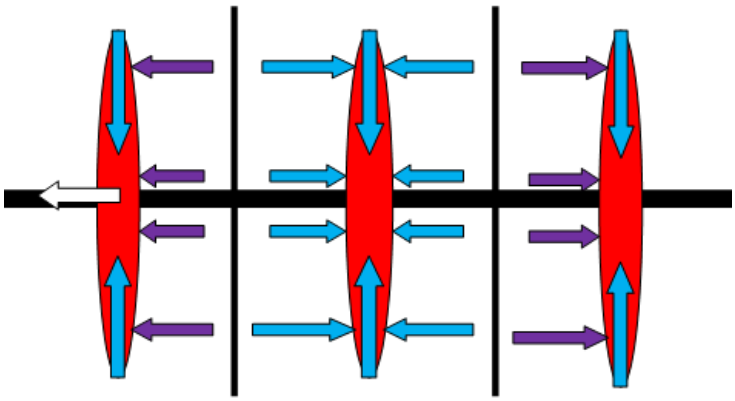

Figure 4.10 Illustration of fluid flow in multi-hydraulic fractured horizontal well

4.3 Basic Simulation Model Validation and Comparison (ECLIPSE Model)

Case 1: The entire reservoir with 10 hydraulic fractures stimulated reservoir volume (DX=2000 ft, DY=1000 ft, DZ=200 ft). Grid dimensions are 210×55×7.

Case 2: Single hydraulic fracture stimulated reservoir volume(simplified model)

(DX=200 ft, DY=1000 ft, DZ=200 ft). Grid dimensions are 21×55×7.

In this thesis, we will compare the solution results from the total 10 hydraulic fractures stimulated volume and single hydraulic fracture stimulated volume to ensure the validity of the simplified model by studying single fracture SRV instead of the entire reservoir. For 10 hydraulic fractures, we use 80850 cells (210×55×7) in total to model the entire reservoir and fractures whose cells width increase as they go away from the fracture. The minimum cells width are 2-ft for hydraulic fractures (k=41.65 md). In case 2, there are 8085 (21×55×7) cells made up for single hydraulic fracture network with the same width and permeability for fracture as we used in case 1. Based on this simplified model and the entire reservoir model, our simulation results indicate that there are excellent solution results matching between the case 1 and case 2.

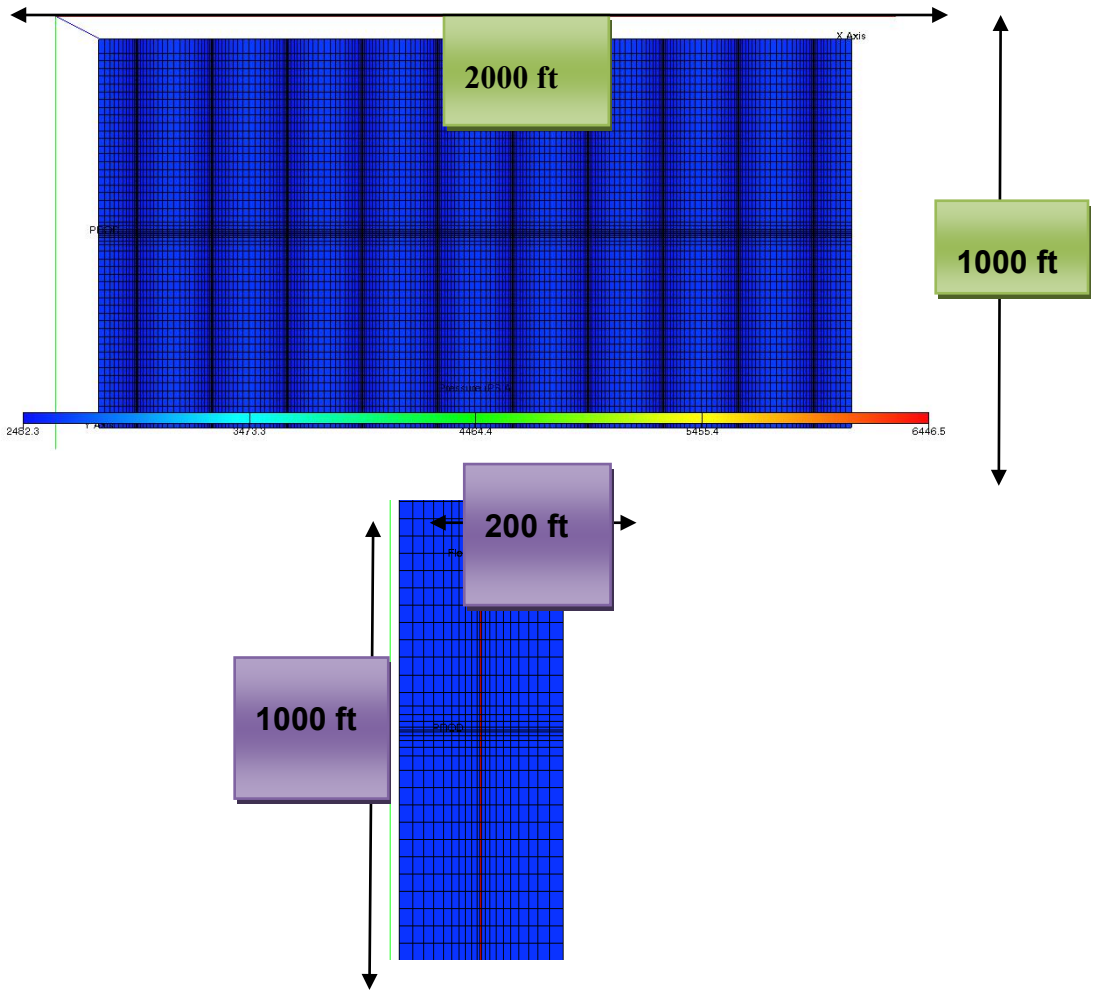

Figure 4.1110 Hydraulic fractures SRV vs. single hydraulic fracture SRV (TOP view)

Fig 4.11 shows the schematic diagram of simulation the whole reservoir with 10 hydraulic fractures and simulation of single hydraulic fracture stimulated reservoir volume. During the primary production process, the well is controlled by bottom-hole pressure (BHP) which is set up as 2500 psi.

When bottom-hole pressure drops below bubble-point pressure, reservoir fluids are subject to solution gas drive, which provides significant energy due to the expansion of the evolved gas. Solution gas drive can provide a lot of energy to drive reservoir fluids towards the wellbore because of the high compressibility of gas. However, in our thesis, we will always keep the BHP above the bubble point pressure in avoid of solution gas liberating from the oil. The reason for us keeping control of BHP above bubble-point is by taking the advantage of avoiding the complex multiple-phase calculations. It also can help us get rid of the confusion caused by the property differences of injected gas and evolved gas in the ensuring miscible cyclic gas injection project.

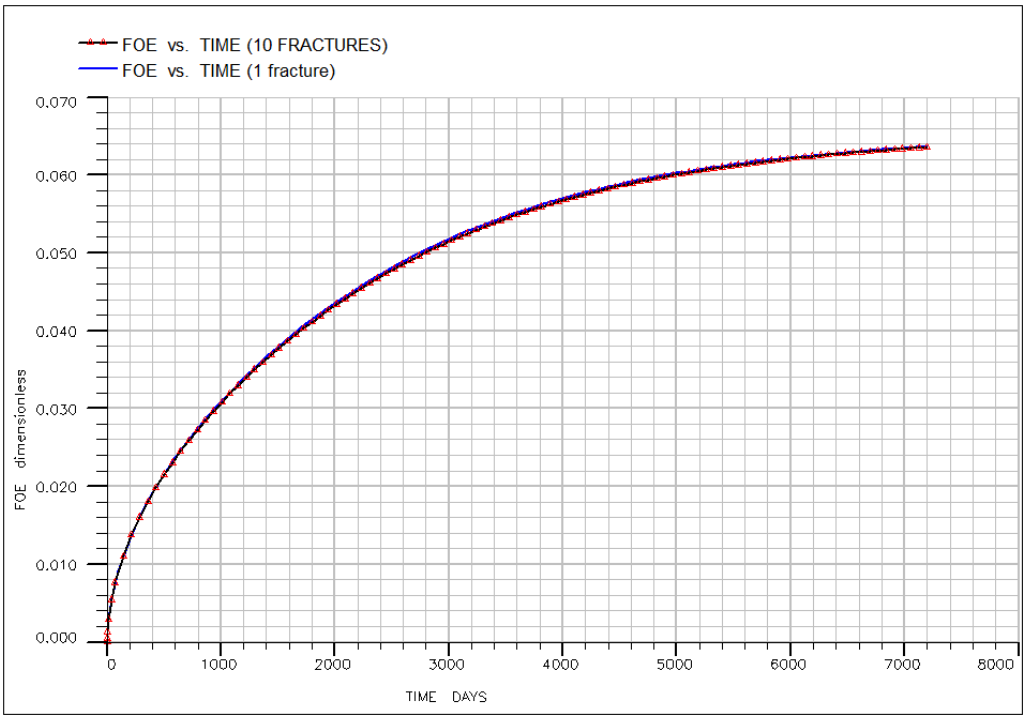

Figure 4.12 Oil Recovery Factor comparison for 10 fractures and 1 fracture

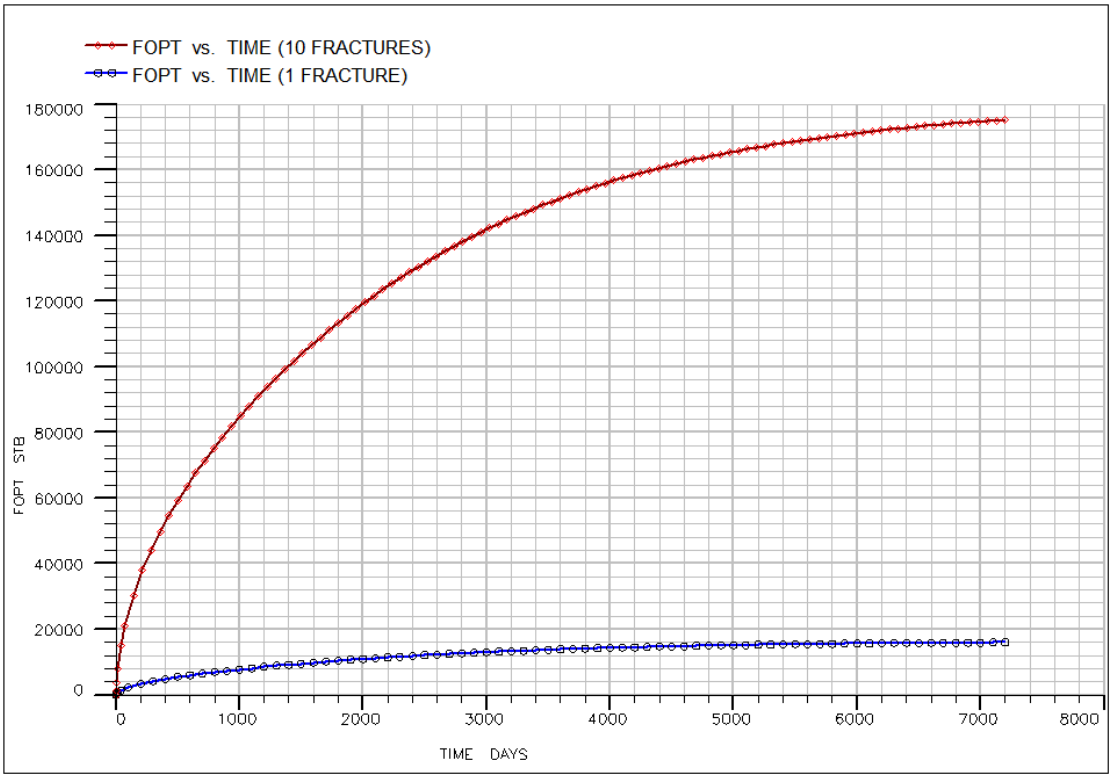

Figure 4.13 Cumulative oil production comparison for 10 fractures and 1 fracture

Results from Fig 4.12 show us that the entire reservoir consisting of 10 fractures and single fracture simulation have the same oil recovery factor matching perfectly for each other at every time step. The whole reservoir cumulative oil production should be 10 times of the single fracture production at a material balance view. Fig 4.13 shows that the oil production from 10 hydraulic fractures, namely, the whole field is 175164 STB, while oil production from single of those hydraulic fractures area is 17847 STB. This is correspondent with anticipated results from our analysis.

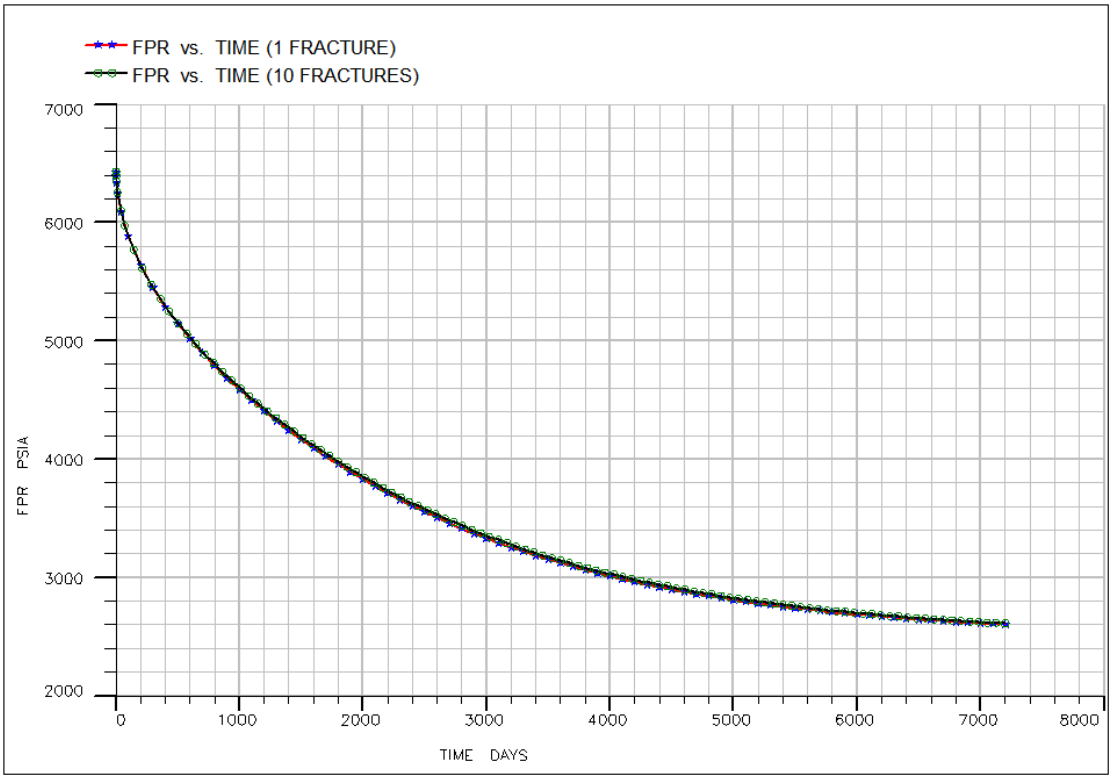

Figure 4.114 Field average pressure vs. time

As shown in Fig 4.14, the average reservoir pressure change of 10 fracture stimulated volume case1 is consistent with the case 2. Case 1 and Case 2 were used to validate the accuracy of the methodology for application of single fracture to replace the simulation of the entire reservoir. The simulation results show that it is accurate enough to simulate single fracture to represent the entire reservoirs for simplicity and saving time.

4.4 Basic Reservoir Model Correction through Comparison by Two Commercial Software (ECLIPSE and CMG)

Now that we have numerically verified the accuracy by using the simplified model for simulating the production behavior of entire reservoir area, we will keep utilizing this simplified method through the whole work. It will greatly reduce the computational complexity especially under multi-cyclic gas injection scenarios.

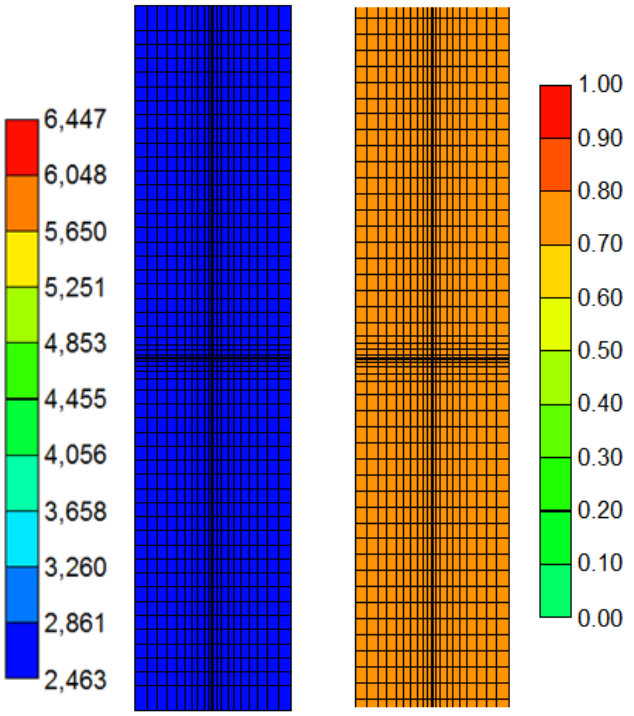

Figure 4.15 Reservoir pressure and oil saturation distribution for primary production

Fig 4.15 shows the reservoir pressure and oil saturation distribution of the simplified model after 7200 days of primary depletion. As shown, most of the pressure drop occurs not far from the fracture because there are nearly no fluids flowing from the shale matrix to matrix if without hydraulic fracture. That is why hydraulic fracturing gained a high recognition for improving the communication between the shale matrix and the fractures that creates a highly conductive flow path to the wellbore. However, primarily it only recovered 6.4% oil from shale oil reservoirs which does not seem to match the high reputation of hydraulic fracturing. Our work in the following would focus on enhancing the secondary recovery in the shale reservoirs by using our developed technique. A prominent increase in the secondary recovery would provide huge incentives for developing the unconventional resources because of increasing energy demand.

We will compare the results obtained from ECLIPSE with CMG further reassuring the correctness of this model. Fig 4.16-4.19 indicate that there are minor errors occurred by using the commercial simulators ECLIPSE and CMG for simulation of cumulative oil

production, oil recovery factor and average reservoir pressure. But this kind of minor errors are acceptable due to different simulators using different internal functions or computing methods.

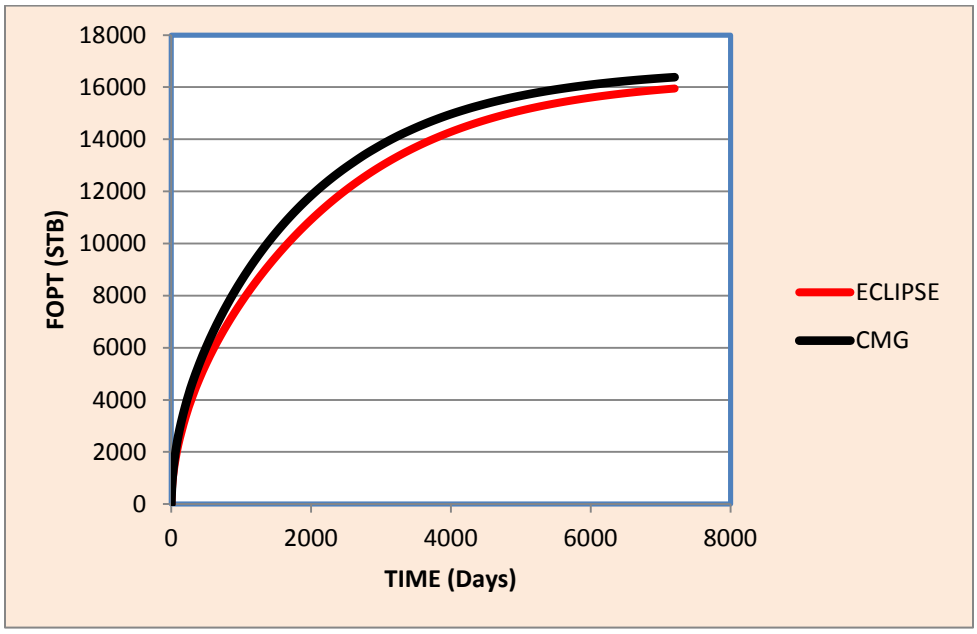

Figure 4.16ECLIPSE and CMG oil production total comparison

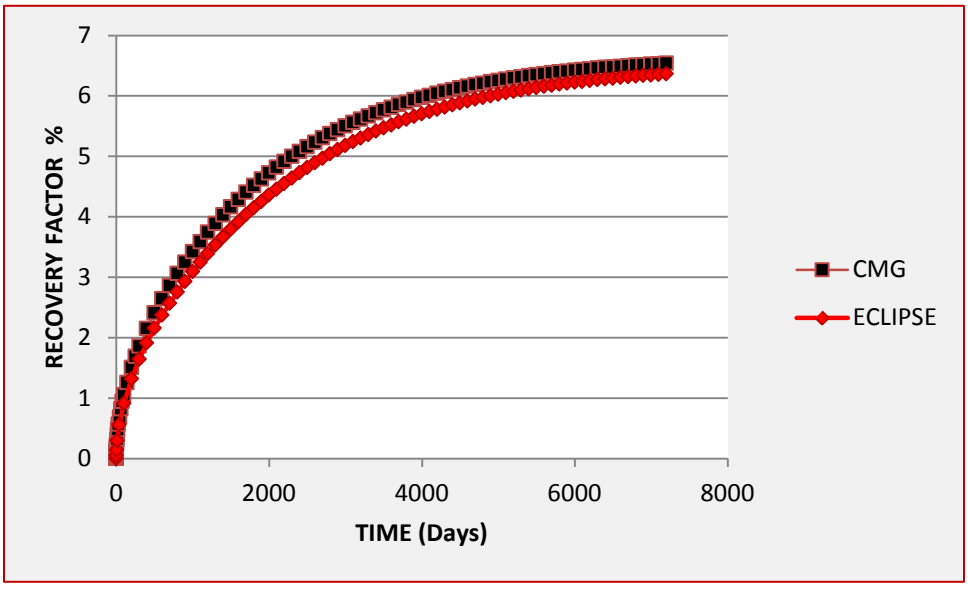

Figure 4.17ECLIPSE and CMG oil recovery factor comparison

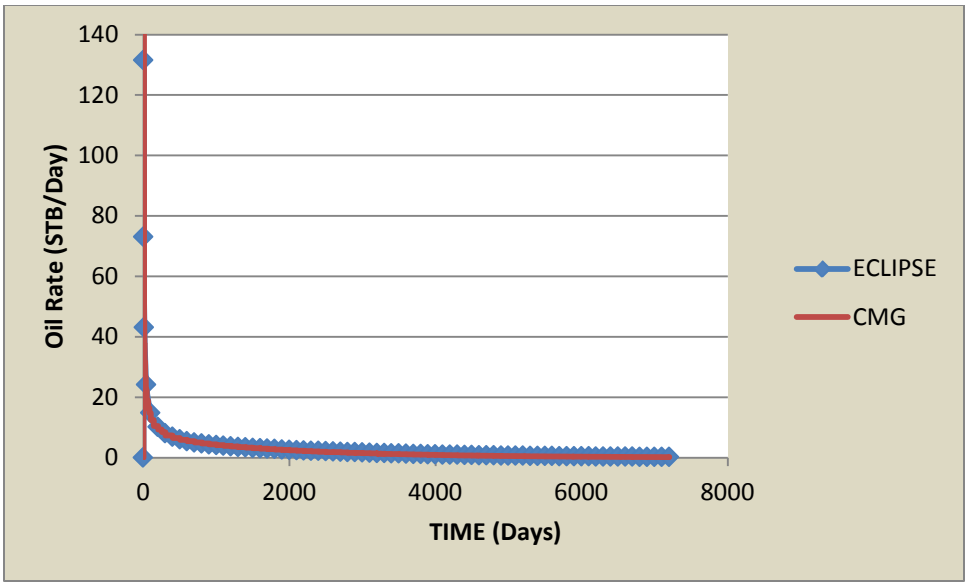

Figure 4.18ECLIPSE and CMG oil rate comparison

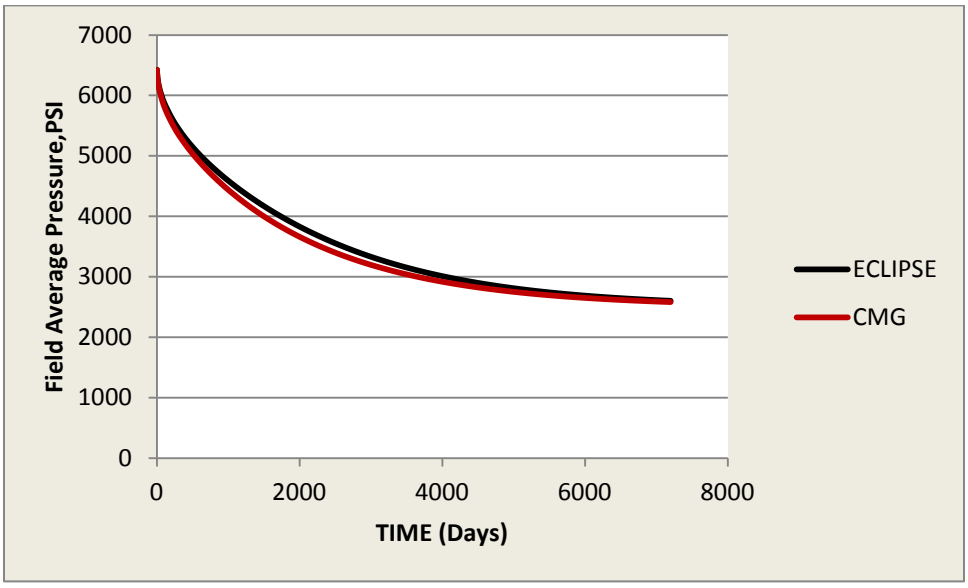

Figure 4.19ECLIPSE and CMG reservoir average pressure comparison

Fig 4.16-4.19 showed the comparison results gained from commercial software CMG and ECLIPSE. These good matching comparison results provide us some confirming information about the correctness of the reservoir model, although there are slight errors

due to the computing issues by these two software.

4.5 Material Balance Calculation Validation for the Model

Havlena and Odeh (1963) expressed Equation in the following form:

$$N_p\left(B_o + (R_p - R_s)B_g\right) + W_pB_w = N\left[(B_o - B_{oi}) + (R_{si} - R_s)B_g\right] + mNB_{oi}\left(\frac{B_g}{B_{gi}} - 1\right) + N(1+m)B_{oi}\left[\frac{c_wS_{wi} + c_f}{1 - S_{wi}}\right]\Delta p + W_e + W_{inj}B_w + G_{inj}B_{inj}$$

4.5.1 Case-Model validation by utilizing material balance before gas injection

Since there is no water injection in our model and this is an undersaturated oil reservoir, we can easily derive the following determined parameters.

W_e=0, since the reservoir is volumetric

m=0, since the reservoir is undersaturated

R_s=R_{si}=R_p, since all produced gas is dissolved in the oil

The above equation can be reduced as:

$$N_pB_o + W_pB_w = N[B_o - B_{oi}] + NB_{oi}\left[\frac{c_wS_{wi} + c_f}{1 - S_{wi}}\right]\Delta p$$

If we assume $k = NB_{oi}\left[\frac{c_wS_{wi}+c_f}{1-S_{wi}}\right]$ and $c = N[B_o - B_{oi}] - W_pB_w$

$$N_pB_o = k\Delta p - c$$

In order to check the soundness and ensure robustness of the model, the results given by Eclipse must be consistent with the results derived from material balance equation. Illustrated as Fig 4.22, the figure of N_p versus p given by material balance calculation can be compared with the output results from ECLIPSE. Predicted production values from

material balance principle can be expressed as:

$$N_p = \frac{N[B_o - B_{oi}] + NB_{oi}\left[\frac{c_w S_{wi} + c_f}{1 - S_{wi}}\right]\Delta p}{B_o}$$

Where $N = Ah\phi(1 - S_w)$, initial oil in place.

Fig 4.22 shows that the results given by ECLIPSE are correspondent with what we expected from theoretical material balance equation.

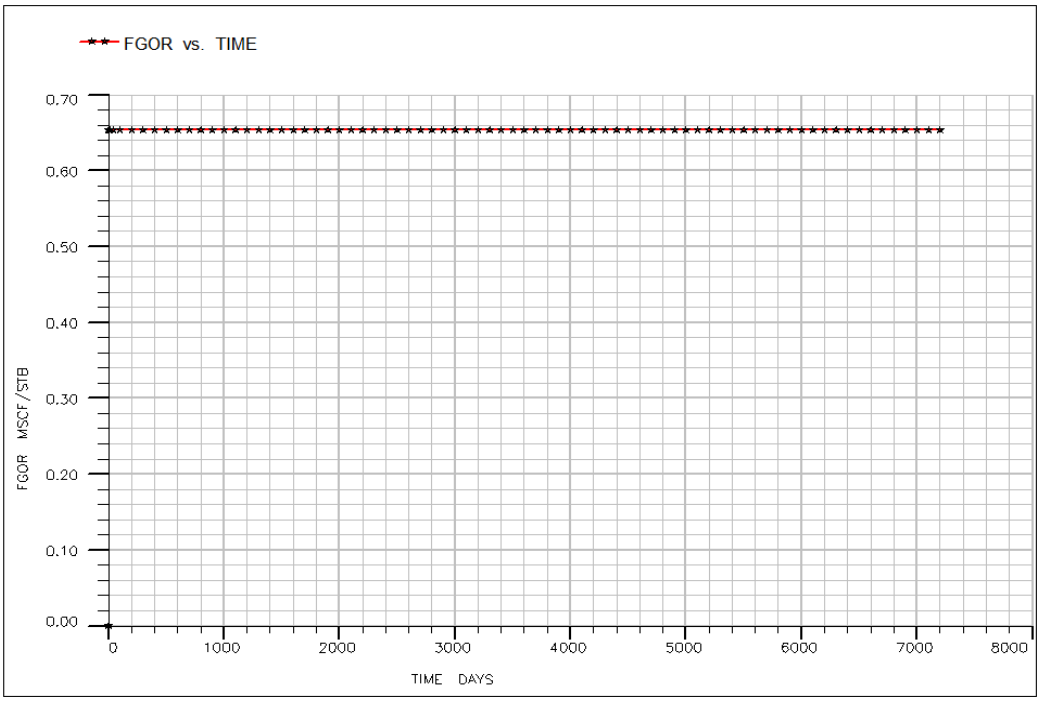

Figure 4.20 GOR vs Time

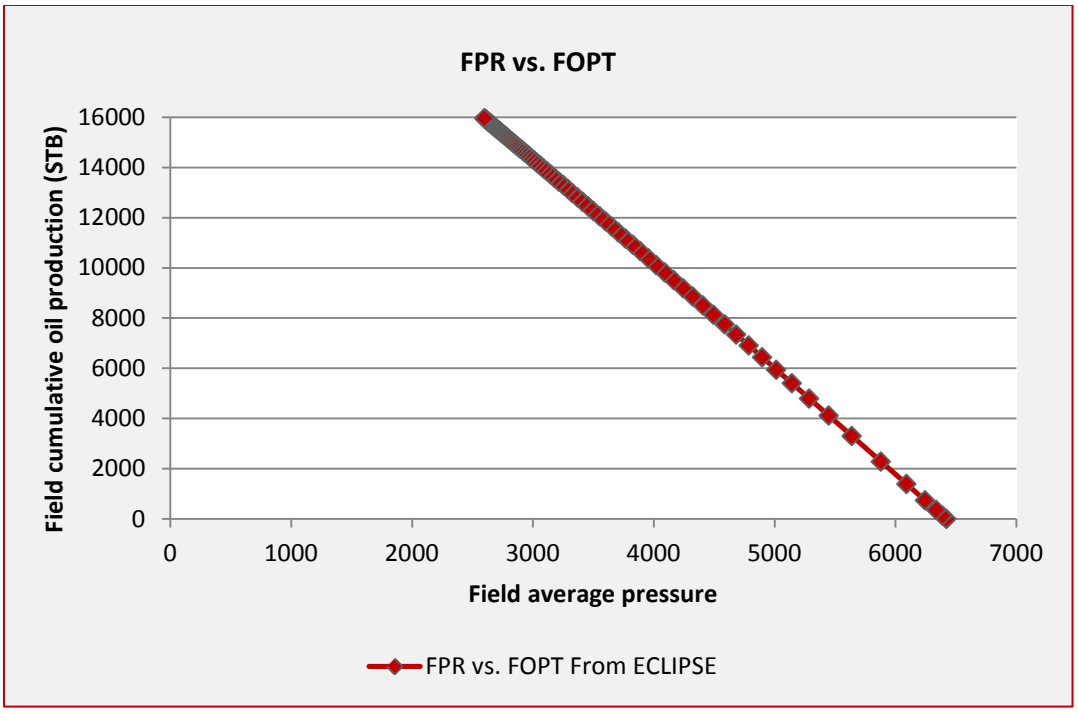

Figure 4.21 ECLIPSE output simulation results

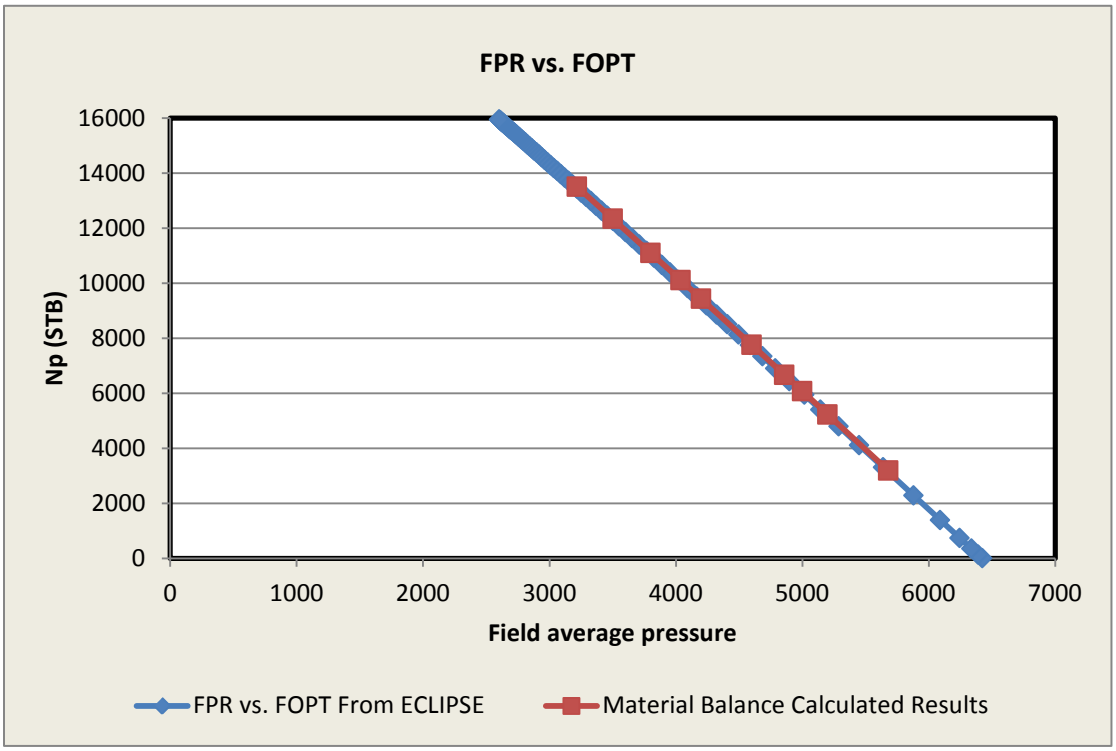

Figure 4.22 ECLIPSE output results match material balance calculated results

Table 4.4 Material Balance Calculation

P	Bo	Bo-Boi	Boi*(Cw*Swi+Cf)/(1-Swi)*Dp	Np (STB)
3218.4	1.42271	0.044897	0.031726684	13496.50101
3500	1.418709	0.040896	0.028940482	12335.74267
3800	1.41446	0.036647	0.025972228	11094.01098
4038.8	1.411086	0.033273	0.023609497	10101.79737
4200	1.408813	0.031	0.022014555	9430.103928
4600	1.403189	0.025376	0.018056882	7756.706355
4859.2	1.399557	0.021744	0.01549231	6667.254
5000	1.397588	0.019775	0.014099209	6073.768917
5200	1.394795	0.016982	0.012120373	5228.707261
5679.6	1.388122	0.010309	0.007375123	3192.444888

Note:

OOIP: N= 250596 STB OOIP= $[Ah \times \emptyset(1 - S_{wc})]_{Matrix} + [Ah \times \emptyset(1 - S_{wc})]_{Fracture}$

Fig 4.20-4.22 repeat checking the robust of the model by introducing the most fundamental material balance calculation. The material balance equation has long been recognized as the basic tools for interpreting and predicting reservoir performance and is widely applied in the simulator. The material balance principle is structured to simply keep inventory of all materials entering, leaving and accumulating in the reservoir. The initial volume equals to the produced out of the reservoir and the volume remaining. Fig 4.22 obtained from material balance calculation perfectly matches the results output from the simulator. By doing this it can avoid some implicit errors caused by input data error or convergence issues.

4.6 Using0.001 ft wide cells and 2 ft wide Fracture Simulation Comparison

Before we move on to the cyclic gas injection project, we are not quite confident about the results by using 2-ft wide cells simulating the actual hydraulic fracture. Although Barry Rubin (2010) investigated using 2-ft wide fracture to represent the 0.001 ft wide fracture to model gas production in unconventional shale gas reservoirs and their work showed excellent matching results between the 2-ft coarse model and the 0.001-ft realistic reference model, we will use our data to complete the procedure. As mentioned above, the fracture conductivity (83.3 md-ft) should be identical in the simulation model using 2-ft wide fracture to the simulation model using a 0.001-ft wide fracture. The blocks surrounding the fracture should vary in a logarithmic fashion away from the fracture in both the direction parallel and perpendicular to the fracture for the sake of adequate representation of flow around the fracture (CMG, 2009).

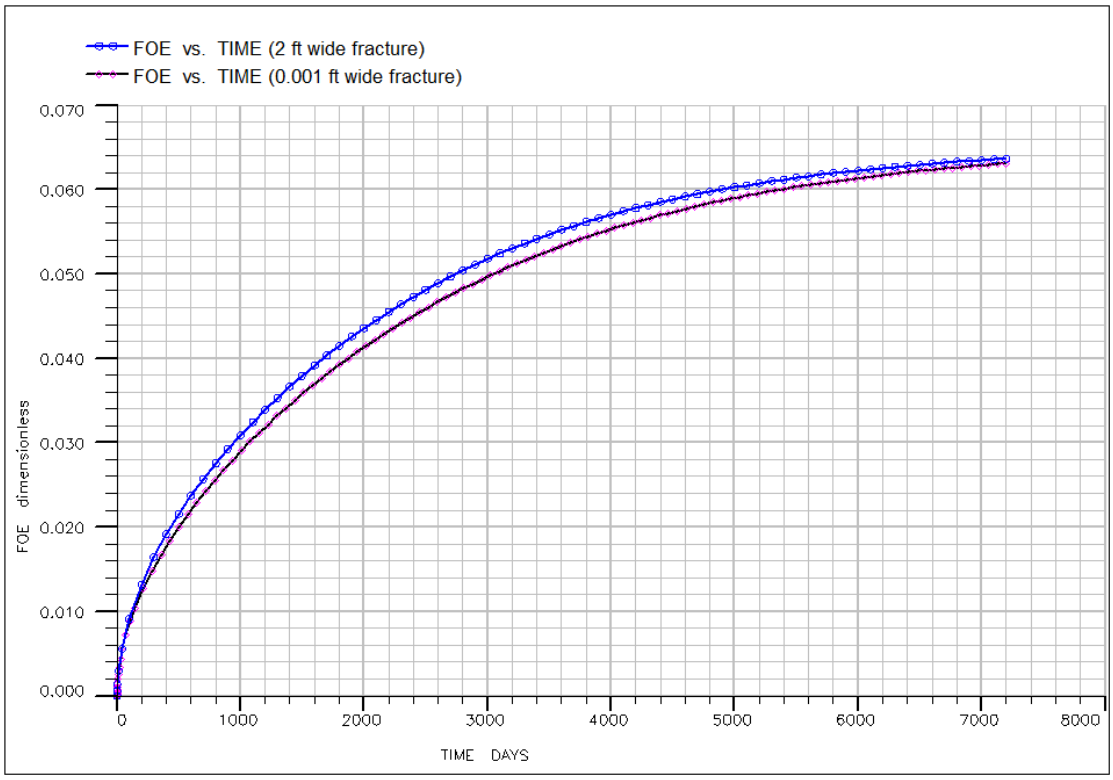

Figure 4.23 Oil recovery factor comparison for 0.001 ft wide fracture and 2-ft wide fracture

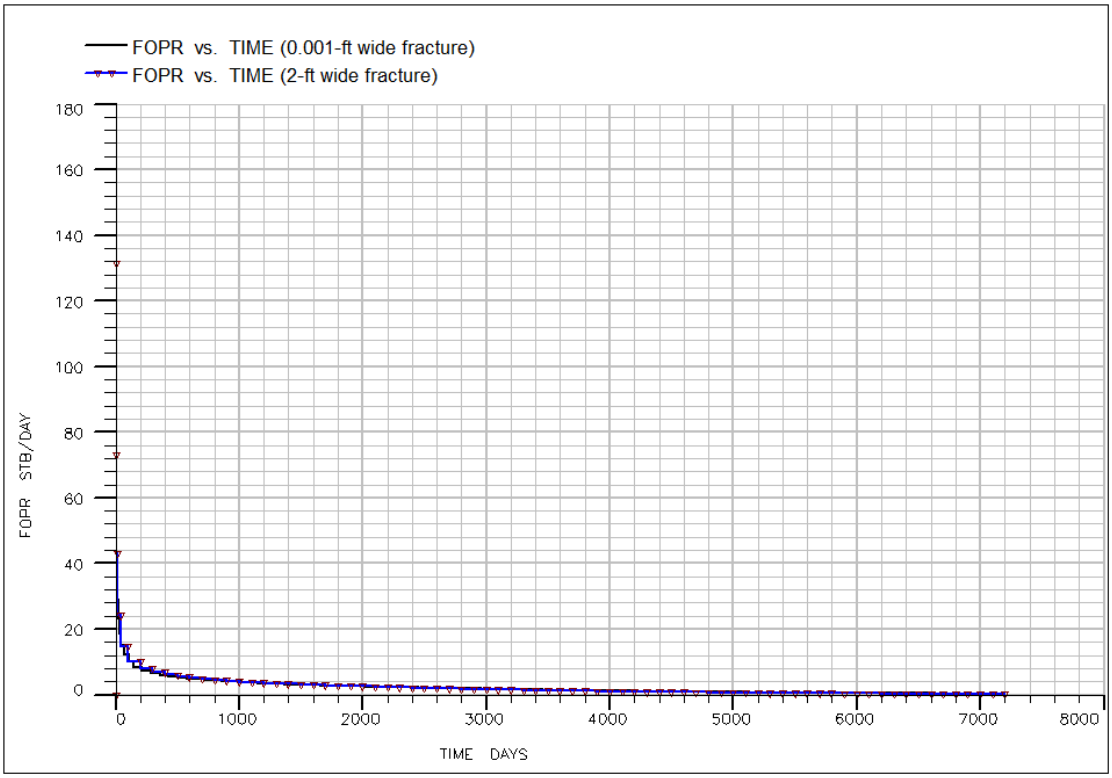

Figure 4.24 0.001-ft wide fracture and 2-ft wide fracture field oil production rate comparison

This part work is to determine if the 2-ft wide fractures could be used to accurately model the fluid flow in the actual extremely narrow fractures. Fig 4.23-4.24 reveal that the methodology documented in lots of literatures by using 2-ft wide grid-block simulating the 0.001 foot wide actual fracture with the same conductivity is legitimate.

It should be noted that the oil recovery factor difference in Fig 4.23 is caused by assigned different relative permeability curves in the matrix and fracture grid blocks (different initial oil saturation for 2 relative permeability curves). The initial oil saturation (S_{oi}) of the relative permeability curve used in the shale matrix was 0.8 and 1 for the fracture. In this case, there are some differences in terms of OOIP for these two cases because 2-ft wide fracture has higher oil storage volume than 0.001-ft wide fracture does (assume 100% oil saturation in the fracture). Oil production rate from 2-ft wide fracture will be higher than 0.001-ft wide fracture at the beginning phase because 2-ft wide fracture can provide the same amount of fluid more quickly than 0.001-ft wide fracture. This can explain why

the oil recovered in 2-ft wide fracture is higher than in the 0.001-ft wide fracture at the early stage. If we use the same relative permeability curve for both the fracture and matrix, we will get the matching results overlapping each other.

Figure 4.25 shows the comparison results of the two cases of 7200 days of primary production. There is slight error for these two cases as has been stated above.

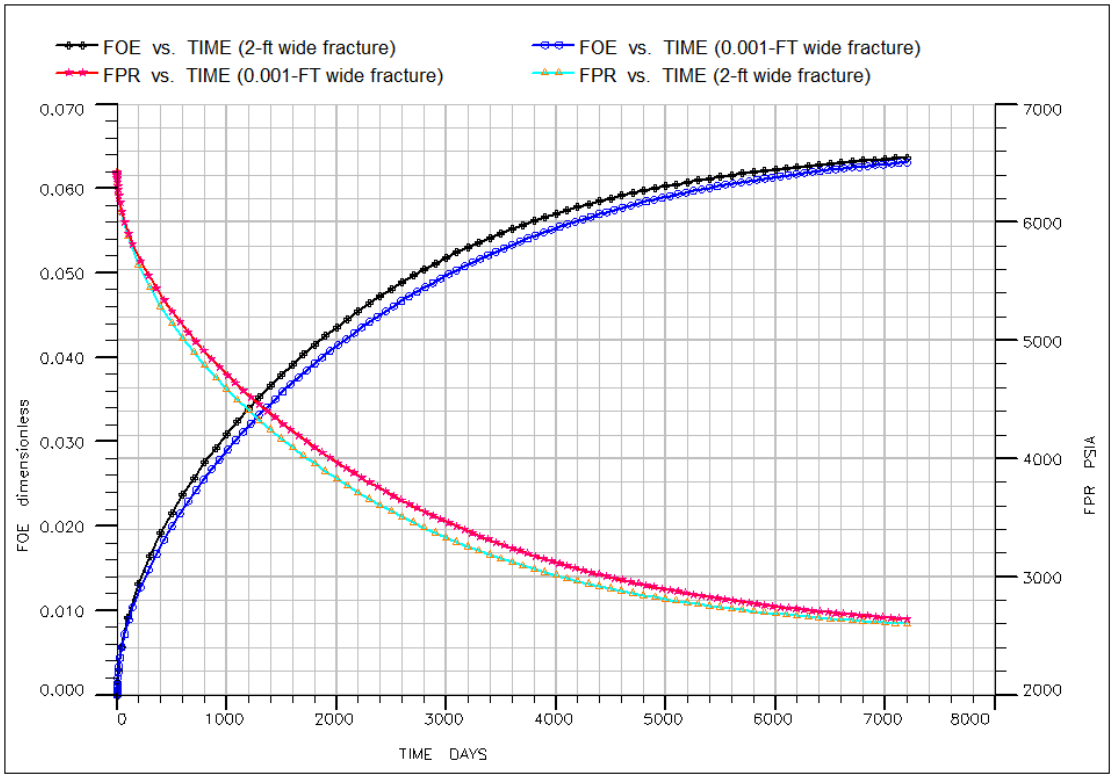

Figure 4.25 Oil RF and average reservoir pressure comparison

4.7 Vertical layers sensitivity study for basic reservoir model

We want to investigate the vertical grid blocks sensitivity for the basic reservoir model. Occasionally, in reservoir simulation, vertical grid sensitivity can cause some kind of error or do not match with production history. We will also investigate the vertical layers sensitivity study to find out whether the production performance is subject to vertical layers influence. The comparison scenarios we will use are 1 layer (21×55×1) and 7 layers (21×55×7) grid dimensions.

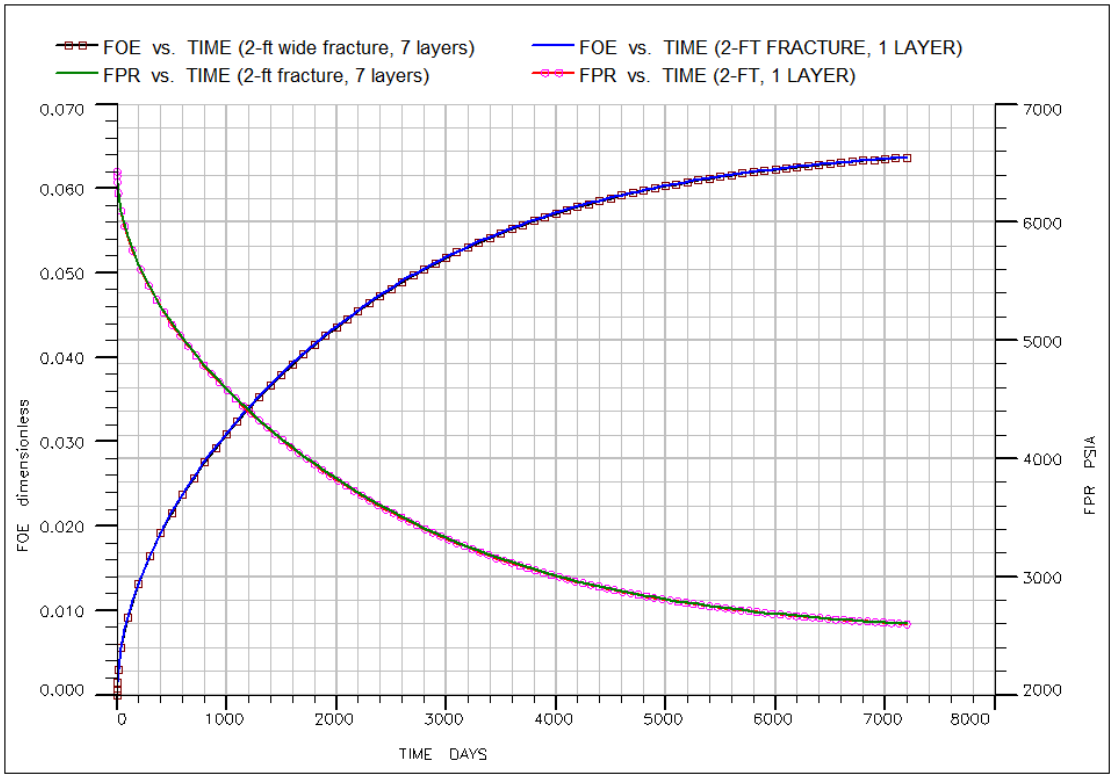

Figure 4.26 Oil RF and field average pressure comparison for vertical layer sensitivity study

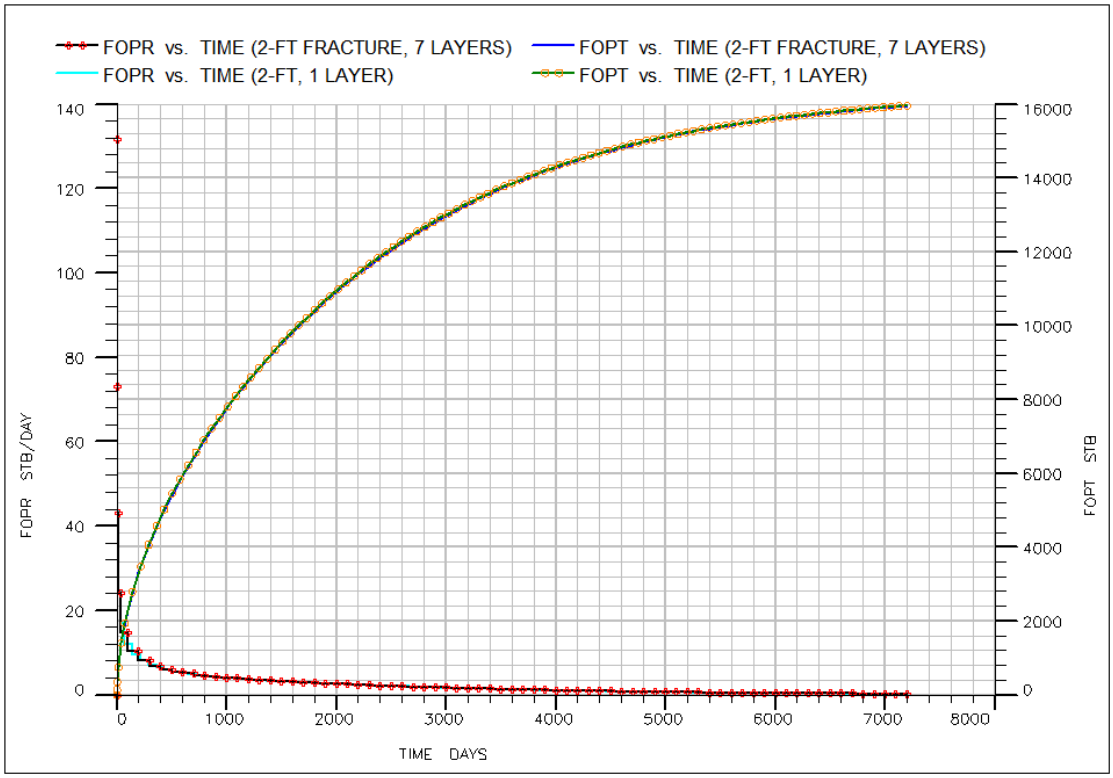

Figure 4.27 Cumulative oil production and oil production rate comparison for vertical layer sensitivity study

The results obtained from Fig 4.26 and Fig 4.27 show that the vertical grid-block layer sensitivity does not have too much effect on this primary recovery from simulation. The reason can be interpreted that the main fluid flow paths in shale oil reservoir rely on highly conductive fractures and vertical flow is not so dominating.

4.8 Vertical Permeability Sensitivity Study

Scenario 1: Kx=Ky=Kz=0.0001 md;

Scenario 2: Kx=Ky =0.0001 md, Kz=0.00005 md; (Kz=0.5Kx=0.5Ky)

Scenario 3: Kx=Ky=0.0001 md, Kz=0.00001 md; (Kz=0.1Kx=0.1Ky)

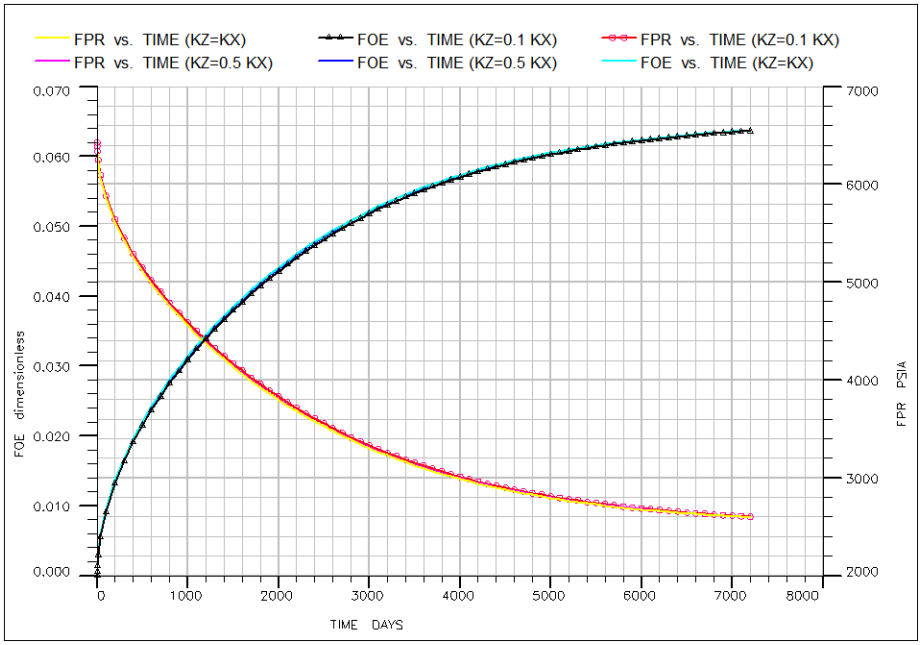

Figure 4.28 Oil RF and average reservoir pressure comparison for vertical permeability sensitivity study

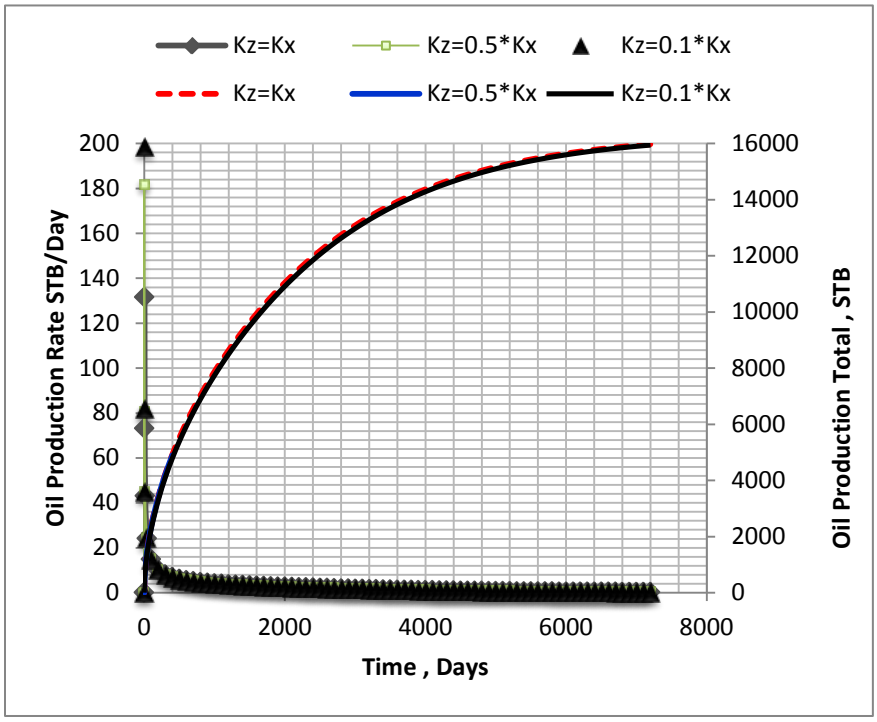

Figure 4.29 Cumulative oil production and oil production rate comparison for vertical permeability sensitivity study

The simulation results obtained from Fig 4.28 and 4.29 after 7,200 days of primary production show that oil production rate and average reservoir pressure decline at the same rates for different vertical permeability scenarios. Fig 4.28 shows that oil recovery is not affected by the matrix vertical permeability difference since most of the fluid drainage comes from the stimulated fracture networks that provide fluids path to the wellbore. The gravity drainage effect in shale oil reservoir can be even minor compared with conventional large permeability reservoirs. In shale oil reservoirs, the main transport of fluids takes places through the fractures, while the matrix blocks supply the fluids to the fractures.

At the depletion process, the fluids are primary produced out of the low-permeability matrix though the conductivity of fracture network. After completing these analyses for vertical permeability influence, we can draw a conclusion about the shale oil reservoir that vertical permeability difference does not have too much influence on well productivity. It is noted that the effective vertical permeability has a great impact on horizontal productivity in conventional reservoirs, which is characterized by anisotropy ratio. The productivity index increases as the anisotropy ratio decreases. Low vertical permeability will lead to a reduction of productivity because it will increase the anisotropy ratio B. Joshi (1991) presented the following expression for estimating the productivity index of a horizontal well accounted for the influence of the reservoir anisotropy, to give(Joshi, 1991):

$$J_h = \frac{0.00708hk_h}{\mu_o B_o \left[\ln(R) + \left(\frac{B^2 h}{L}\right)\ln\left(\frac{h}{2r_w}\right)\right]}$$

Where the parameter B as defined by:

$$B = \sqrt{\frac{k_h}{k_v}}$$

However, in shale reservoir it is widely accepted that most of the fluid flow comes from the stimulated fracture network without too much flow rate directly coming from matrix

flow. That can show why stimulated reservoir volume is vital important to shale oil/gas reservoir productivity.

Chapter 5

Miscible Cyclic Gas Injection Simulation

The model we consider is by using a 4-component system consisting of water, oil, dissolved gas and an injected solvent to replace a full compositional simulation without going to the complexity and expense of using a compositional model. This model assumes that hydrocarbon fluid composition remain constant during the simulation. All fluid properties are assumed to be determined by oil pressure and bubble point pressure only. The solubility of gas in the oil phase is taken into account by using the solution gas-oil ratio (R_s). While the compositional model is different, the reservoir fluid properties are dependent not only on the reservoir temperature and pressure but also on the compositions of the reservoir fluid which are not constant. Oil and gas phases are represented by multi-component mixtures in compositional model and we have to calculate the composition of each phase. To decide how many phases are present, we have to perform the flush calculation. We also have to calibrate the equation of state (EOS) for the determination of the physical properties of the oil and gas.

P. Ceragioli & EniSpA (2008) presents a paper that provided some guidelines about choosing the black-oil model or fast compositional model. Their paper shows that full compositional simulation reliability is dependent on a proper space-time discretization on a well characterized reservoir and by an equation of state with an enough detailed pseudo-composition of the reservoir fluid. In most cases, spurred by an effort to reduce the computing time people will use reduced pseudo-components and coarser grid blocks compositional model that implicitly assumes a too homogeneous reservoir. Therefore a robust black-oil model, properly calibrated on a well-defined compositional model, sometimes can be more reliable than a reduced compositional model that may make unknown assumptions for a significant amount of necessary composition data of the reservoir fluids (P.Ceragioli, 2008). We don't have too much detailed data about the composition of the reservoir fluids in Eagle Ford Shale. In our case, we would rather use a black-oil model than make lots of unknown assumptions for a significant amount of

composition data of the reservoir fluids. The purpose for us to use a black-oil model is self-evident by reducing the computing time and complexity, especially when we will meet 60 cycles of gas injection later on.

5.1 Feasibility of miscible flooding evaluation

In this paper, we talked about using cyclic gas injection for achieving a certain degree of miscibility to improve oil recovery. But we do not specify what kind of gas we need to meet our purpose. It can be LPG or propane which is injected as a primary slug to be followed by an extended period of lean gas injection, and it also can be CO_2 miscible flooding under MCM process. The important point is that we have to control the pressure above MMP at which in-situ miscibility can be achieved for a specified fluid system.

There are some limitations for the miscible flooding. The reservoir is required to be minimum depth to have the pressure needed to maintain the generated miscibility. The required pressure ranges from about 1,200 psi for the LPG process to 3,000~5,000 psi for the high pressure gas drive, depending on the oil composition (Satter, March 2008). In our work, the reservoir depth of Eagle Ford field can reach 9884 ft and the initial reservoir pressure is 6425 psi. We don't need to consider the minimum pressure required for miscibility problems.

5.2 Minimum Miscibility Pressure (MMP) Determination

The miscible displacement process can be defined as processes where the displacing fluid is miscible with the displaced fluid at conditions in which interfacial tension (IFT) is eliminated. Miscible displacing fluids are often referred as a solvent such as LPG or propane which is injected as a slug to be followed by an extended period of lean gas injection. Certain non-hydrocarbon gases such as carbon dioxide (CO_2) also could achieve miscible displacement of oil at pressures above MMP. If under the proper conditions, the injected gas is miscible in all proportions with oil, the oil is displaced efficiently leaving with little or no residual oil. The pressure at which the interfacial tension of displacing fluid and displaced fluids become zero is called as Minimum Miscibility Pressure (MMP).

5.2.1 Vaporizing-Gas displacement MMP determination

In the vaporizing gas displacement process, the injected fluid is generally a relatively lean gas in which it mostly consists of methane and other low molecular weight hydrocarbons.

The displacement processes were conventionally classified as first-contact miscible (FCM) or multiple-contact miscible (MCM) depend on the manner in which miscibility is achieved. An FCM process normally consists of injecting a relatively small primary slug that is miscible with the crude oil, followed by the injection of a larger and less expensive secondary slug. This concept of FCM flooding is very similar to the manner of polymer flooding we used in which small primary slug of polymer is injected, followed by large secondary slug of water. Clark (1958) discovered that methane and crude oil are partially soluble in one another and can't form 100% miscible displacement that usually requires higher pressure for miscibility than with CO_2. But under most reservoir conditions, LPG or propane can achieve good miscibility with the crude oil. On the other hand, it was also found that methane and propane will mix in all proportions and appear to be a single phase at reservoir conditions. The most economic and proper solution is by injection of a small primary slug of propane and followed by an extended period of secondary slug of methane injection. Then the FCM miscible displacement should be designed as a small primary slug of butane or propane displacing the crude oil. The butane or propane is displaced by methane

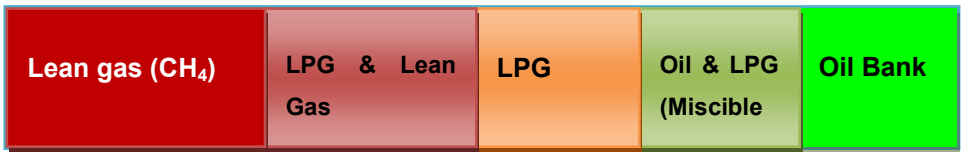

Figure 5.1 Miscible displacement

5.2.2 CO_2 miscible displacement MMP determination

Carbon dioxide flooding has a long history for recovering oil from reservoirs in which the initial pressure has been depleted through primary production and possibly waterflooding.

CO_2 miscible flooding can be treated as MCM process in which oil and injected solvent

are not miscible on first contact. However, there is compositions modification during the process between injected phase and oil phase. Through multiple contacts between the CO_2 and oil phase, intermediate and higher molecular weight hydrocarbons are extracted into the CO_2 rich phase. Under proper conditions, the CO_2 rich phase will achieve a composition that is miscible with crude oil. But this application depends on the reservoir pressure, temperature, and compositions of the crude oil and injected fluid. Local displacement efficiency of CO_2 flooding is closely correlating with the minimum miscibility pressure (MMP).

Another significant reason why industries are interested in CO2 is that the pressure required for miscibility with CO2 is usually significantly lower than the pressure required for miscible displacement with either natural gas, flue gas, or nitrogen.

MMP is commonly determined from empirical correlations based on experimental results or using EOS modeling for phase behavior calculations. EOS approach requires availability of a significant amount of composition data for the reservoir fluids. Such data often are not available, although they can be obtained from laboratory analyses which are somewhat laborious and time-consuming.

A variety of correlations for the prediction of MMP have been developed from regression of slimtube data. Yellig and Metcalfe (1980) developed a simple correlation for pure CO_2 injection in which MMP is correlated as a single curve as a function of temperature. They did not take account the compositions of reservoir fluids and pressure.

$$MMP_{pure} = 1833.717 + 2.2518055T + 0.01800674T^2 - \frac{103949.93}{T}$$

H.Yuan (2005) developed a new method for combining analytic multi-component multi-phase flow theory to calculate MMPs for a variety of reservoir temperatures, and injection compositions. Their paper shows that they used 41 experimental slimtube MMPs that were regressed to obtain a set of coefficients for the quadratic model. They also compared the calculated MMPs by using this new correlation to the estimated MMPs from the fit to the analytical MMPs to several other correlations and also with the

slimtube MMPs. The new correlation is superior to all others in predicting the slimtube MMPs (Yuan, 2004).

$$MMP_{pure} = a_1 + a_2 M_{C_{7+}} + a_3 P_{C_{2-6}} + \left(a_4 + a_5 M_{C_{7+}} + a_6 \frac{P_{C_{2-6}}}{M^2_{C_{7+}}}\right) T + \left(a_7 + a_8 M_{C_{7+}} + a_9 M^2_{C_{7+}} + a_{10} P_{C_{2-6}}\right) T^2$$

They found used fitting regression data to find the fitting coefficient:

$a_1 = -1.4634E + 03$, $a_2 = 0.6612E + 01$

$a_3 = -4.4979E + 01$, $a_4 = 0.2139E + 01$, $a_5 = 1.1167E - 01$, $a_6 = 8.1661E + 03$, $a_7 = -1.2258E - 01$, $a_8 = 1.2283E - 03$, $a_9 = -4.0125E - 06$ and $a_{10} = -9.2577E - 04$

Where MMP_{pure} is estimated MMP from the correlation for pure CO_2 injection. $M_{C_{7+}}$ is the molecular weight of C_{7+}, $P_{C_{2-6}}$ is the total molar percentage of C_2-C_6, and T is the reservoir temperature. $M_{C_{7+}}$ ranged from 139 to 319, $P_{C_{2-6}}$ ranged from 2.0 to 40.3%.

Table 5.1 MMPs calculation from this new correlation (at T=255 F)

	MMP at (Mc_{7+}=140)	160	180	200	220	240	260	280	300	320
$P_{C_{2-6}} = 2\%$	2266.6	3024.2	3573.1	3913.3	4044.6	3967.1	3680.8	3185.6	2481.6	1568.7
7%	2266.7	3023.0	3571.1	3910.6	4041.5	3963.7	3677.1	3181.7	2477.5	1564.5
12%	2266.7	3021.8	3569.1	3908.0	4038.4	3960.2	3673.4	3177.8	2473.4	1560.2
17%	2266.8	3020.7	3567.0	3905.3	4035.3	3956.8	3669.7	3173.8	2469.3	1556.0
22%	2266.8	3019.5	3565.0	3902.7	4032.2	3953.3	3665.9	3169.9	2465.2	1551.7
27%	2266.9	3018.3	3562.9	3900.0	4029.1	3949.9	3662.2	3166.0	2461.1	1547.5
32%	2266.9	3017.1	3560.9	3897.4	4026.0	3946.4	3658.5	3162.1	2457.0	1543.3
37%	2267.0	3015.9	3558.8	3894.7	4022.9	3943.0	3654.8	3158.1	2452.9	1539.0

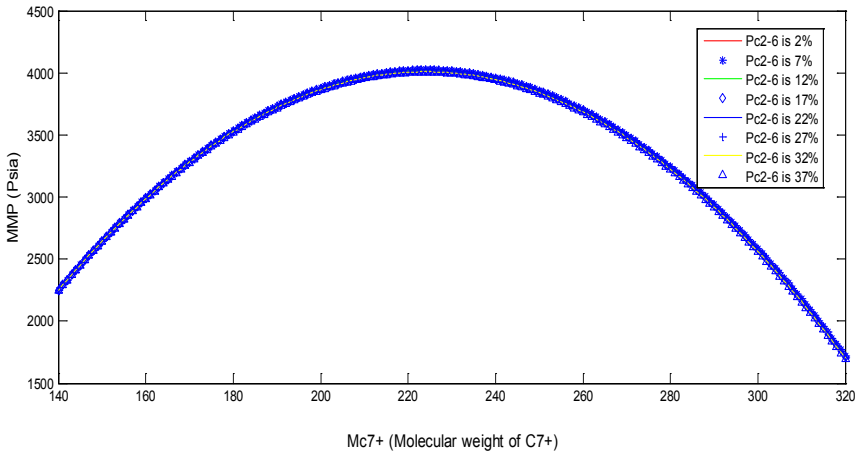

Figure 5.2 Calculated MMPs from new correlations

After we spent some efforts on investigating this new correlation, it turns out not so accurate a method because generally MMP should increase with the increasing molecular weight of Mc_{7+}, while it is not the case. MMP determination is closely dependent on the compositions of reservoir fluids. It is also easy to conclude from Fig 22 that MMP is not strongly dependent on the molecular percentage of C_{2-6} so that some other correlations do not include this part in the MMP prediction. Without acquisition of these data, we can make up some reasonable data about reservoir fluids to predict MMP with pure or impure CO_2 injection. The purpose for MMP determination is to acquire some criteria to control the reservoir pressure staying above the MMP to achieve miscible displacement.

5.3 Miscible Viscosity Calculation in the Simulator

In this work, we will keep on using the black-oil solvent model to model gas injection without going to the complexity and expense of using a compositional model. Todd and Longstaff proposed a method of simulating miscible displacement performance without reproducing the fine structure of the flow. Their method involves modifying the physical properties and flowing characteristic of the miscible fluids in a three-phase black-oil model. They introduced a mixing parameter ω, which determines the amount of miscibility between the miscible fluids within a grid block.

ECLIPSE uses the Todd-Longstaff model for effective oil and solvent viscosities calculation:

$$\mu_{o,eff} = \mu_o^{1-\omega} * \mu_m^{\omega}$$

$$\mu_{s,eff} = \mu_s^{1-\omega} * \mu_m^{\omega}$$

If $\omega = 1$ then $\mu_{o,eff} = \mu_{s,eff} = \mu_m$ where μ_m is the viscosity of a fully mixed oil-solvent system. Then formula to be used for μ_m is the 1/4th-power fluid mixing rule(E.J, 1963)

$$\left(\frac{1}{\mu_m}\right)^{1/4} = \frac{S_s}{S_n}\left(\frac{1}{\mu_s}\right)^{1/4} + \frac{S_o}{S_n}\left(\frac{1}{\mu_o}\right)^{1/4}$$

$$\mu_m = \frac{\mu_o \mu_s}{\left(\frac{S_s}{S_n}\mu_o^{1/4} + \frac{S_o}{S_n}\mu_s^{1/4}\right)^4}$$

$$S_n = S_o + S_s$$

$\mu_m$isthe unmixed viscosities of oil and solvent.

S_o, S_s, S_n are the oil saturation, solvent saturation and hydrocarbon phase saturation

ω is the Todd-Longstaff parameter.

The mixing parameter approach allows the case of a partial mixing zone to be modeled

by choosing an intermediate value of ω.

If $\omega = 0$then $\mu_{o,eff} = \mu_o$, $\mu_{s,eff} = \mu_s$ and each component has an effective viscosity equal to its pure value. If $\omega = 1$ then $\mu_{o,eff} = \mu_{s,eff} = \mu_m$ where μ_m is the viscosity of a fully mixed oil-solvent system.

For our case, we have oil, gas, water, and injected gas (solvent) which is a 4-phase component blackoil model. The following form for the effective oil and solvent viscosities is used in an immiscible simulator:

$$\mu_{o,eff} = \mu_o^{1-\omega} * \mu_{mos}^{\omega}$$

$$\mu_{s,eff} = \mu_s^{1-\omega} * \mu_m^{\omega}$$

$$\mu_{g,eff} = \mu_g^{1-\omega} * \mu_{msg}^{\omega}$$

Where

μ_o,μ_s,μ_g are the unmixed viscosities of oil, solvent and gas.

$\mu_{mos}$is the fully mixed viscosity of oil+solvent

$\mu_{msg}$is the fully mixed viscosity of solvent and gas

$\mu_m$is the fully mixed viscosity of oil+solvent+gas

ω is the Todd-Longstaff parameter.

The mixture viscosities μ_{mos}, μ_{msg}, μ_m are defined using the 1/4th power fluid mixing rule, as follows:

$$\mu_{mos} = \frac{\mu_o \mu_s}{\left(\frac{S_o}{S_{os}}\mu_s^{1/4} + \frac{S_s}{S_{os}}\mu_s^{1/4}\right)^4}$$

$$\mu_m = \frac{\mu_o \mu_s \mu_g}{\left(\frac{S_o}{S_n}\mu_s^{1/4}\mu_g^{1/4} + \frac{S_s}{S_n}\mu_o^{1/4}\mu_g^{1/4} + \frac{S_g}{S_n}\mu_o^{1/4}\mu_s^{1/4}\right)^4}$$

$$\mu_{msg} = \frac{\mu_s \mu_g}{\left(\frac{S_s}{S_{sg}}\mu_g^{1/4} + \frac{S_g}{S_{sg}}\mu_s^{1/4}\right)^4}$$

Where $S_n = S_{oil} + S_{solvent} + S_{gas}$

For example, at the pressure 2398, μ_o=0.337718 cp, μ_g=0.0192317, μ_s=0.0192317

Assume $\frac{S_o}{S_n} = 0.5, \frac{S_s}{S_n} = 0.2, \frac{S_g}{S_n} = 0.3$

$$\mu_m = \frac{0.337718 \times 0.0192317 \times 0.0192317}{(0.5 * (0.0192317)^{1/4} \times (0.0192317)^{1/4} + 0.2 * (0.337718)^{1/4} \times (0.0192317)^{1/4} + 0.3 * (0.337718)^{1/4} \times (0.0192317)^{1/4})^4}$$

=0.06268cp

This example shows when oil mixed with injected gas it can effectively reduce the system viscosity. The lean gas or CO_2 injected into the reservoir that can dissolve in the oil to lower its viscosity and improves the mobility of the oil mixtures.

In the vaporizing gas process, the injected gas (lean gas) composition is modified as it moves through the reservoir. The injected fluid is enriched in composition through multiple contacts with the oil, during which intermediate components in the oil are vaporized into the injected gas. Oil will absorb some of these components from the enriched gas and the oil will get lighter as it moves as more gas flows through it. Under proper conditions, all possible combinations of the injection gas and the lighter reservoir oil will result in a one-phase fluid, miscibility is achieved.

5.4 Cyclic gas injection applied after primary production modeling

In many miscible displacements, the gas is only miscible with the reservoir oil at high pressure. Typically the gas oil capillary pressure reduces with increasing pressure, and

only when it has reduced to zero can the two fluids be miscible. When the block pressure is so much lower than the minimum miscibility pressure (MMP) that ω should be 0, solvent is displacing oil immiscibility. As the block pressure increases, this mixing parameter reaches its maximum value ω_{omax} at the MMP. However, there are only limited amount of published literatures to assist for estimation of ω_{omax}. When no better data is available, the CMG manual recommends a value in the range of 0.5 to 0.8 as a first approximation.

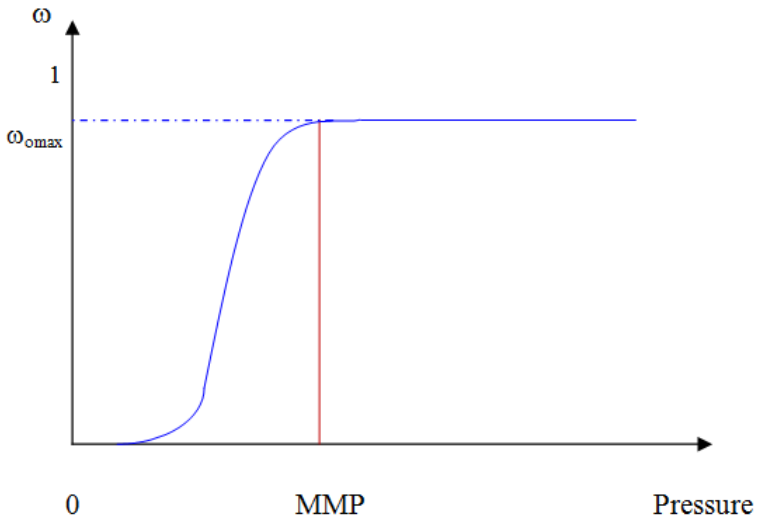

Figure 5.3 ω versus P

In the simulator it provides the option to model the pressure dependent miscibility that controls the transition between immiscible and miscible displacement as a function of oil pressure. If this keyword is not present in miscible runs, miscible displacement is assumed to occur at all pressures. In CMG, we can input the pressure dependent miscibility tables in the PVTS section.

We set up an oil pressure which should be above MMP for miscibility to be a value that approaches 1. In our work we chose ω_{omax} as 0.74 as suggested by the sample data by CMG.

5.4.1 Reservoir fluids and injected solvent properties

The reservoir fluid selected for this study was that from Eagle Ford Shale reservoirs. The density of original gas in place is 0.06108 lb/ft^3 (Specific Gravity=0.8). Oil compressibility is 1*10E-5 psi-1 as we stated before. The composition of injector fluid can be specified as 77% C1, 20% C2, 3% C6. Most of the injected gas should be C1 with trace amounts of C2 and C6. The injected solvent density is 0.06248 lb/ft^3, which is close to the density of original solution gas. Gas and solvent mixing parameter OMEGASG was set as 0.77. When there is free gas (chase gas or original gas in place) this parameter determines the mixing of free gas with solvent. Minimum solvent saturation MINSS was set at 0.2. The minimum solvent saturation is the solvent saturation in the presence of gas below which mixing is not possible.

5.4.2 Well Operating Constraints

We specified the maximum surface solvent rate as 800 Mscf/day for injector and the maximum allowable bottom-hole injection pressure is 7000 psi, the minimum BHP for producer is 2500 psi. There are two limiting controls for the injector, that is, upper injection rates and upper injection pressure. The injector will automatically change its mode of control whenever the existing control mode would violate one of these limits. In other words, the well will inject 800 Mscf/day of solvent until the bottom-hole pressure exceeds 7000 psi. The well's control mode will then change automatically to maintain a constant BHP of 7000 psi injection pressure. The reason why we choose 800Mscf/day for gas injection rate is because we went through several simulations cases before about the gas injection in shale reservoirs. We know that if the injection rate is set too high it will result in the simulator convergence issue.

5.5 Design of Well Schedule

Well Schedule 1: 10950 days (30 years) of Primary production+60 cycles of gas injection, each cycle including: 100 days injection and 100 days production.

The process of cyclic solvent injection is sometimes called "huff and puff" as EOR

method used in heavy oil reservoirs. This is a cyclic process in which the same horizontal well is used for injection and production. The cyclic gas injection process is applied after 10950 days of primary production. Each cycle consists of 100 days injection followed by 100 days production, which will be repeated 60 cycles. As what is the optimized cycle schedule for recovering the most oil with least time, it is a sort of trial and error process and we will go through several cycle schedules for making the best decision.

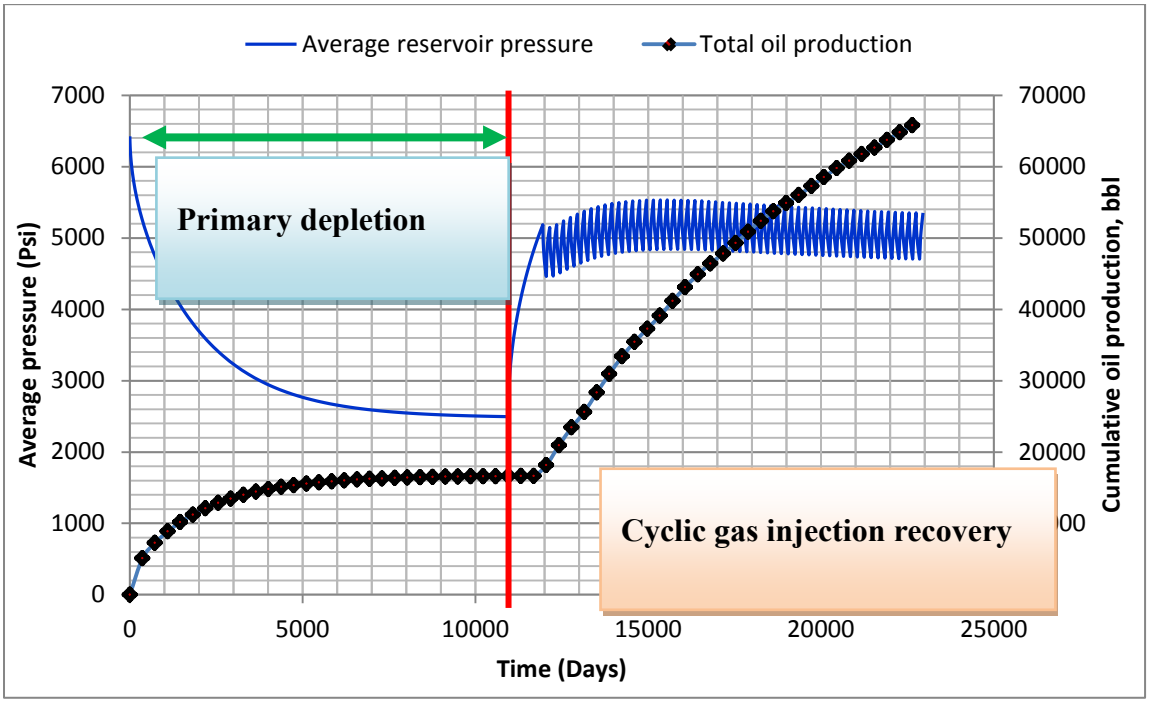

Figure 5.4 Cumulative oil production and average reservoir pressure variations for cyclic gas injection

In Fig 5.4 there are some time lagged for cumulative oil production behind the average reservoir pressure because during this time it is implementing the gas injection so that there are no incremental oil producing yet. We implement 1000 days gas injection for the first cycle in order to increase the reservoir pressure to a high value, increasing from 2450 psi to more than 5000 psi. In the following repeating 60 cycles of gas injection, the average reservoir pressure variations almost follow the same magnitude of fluctuation for each cycle.

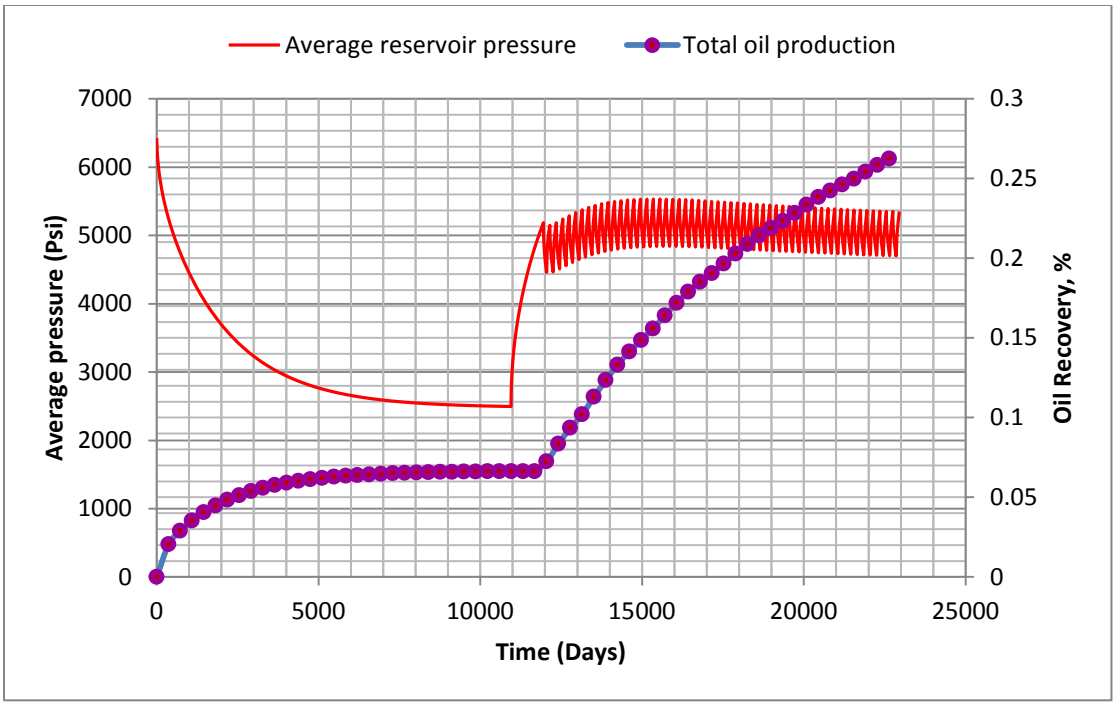

Figure 5.5 Enhanced oil recovery for implementing cyclic gas injection

Fig 5.5 above shows that primary recovery factor is 6.5% which is not a good inspiring number after spending enormous cost on hydraulic fracturing. But after we start the 60 cycles of gas injection process, finally it gets 27.3% oil recovery which is almost 4 times of primary recovery.

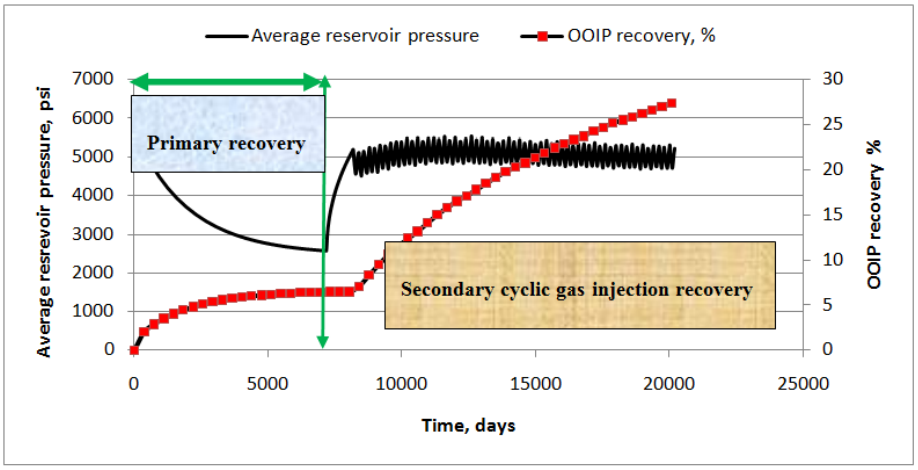

Figure 5.6 Enhanced oil recovery for implementing cyclic gas injection

It should be noticed that there are almost no differences for primary recovery from 7200 days of primary production (Fig 5.6) and 10950 days of primary production (Fig 5.5). Fig 5.6 shows the case of 7200 primary production followed by the same 60 cycles of gas injection which acquires 6.5% for primary recovery and 27.34% for overall recovery. In the following cases, we will all use 7200 days as the primary depletion period.

Table 5.2 Field cumulative oil production and solvent injection

Well Schedule 1 Each cycle schedule (100 days injection, 100 days production), for 60 cycles		
	Oil(MSTB)	Solvent (MMSCF)
Cumulative Production	68.593	1797.6
Cumulative Injection	NA	1934.5
Current Fluids In Place	182.23	135.52

Table 5.3 Field OOIP recovery after miscible cyclic gas injection

Mechanism	OOIP Recovery (%)
Primary Recovery	6.5
Miscible cyclic gas incremental recovery	20.84
Overall Recovery	27.34
Remaining	72.66

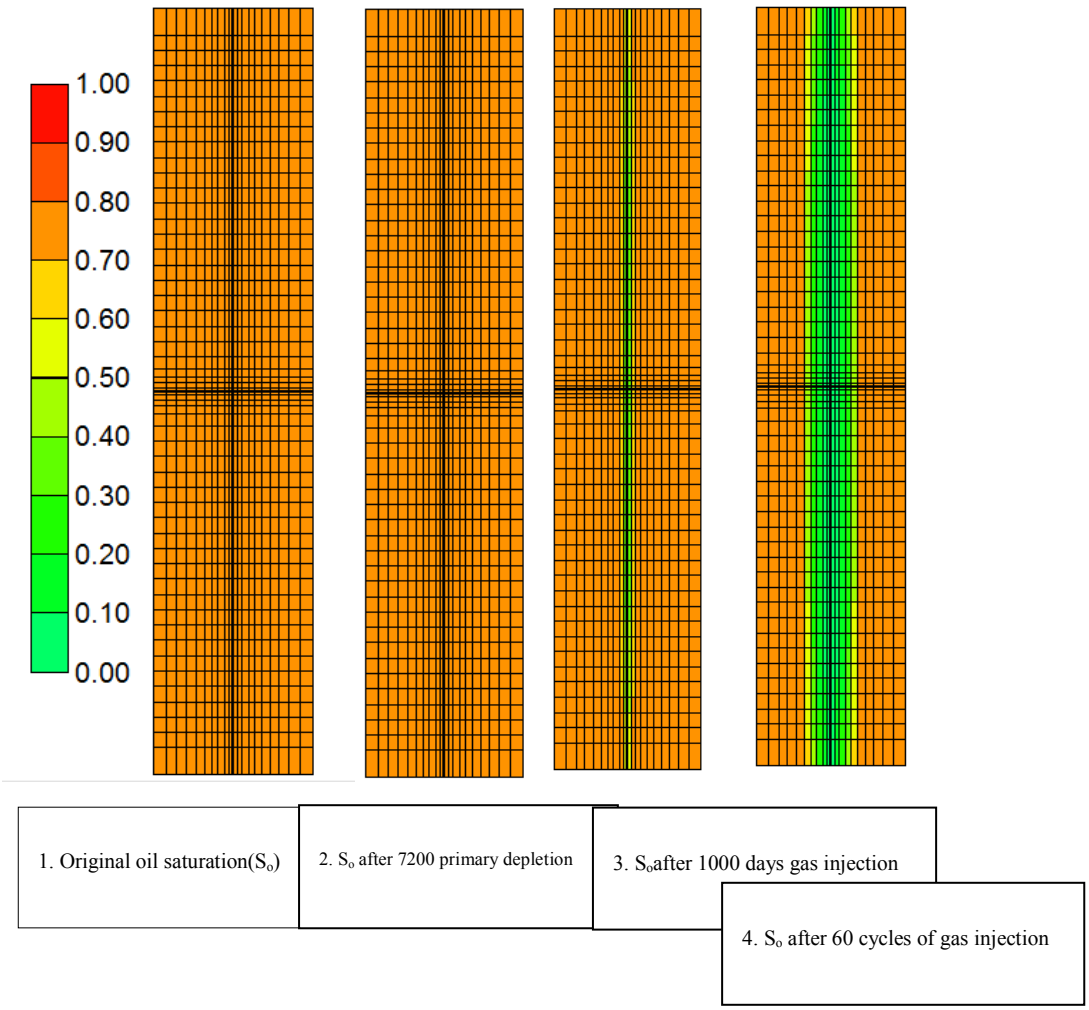

Figure 5.7 Oil saturation distribution during cyclic gas injection process

In shale oil reservoirs, the main transport of fluids takes place through the fractures, while the matrix blocks supply the fluids to the fractures. By implementing cyclic gas injection, the injected solvent pushes oil away from the fracture but at the same time acts as pressure maintenance for building up the reservoir pressure (Fig 5.8). As shown from Fig 5.7 oil saturation distribution, oil is pushed away from the fracture during the gas injection period. More importantly, if the reservoir pressure stays above MMP, the injected solvent will be fully miscible with oil, which can greatly reduce the oil viscosity and make the system much more mobile. When the production process begins, the mixed oil and solvent will flow out of the matrix into the highly conductive fracture, then into the wellbore. However, in a 200 ft (X direction) wide shale oil reservoir model, the stimulated oil volume (mobile oil grid blocks) by cyclic gas injection processes is only 35

ft far away from the fracture, symmetrically (Shown by Fig 5.7). If we can think of ways to enhance the macroscopic displacement efficiency, it will bring a revolution to shale oil reservoirs development.

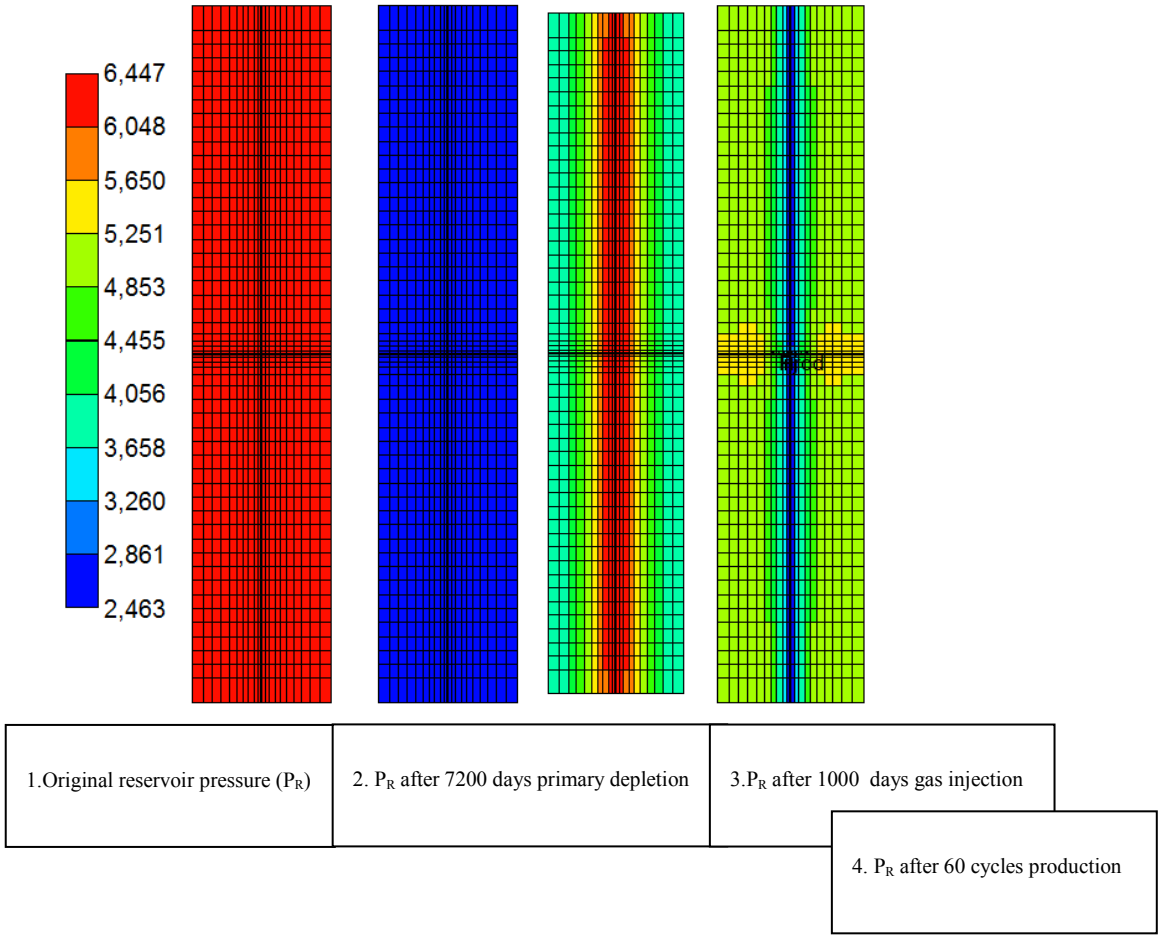

Figure 5.8 Reservoir pressure distribution during the cyclic gas injection process

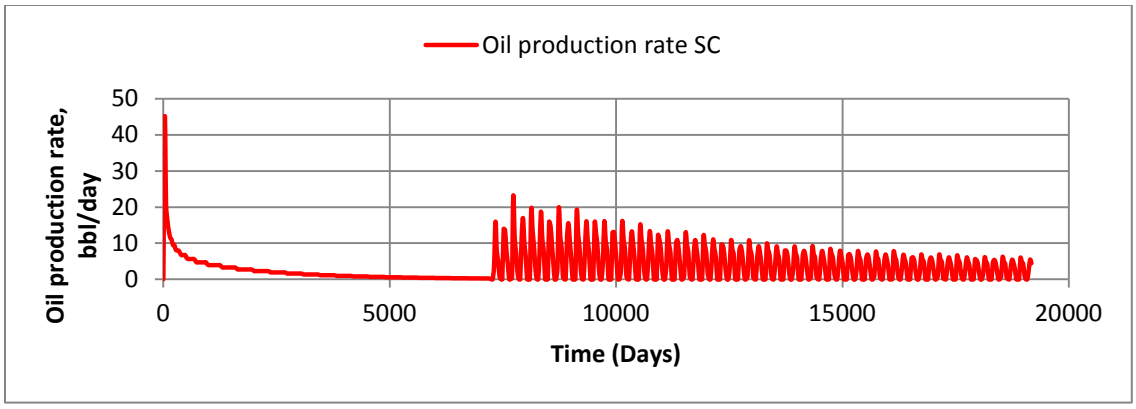

Figure 5.9 Oil production rate for well schedule 1

Fig 5.9 shows that oil production rate is decreasing with the increasing of cyclic gas injection application. It should be noticed that if we increase the injection time and production time for each cycle, which would not be a good option. Because gas injection rate or oil production rate decrease very fast within a particular cycle after a short period of time.

Well Schedule 2: 7200 days of Primary production+30 cycles of gas injection

Each cycle including: 200 days injection and 200 days production

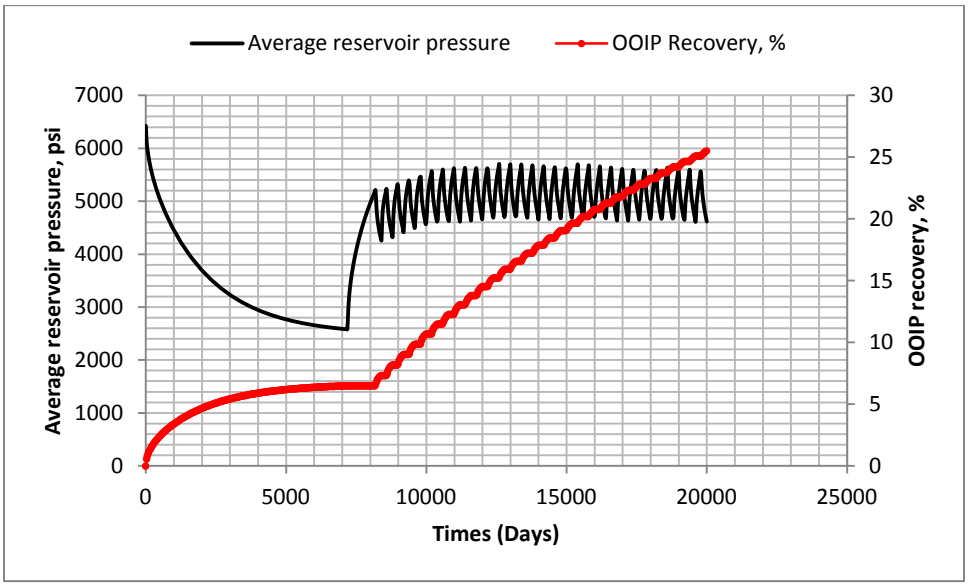

Figure 5.10 OOIP recovery and P_{av} versus time

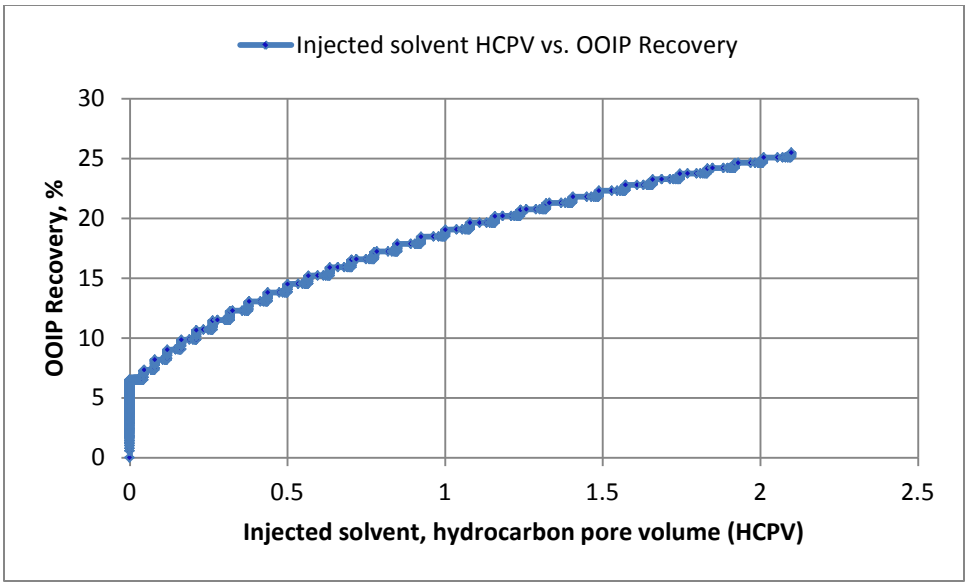

Figure 5.11 Injected solvent HCPV versus OOIP recovery

Note: Hydrocarbon pore volume (HCPV)=$V\phi(1-S_{wc})$=$200\times1000\times200\times0.06\times(1-0.2)=1{,}920{,}000$ ft^3

Table 5.4 Field cumulative oil production and solvent injection

Well Schedule 2 Each cycle schedule (200 days injection, 200 days production), for 30 cycles		
	Oil(MSTB)	Solvent (MMSCF)
Cumulative Production	63.979	1041.7
Cumulative Injection	NA	1126.5
Current Fluids In Place	186.84	84.412

Table 5.5 Field OOIP recovery after miscible cyclic gas injection

Well schedule 2	
Mechanism	OOIP Recovery (%)
Primary Recovery	6.5
Miscible cyclic gas incremental recovery	19
Overall Recovery	25.5
Remaining	74.5

Well Schedule 3:7200 days of Primary production+120 cycles of gas injection

Each cycle consists of 50 days injection and 50 days production

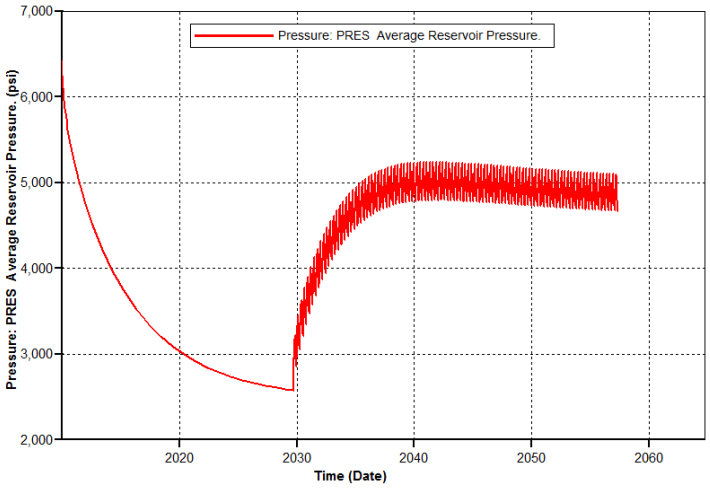

Figure 5.12 Average reservoir pressure versus time

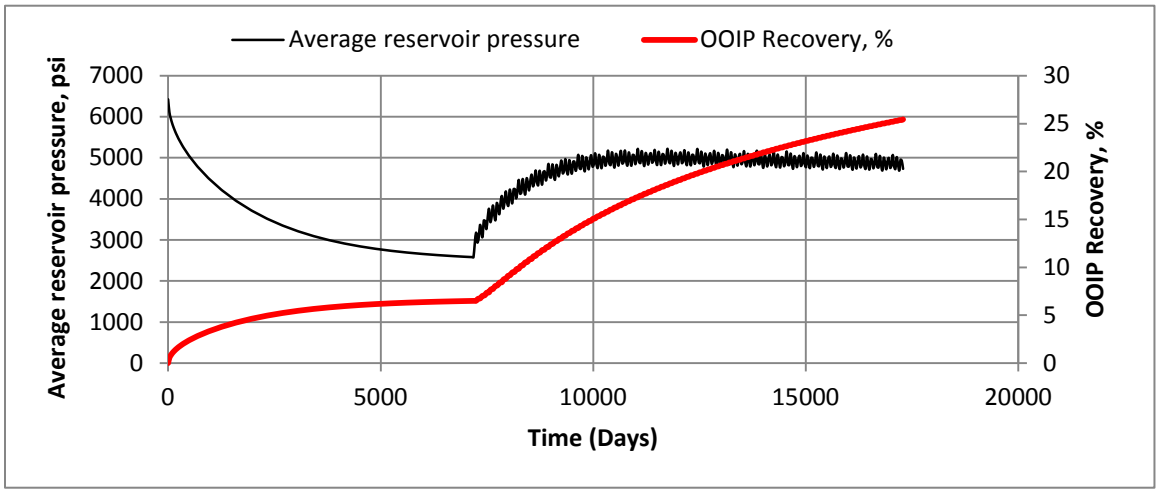

Figure 5.13 OOIP recovery and P_{av} versus time of schedule 2

Table 5.6 Field cumulative oil production and solvent injection

Well Schedule 3 Each cycle schedule (50 days injection, 50 days production), for 120 cycles		
	Oil(MSTB)	Solvent (MMSCF)
Cumulative Production	63.850	2205.0
Cumulative Injection	NA	2301.0
Current Fluids In Place	186.98	93.319

Table 5.7 Field OOIP recovery after miscible cyclic gas injection

Well schedule 3	
Mechanism	OOIP Recovery (%)
Primary Recovery	6.5
Miscible cyclic gas incremental recovery	18.93
Overall Recovery	25.43
Remaining	74.57

Well Schedule 4: 7200 days of primary production+60 cycles of gas injection

Each cycle consists of 50 days injection and200 days production

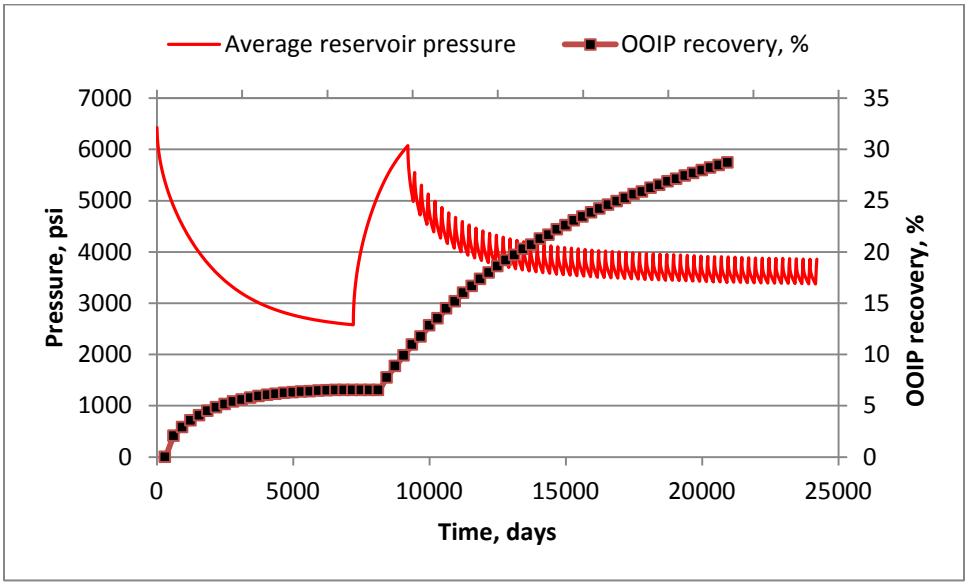

Figure 5.14 OOIP recovery and P_{av} versus time of schedule 2

Table 5.8 Field cumulative oil production and solvent injection

Well Schedule 4 Each cycle schedule (50 days injection, 200 days production), for 60 cycles		
	Oil(MSTB)	Solvent (MMSCF)
Cumulative Production	71.878	1704.5
Cumulative Injection	NA	1817.8
Current Fluids In Place	186.98	111.67

Table 5.9 Field OOIP recovery after miscible cyclic gas injection

Well schedule 4	
Mechanism	OOIP Recovery (%)
Primary Recovery	6.5
Miscible cyclic gas incremental recovery	22.15
Overall Recovery	28.65
Remaining	71.35

Well production performance summary for different well schedules

Well schedule 1: Total project duration =7200+1000+200*60=20200 days

(1000 days for first cycle of gas injection)

Well schedule 2: Total project duration =7200+1000+400*30=20200 days

Well schedule 3: Total project duration =7200+100*120=19200 days

Well schedule 4: Total project duration =7200+1000+250*60=23200 days

Table 5-10Well production performance summary for different well schedules

	Injection time in each cycle (Days)	Production time in each cycle (Days)	Cycles used	Total project duration (Days)	Overall OOIP Recovery, %
Well schedule 1	100	100	60	20200	27.34
Well schedule 2	200	200	30	20200	25.5
Well schedule 3	50	50	120	19200	25.43
Well schedule 4	50	200	60	23200	28.65

Well Schedule 5

After completing the analysis for those different cyclic schedule variations, it is realized that the differentials in cyclic schedules do not have too prominent effects on the ultimate OOIP recovery. Further improvement of oil recovery in shale oil reservoirs can't dependent on manipulations of cyclic well schedules. Basically, the macroscopic sweep efficiency of these four different cyclic schedules is almost the same. The stimulated oil volume by cyclic gas injection remains near to the fracture as we analyzed in well schedule 1.

However, as the production performance in unconventional reservoirs is different from the conventional reservoirs, care should be taken when we design the well schedule or seek for the optimization of cycle schedule. Fig 5.15 and 5.16 are the simulation results for the case of 6 cycles of solvent injection, each cycle consists of 1000 days of solvent injection and 1000 days of production. The reason underlying why we picked up 100 days or 200 days for injection or production period in each cycle through *well schedule 1 to 4* can also be interpreted by Fig 5.15 and 5.16. Fig 5.15 shows that the solvent injection rate in shale reservoirs declines very quickly. Fig 5.16 intends to show that oil

rate also decreases very quickly in shale reservoirs in similar to solvent injection rate. Elongating the injection or production period in each cycle is not helpful to improving the well production performance, because the injection rate declines so fast that it keeps quite low at most of the time during 1000 days injection period. By utilizing longer injection or production period in each cycle can be considered as wasting the injection time or production time. As we can't maintain 800 Mscf/day injection rate for a long time, therefore, it is suggested to use relatively short period of injection or production period in each cycle.

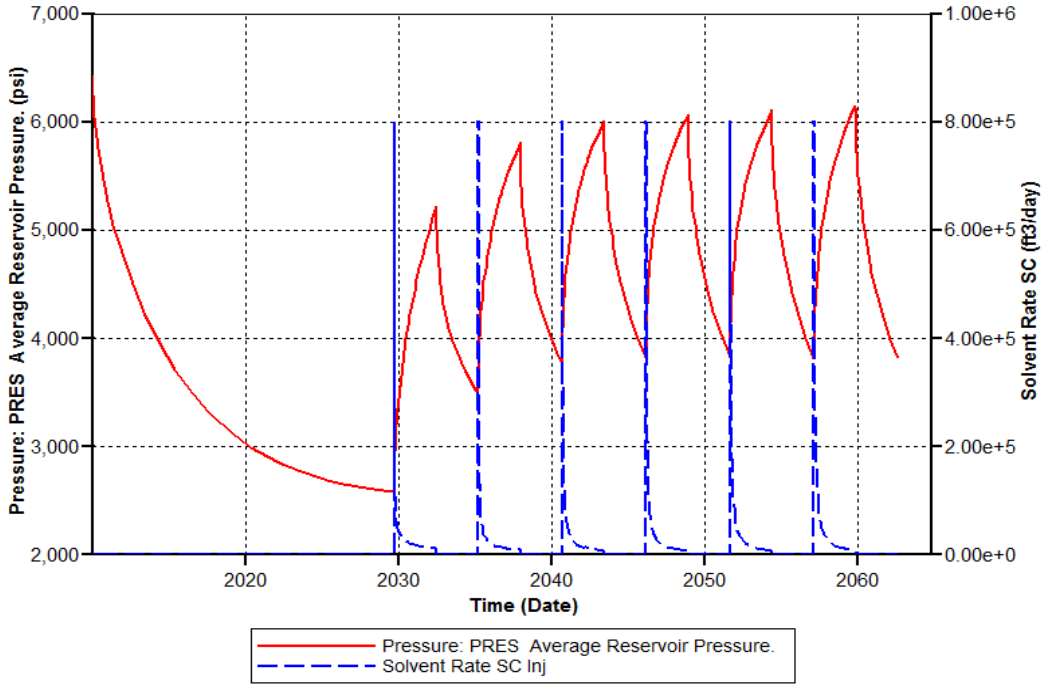

Figure 5.15 Injection rate variations during the cyclic gas injection process (each cycle consists of 1000 days production and 1000 days injection, lasting for 6 cycles)

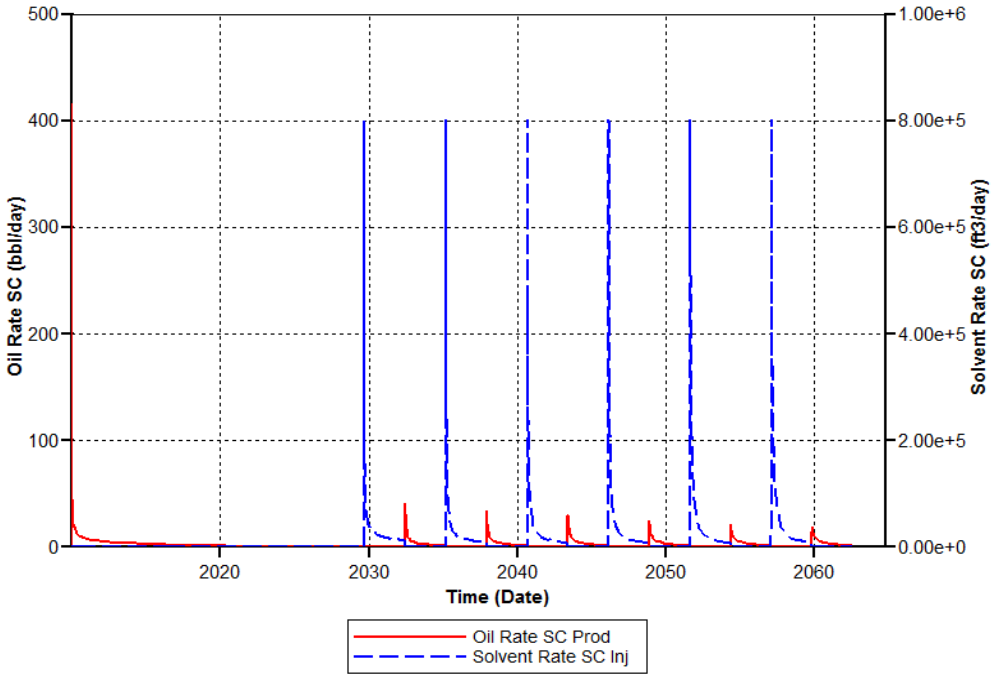

Figure 5.16 Oil production rate vs. Solvent injection rate during the cyclic injection process

However, the following case shows another complicating cyclic gas injection process that is able to cause huge magnitude of reservoir pressure fluctuations. At the beginning phase, we implement 10 cycles of steady production (each cycle consists of 100 days injection and 100 days production). At the following stage, we want to enhance the reservoir pressure into a higher level which can be achieved by 1000 days of gas injection. Later on, it includes 6 big cycles of decaying (each cycle including 200 days production and 50 days injection) and booming (each cycle including 100 days injection and 50 days production), as shown by Fig 5.17. The total project duration are 24600 days.

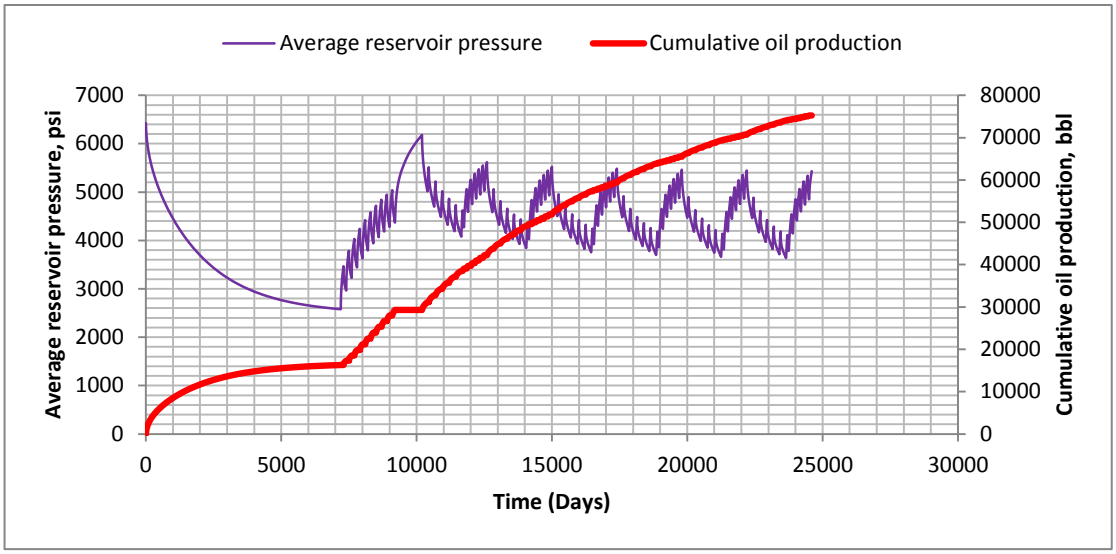

Figure 5.17 Cumulative oil production and P_{av} versus time

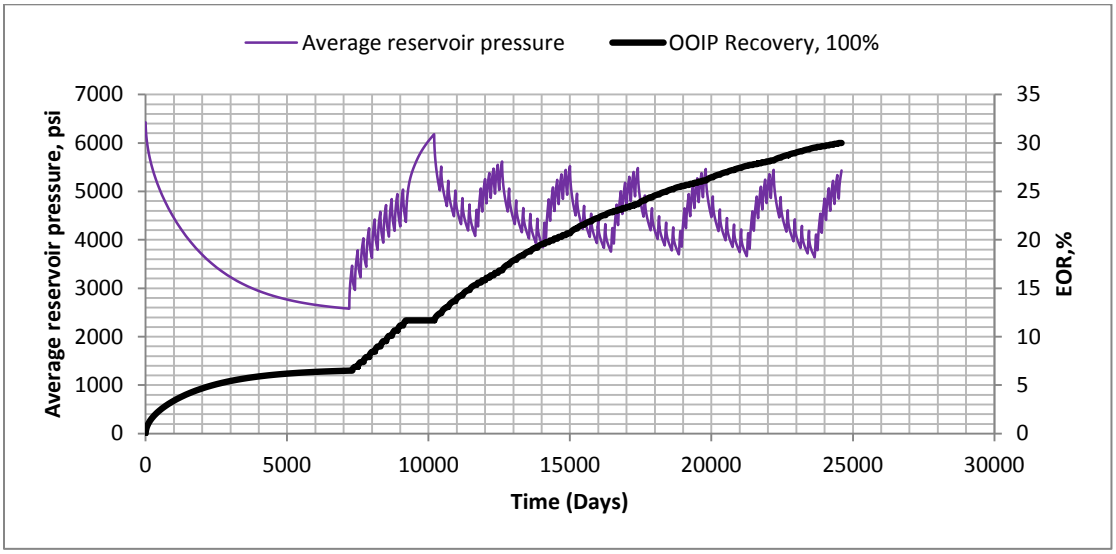

Figure 5.18 OOIP recovery and P_{av} versus time

Table 5.11 Field cumulative oil production and solvent injection

Multiple cyclic gas injection		
	Oil(MSTB)	Solvent (MMSCF)
Cumulative Production	75.237	2258.4
Cumulative Injection	NA	2414.1
Current Fluids In Place	175.59	153.31

Table 5.12 Field OOIP recovery after miscible cyclic gas injection

Well schedule 4	
Mechanism	OOIP Recovery (%)
Primary Recovery	6.5
Miscible cyclic gas incremental recovery	23.45
Overall Recovery	29.95
Remaining	70.05

After we complete these five different cycle schedule simulations and analyses, it can be concluded that improving oil recovery in shale oil reservoirs can't rely on optimization the cycle schedules. Cycle schedule variations do not bring too much prominent influence on ultimate oil recovery.

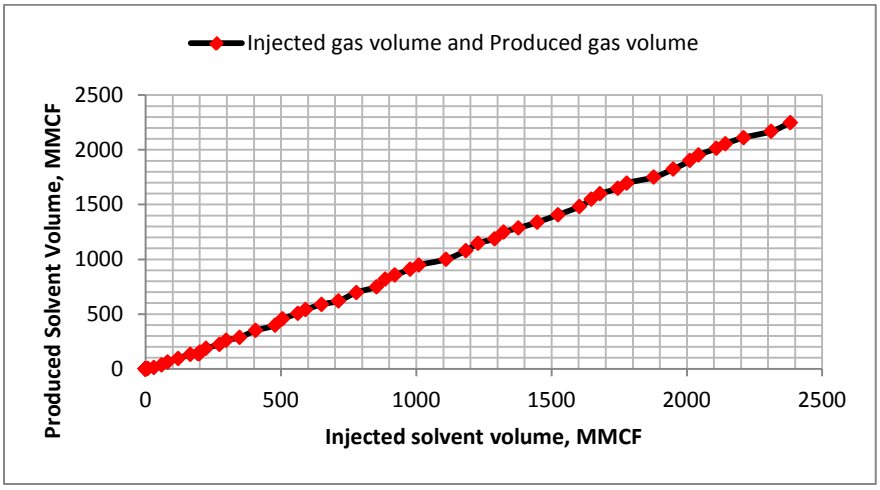

Figure 5.19 Injected solvent volume versus produced back solvent volume

At the wellhead, injected gas is typically composed of a mixture of propane and methane and recycled gas from gas plant operations. Some projects were abandoned due to key considerations of high cost of compression and capture of the injection gas or shortage of injection gas source. Fig 5.19shows the gas being produced back is almost amount to the injected gas volume which is a good characterization for recycling this gas for reinjection. The produced solvent is separated and recompressed for reinjection along with additional volumes of newly-purchased solvent. As produced solvent volume is almost equivalent to the injected gas volume, it will save a lot of cost for purchasing new gas.

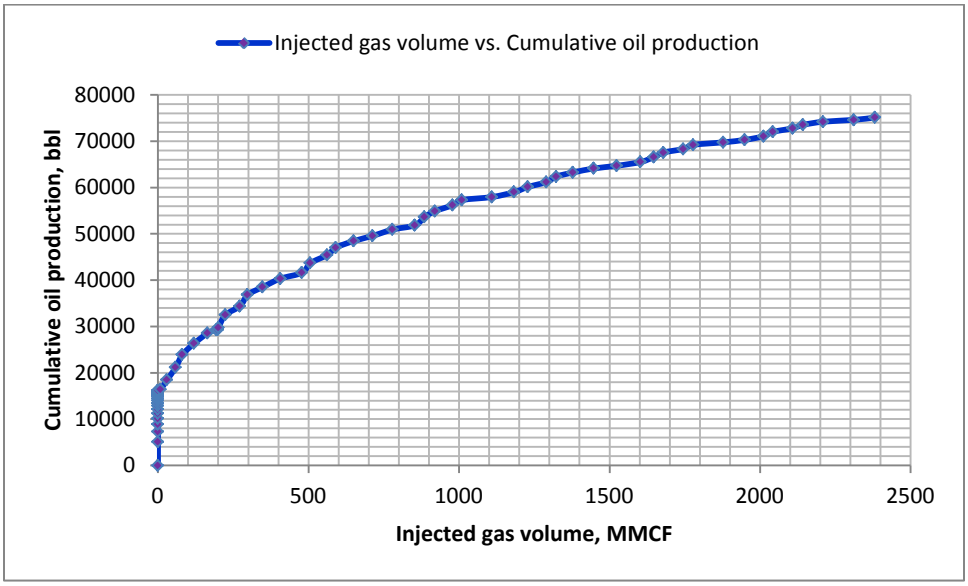

Figure 5.20 Injected gas volume versus cumulative oil production

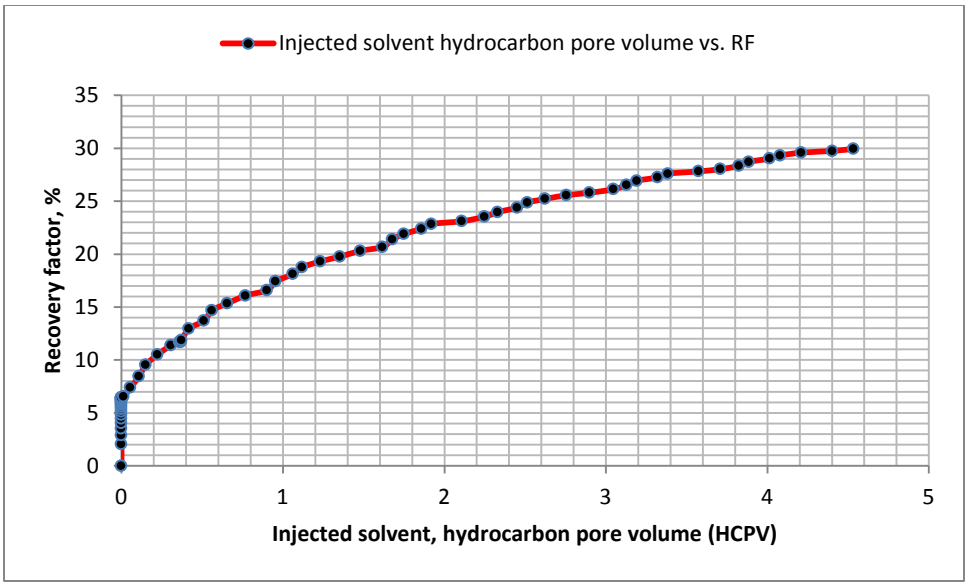

Figure 5.21 Injected solvent HCPV versus OOIP recovery

As shown by Fig 5.21, Oil recovery is achieved 30% after injection of 4.5 hydrocarbon pore volume of solvent. Compared with well schedule 2, in which injection of 2.1 hydrocarbon pore volume of solvent and oil recovery is 25.5%, 4.5 HCPV of solvent injection for the purpose of pursing 30% recovery may not be an economic option.

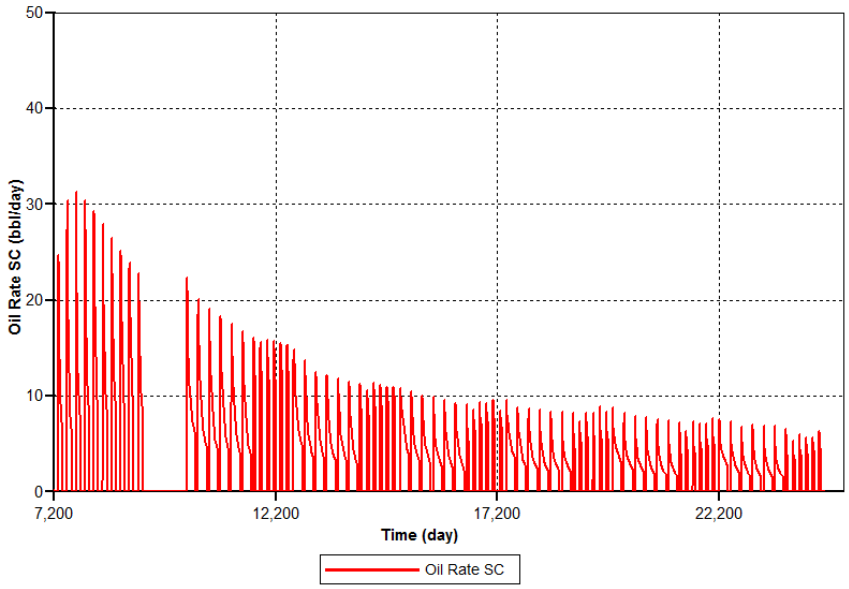

Figure 5.22 Oil production rate versus time (well schedule 5)

Fig 22 shows that oil production rate is declining with the increasing cycles of gas injection processes.

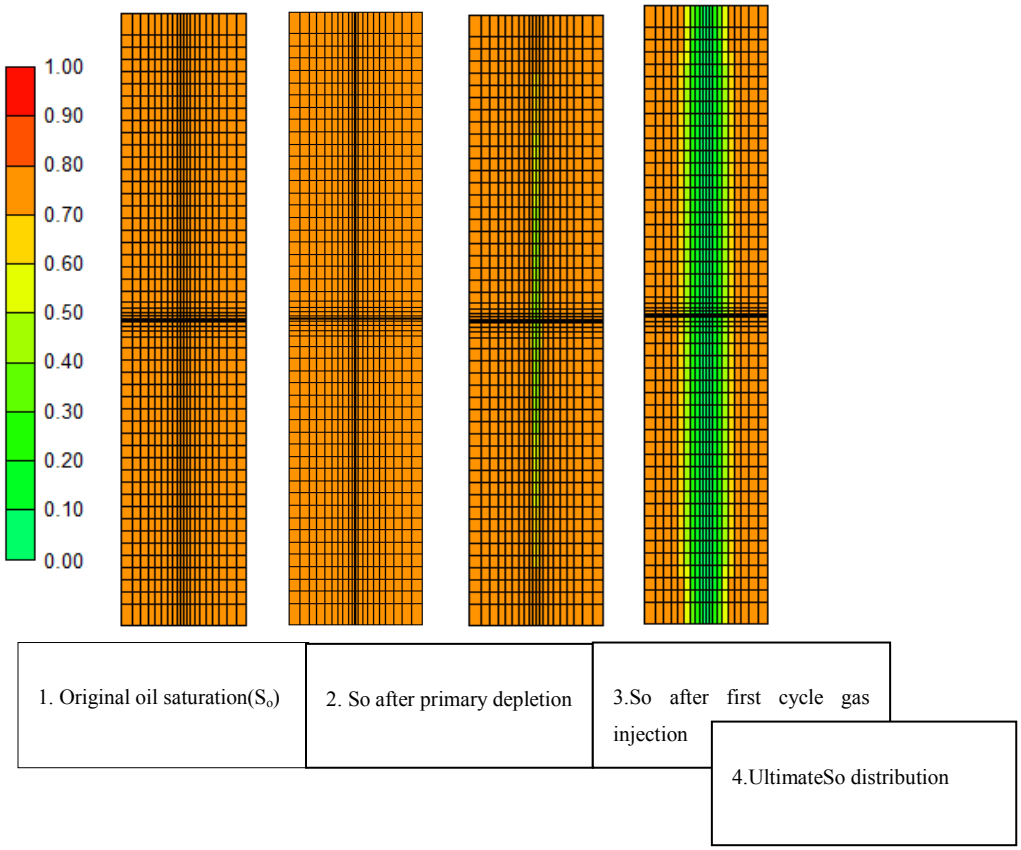

Figure 5.23 Oil saturation variations during cyclic gas injection process (well schedule 5)

In a 200 ft (X direction) wide shale oil reservoir model, the stimulated oil volume by cyclic gas injection processes isalmost45 ft far away from the fracture, symmetrically (As shown by Fig 5.23). While overall displacement efficiency in a process is defined as a product of volumetric sweep efficiency E_v and the microscopic efficiency E_D.

$E= E_v E_D$.

Miscible flooding implies that the interfacial tension between the displacing fluid and oil becomes zero and the residual oil saturation in the swept region is nearly 0. In a miscible flooding, the microscopic displacement efficiency, E_D is generally approaching unity. So oil recovery in miscible displacement primarily depends on the volumetric sweep

efficiency, the volume of reservoir contacted by the injected fluid. If we can think of ways to increase the macroscopic displacement efficiency by miscible cyclic gas injection technique, it will bring a shale oil reservoirs revolution.

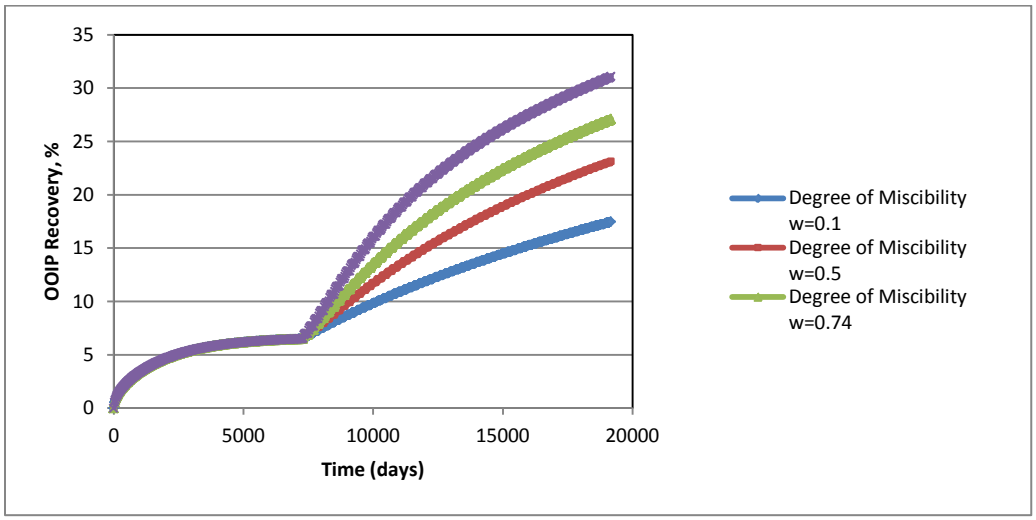

Figure 5.24 Different degree of miscibility effect on the ultimate OOIP recovery

This graph was plotted on the basis of well schedule for each cycle consisting of 100 days of gas injection and 100 days of well producing. It shows the effect of the degree of miscibility on the ultimate OOIP recovery.

The technique of cyclic gas injection can avoid some sorts of conventional miscible flooding problems including viscous fingering results in poor vertical and horizontal sweep efficiency, large quantities of expensive products required and the solvent being trapped and not recovered (Shown by Fig 5.19, most injected solvent was produced back). In this cyclic gas injection project, we only drill a horizontal well at the same time implementing hydraulic fracturing to obtain 10 hydraulic fractures for efficient production. Therefore, the viscous fingering and early breakthrough of injected gas would not occur by using this technique. As shown in Fig 5.19, there is almost no solvent trapped such that more oil will be produced as solvent will mix fully with oil acting much like a thinning agent. It becomes more mobile to flow into the wellbore.

5.6 Economic Analysis of the Cyclic Gas Injection Process

Table 5.13 shows the results of cumulative oil production and solvent injection from the entire horizontal well which consists of 10 hydraulic fractures for well schedule 1. Table 5.14 presents results of the economic analysis for the secondary recovery. The work interest and revenue interest are assumed to be 100%. The adiabatic horsepower required to compress 1 MMscfd of a 0.8 gravity natural gas to 7000 psi can be calculated by the use of an analytic method (Kelkar, 2008). Most of the capital expenses invested at the initial stage including horizontal well construction (drilling and completion) and fracturing execution cost. The primary oil recovery is 6.5% only. If we assume the oil price is $100 per barrel and gas price is $3 per MSCF, evaluation of net revenue from the secondary recovery can be done by excluding the initial capital expenses such as horizontal well construction cost and fracturing treatment costs. From the economic analysis of the secondary cyclic gas injection recovery process, more than $48 million net revenue (not NPV) will be obtained for the horizontal well if without considering any other costs. This economic evaluation maybe not exactly accurate but it gives us an assessment that if implementing secondary cyclic gas injection in shale oil reservoirs could lead to a profitable project.

Table 5.13 Cumulative oil production and solvent

A horizontal	Oil(M	Solvent
Cumulative	685.93	17976
Cumulative	NA	19345
Current Fluids In	1822.3	1355

Table 5.14 Economic analysis for the secondary recovery

Economic parameters	
Secondary incremental oil production (Barrels)	524,211.7
Incremental oil revenue ($100/Barrel), $	52,421,170
Horsepower required for compressing gas to 7000 psi (Kilowatthour)	1,180,022
Electricity charges (12cents/KWH), $	141,602.6
Gas purchasing for lost gas (MMSCF)	1369
Gas purchasing cost ($3/MSCF), $	4,107,000
Net revenue for the horizontal well, $	48,172,567

Chapter 6

Summary

The goal of this thesis is to demonstrate that the developed technique of cyclic gas injection have the potential for improving oil recovery in shale oil reservoirs. In our work, we use a black-oil solvent model to simulate cyclic gas injection process without going to the complexity and expense of using a compositional model. P. Ceragioli & EniSpA (2008) presents a paper that provided some guidelines about choosing the black-oil model or fast compositional model. Their paper shows that full compositional simulation reliability is dependent on a proper space-time discretization on a well characterized reservoir and by an equation of state with an enough detailed pseudo-composition of the reservoir fluid. We don't have too much detailed data about the composition of the reservoir fluids in Eagle Ford Shale. In our case, we would rather use a black-oil model than make lots of unknown assumptions for a significant amount of composition data of the reservoir fluids. "A robust black-oil model, properly calibrated on a well defined compositional model, sometimes can be more reliable than a reduced compositional model" (Ceragioli, 2008).

In shale oil reservoirs, the main transport of fluids takes place through the fractures, while the matrix blocks supply the fluids to the fractures. By implementing cyclic gas injection, the injected solvent pushes oil away from the fracture but acts as pressure maintenance for the reservoir. More importantly, when the reservoir pressure stays above MMP, the injected solvent can be fully miscible with oil, which can greatly reduce the oil viscosity and make the system much more mobile. When the production process begins, the mixed oil and solvent will flow out of the matrix into the highly conductive fracture, then into the wellbore. However, in a 200 ft (X direction) wide shale oil reservoir model, the stimulated oil volume (mobile oil grid blocks) by cyclic gas injection processes is only 35 ft far away from the fracture, symmetrically. If we can think of ways to enhance the macroscopic displacement efficiency, it will bring a revolution to shale oil reservoirs development. Primary recovery from shale oil reservoirs by hydraulic fracturing

technology and horizontal well drilling is 6.5%. But generally by application of miscible cyclic gas injection technique, it is able to acquire 22% incremental oil recovery, no matter which well schedule we select.

Chapter 1 of the thesis makes a statement about the problems existing in current unconventional reservoirs development. Unlike conventional reservoirs, water flooding does not seem to be a good option in shale oil reservoir because of its injectivity issue. Historically, primary production from shale oil reservoirs even applied with hydraulic fracturing techniques was 6% OOIP or less. There are potential difficulties for conventional cyclic gas injection application such as bypassing oil and disconnected oil zones caused by massive viscous fingering and channeling by high pressures in injection cycles, combined with poor mobility ratios and high permeability streaks.

Chapter 2 focuses on the literature review about the existing technology applied in developing unconventional reservoirs including horizontal drilling and multi-stage hydraulic fracturing techniques. Also it introduces some background about shale reservoir characteristics such as lithology, assessment of the quality, type and thermal maturity of the rock and kerogen samples. Additionally, it gives a simple history introduction about cyclic steam stimulation that used to be applied in heavy oil reservoirs. We modify it, combined with existing horizontal drilling and multi-stage hydraulic fracturing technology. Studies show the technique we developed can provide significant contribution to incremental oil recovery in shale oil reservoirs.

Chapter 3 illustrates five flow patterns in hydraulically fractured well: fracture linear, bilinear, formation linear, elliptical and pseudo-radial flow. It also proposes some after closure analysis for determination of important reservoir parameters from different flow regimes. Chapter 3 also consists of non-Darcy flow description that should happen in gas reservoirs in hydraulically fractured wells.

Chapter 4 focuses on the basic reservoir model setting up, sensitivity studies and validation. It lists the basic reservoir properties for Eagle Ford Shale, reservoir fluids properties and fracture properties. We also completed the grid sensitivity study, different

commercial softwares simulation results comparison and material balance calculation for the validation of the model.

Chapter 5 shows the detailed work for implementing cyclic gas injection and the incremental oil recovery for each well schedule scenario. In conclusion, cyclic gas injection can be considered as an effective way for improving oil recovery in shale oil reservoirs.

6.1 Recommendations and Future Works

1. There are some limitations for the miscible flooding that is the reservoir is required to be minimum depth to have the pressure needed to maintain the generated miscibility. We have to consider the required reservoir pressure, temperature and reservoir fluids compositions when we want to use this technique.

2. In our paper, we are short of the solvent PVT data, for convenience, we use the reservoir gas PVT data replacing for solvent, which is reasonable. However, if we use compositional model, it will be easier to acquire the solvent PVT data from EOS.

3. In the future, we will complete the economic analysis for miscible cyclic gas injection to optimize what kind of reservoir condition is applicable, when is the best time to begin the cyclic gas injection and what kind of well schedule cycles will achieve the most recovery with least time.

4. We will consider using a compositional model by adjusting the injected solvent compositions to simulate the whole miscible cyclic gas injection process again. It would be more practically applicable and meaningful to optimize what fraction of primary slug, what fraction of secondary slug of solvent is and if some other extra gas supplement like nitrogen will acquire the more oil recovery.

5. We want to take into account the thermal effects brought by the injected solvent on reservoir fluids properties. It would be innovative to initiate a new study for

cyclic steam stimulation for shale oil reservoir by taking into considerations of the energy of injected gas. We believe the mechanism of thermal recovery combined with miscible cyclic flooding will achieve better results and acquire much more incremental oil recovery.

References

1. Ahmed, T. 2010. *Reservoir Engineering Handbook.* Gulf Professional Publishing, PP. 711-750.

2. Chaudhary, A.S.,Texas A&M University, Ehlig-Economides, C.,Texas A&M University, Wattenbarger, R.,Texas A&M University. 2011. *Shale Oil Production Performance from a Stimulated Reservoir Volume*. SPE 147596 presented at Annual Technical Conference and Exhibition, Denver, Colorado, USA, 30 October-2 November .

3. Baihly J.D., SPE, Malpani, R., SPE, Schlumberger; Edwards, C., Anadarko; Han, S.Y., SPE, Kok, J.C.L. ,SPE, Tollefsen, E.M., SPE, Wheeler, C.W., Schlumberger, 2010. *Unlocking the Shale Mystery: How Lateral Measurements and Well Placement Impact Completions and Resultant Production.* SPE 138427 presented at Tight Gas Completions Conference, San Antonio, Texas, USA, November 2010.

4. Bazan, Lucas W., SPE, Bazan Consulting, Inc.; Larkin, Sam D.,SPE, Larkin Consulting, Inc.; and Lattibeaudiere, Michael G., SPE, Rosetta Resources Inc. and Palisch, Terry T., SPE, CARBO Ceramics. 2010. *Improving Production in the Eagle Ford Shale with Fracture Modeling, Increased Fracture Conductivity, and Optimized Stage and Cluster Spacing Along the Horizontal Wellbore.* SPE 138425 presented at Tight Gas Completions Conference, San Antonio, Texas, USA, November 2010.

5. CMG. 2009. *Modelling Non Darcy Flow in Hydraulic Fractures Accurately Using a Grid Based Approach*. IMEX, Advanced Oil/Gas Reservoir Simulator Version, PP. 167-190 .

6. Dake, L. 1978. Fundamentals of Reservoir Engineering.

7. Green,W.D., Willhite,G.P. 1998. Enhanced Oil Recovery . SPE Textbook Series Vol. 6.

8. Dusseault, M. 2002. Cold Heavy Oil Production with Sand in the Canadian Heavy Oil Industry.

9. Schlumberger, 2010. *ECLIPSE Technical Description,* PP. 613-650.

10. Economides, M.J., Nolte, K.G. 1987. Post-Treatment Evaluation and Fractured Well Performance. Reservoir stimulation, Schlumberger Educational services, Houston. Chap, 11,1-17.

11. Yuan,H., Egwuenu, A.M., Dinodoruk, B. 2004. Improved MMP Correlations for CO2 Floods Using Analytical Gasflooding Theory. Tulsa: Paper SPE 89359 presented at the 2004 SPE symposium on improved oil recovery, Tulsa, 17-21 April.

12. Hollabaugh, G.S., Dees, J.M. 1993. Propellant Gas Fracture Stimulation of a Horizontal Austin Chalk Wellbore. Paper SPE 26584 presented at the SPE Annual Technical Conference and Exhibition, Houston, Texas, 3-6 October.

13. Joshi, S. D.1991. Horizontal Well Technology. PennWell Publishing.

14. McCarthy,K., Niemann,M., Palmowski, D. 2011. Basic Petroleum Geochemistry for Source Rock Evaluation. Schlumberger.

15. Koval, E.J. 1963. *A Method for Predicting the Performance of Unstable Miscible Displacement in Heterogeneous Media,* SPE Journal, Volume 3, Number 2.

16. Gidley, J.L., Holditch, S.A., Nierode, D.E. et al. 1989. Postfracture Formation Evaluation. In Recent Advances in Hydraulic Fracturing, 12. Chap. 15, 317. Richardson, Texas: Monograph Series, SPE.

17. Lee, J. (2003). Pressure Transient Testing. SPE Textbook Series, Vol.9.

18. Martin, R., Baihly, J. et al. 2011. Understanding Production from Eagle Ford-Austin Chalk System. Paper SPE 145117 presented at the SPE Annual Technical

Conference and Exhibition, Denver, Colorado, USA. 30 October-2 November.

19. Mendoza, E., SPE, Aular, J.,AAPG, Halliburton; Sousa, L.,SPE, formerly Halliburton. 2011. *Optimizing Horizontal-Well Hydraulic-Fracture spacing in the Eagle Ford Formation, Texas.* SPE 143681 presented at North American Unconventional Gas Conference and Exhibition, The Woodlands, Texas, USA, 14-16 June.

20. Economides,M.J., Martin, T. 2007. Modern Fracturing: Enhancing Natural Gas Production. BJ Services Company, Houston.

21. P.Ceragioli, E. S. 2008. Gas Injection: Rigorous Black-Oil or Fast Compositional Model. Paper SPE 12867 presented at the International Petroleum Technology Conference, Kuala Lumpur, Malaysia. 3-5 December.

22. Borstmayer, R., Stegent, N. 2011. Approach Optimizes Completion Design. The American Oil & Gas Reporter.

23. Rubin, B. 2010. *Accurate Simulation of Non Darcy Flow in Stimulated Fractured Shale Reservoirs*. Paper SPE 132093 presented at Western Regional Meeting, Anaheim, California, USA, 27-29 May.

24. Satter, A. 2008. Practical Enhanced Reservoir Engineering. PennWell.

25. Soliman, M.Y., Craig,D. et al. 2005. New Method for Determination of Formation Permeability, Reservoir Pressure, and Fracture Properties from a Minifrac Test. Paper 05-658 Presented at Alaska: American Rock Mechanics Association.

26. Todd, M.R., Longstaff, W.J, 1972, *The Development, Testing, and Application Of a Numerical Simulator for Predicting Miscible Flood Performance,* Journal of Petroleum Technology, Volume 24, Number 7.

27. Tom Alexander, J. B. 2011. Shale Gas Revolution. Schlumberger.

Appendix A

Oil Compressibility above bubble point

Vasquez and Beggs (1980) correlated the isothermal oil compressibilitycoefficients with R_s, T, °API, γ_g, and p. They proposed thefollowing expression:

$$C_o = \frac{-1433 + 5R_{sb} + 17.2(T - 460) - 1180\gamma_{gs} + 12.61API}{10^5 p}$$

$$B_o = B_{ob}\exp\left(C_o\left(P_{bp} - P\right)\right)$$

P		C_o	B_o
Pb	Pb=2398	2.42207E-05	1.43443
Undersaturated	2800	2.07433E-05	1.422518
	3200	1.81504E-05	1.413701
	3800	1.52845E-05	1.404019
	4400	1.32003E-05	1.397019
	5000	1.16162E-05	1.391722
	5600	1.03716E-05	1.387575
	6500	8.93557E-06	1.382805

Vasquez and Beggs (1980) proposedthe following expression for estimating the viscosity of undersaturatedcrude oil:

$$\mu_o = \mu_{ob}\left(\frac{p}{p_b}\right)^m$$

Where $m = 2.6\, p^{1.187} 10^a$,with$a = -3.9(10^{-5})\, p - 5$

P		a	m	μ_o
Pb	Pb=2398			0.337718

Undersaturated	2800	-5.1092	0.249776	0.351048
	3200	-5.1248	0.282349	0.366381
	3800	-5.1482	0.328078	0.392779
	4400	-5.1716	0.369957	0.422743
	5000	-5.195	0.407991	0.455777
	5600	-5.2184	0.442255	0.491421
	6500	-5.2535	0.486857	0.548775

Appendix B

Data File

```
INUNIT FIELD

WSRF WELL 1

WSRF GRID TIME

WSRF SECTOR TIME

OUTSRF WELL

OUTSRF RES ALL

OUTSRF GRID BPP KRG KRO KRW PRES SG SO SSPRES SW VISG VISO

*OUTPRN *GRID *SO *PRES

WPRN GRID TIME

WPRN WELL TIME

**$ Distance units: ft

RESULTS XOFFSET 0.0000

  **************************************************************************

  ** Reservoir Description Section

  **************************************************************************

GRID VARI 21 55 7

KDIR DOWN

DI IVAR

16      14      12      12      10      9       8       8       6       4       2
4       6       8       8       9       10      12      12      14      16
```

DJ JVAR

35 21*20 16 10 8 6 4 2 4 6 8 10 16 21*20 35

DK ALL

1155*52.8 1155*26.4 1155*14.2 1155*13.2 1155*14.2 1155*26.4 1155*52.8

DTOP

1155*9884

**$ Property: Permeability I (md) Max: 0.0001 Min: 0.0001

**$ Property: Permeability I (md) Max: 41.65 Min: 0.0001

PERMI ALL

10*0.0001 41.65 20*0.0001 41.65 20*0.0001 41.65 20*0.0001 41.65 20*0.0001 41.65 10*0.0001

10*0.0001 41.65 20*0.0001 41.65 20*0.0001 41.65 20*0.0001 41.65 20*0.0001 41.65 10*0.0001

10*0.0001 41.65 20*0.0001 41.65 20*0.0001 41.65 20*0.0001 41.65 20*0.0001 41.65 10*0.0001

10*0.0001 41.65 20*0.0001 41.65 20*0.0001 41.65 20*0.0001 41.65 20*0.0001 41.65 10*0.0001

10*0.0001 41.65 20*0.0001 41.65 20*0.0001 41.65 20*0.0001 41.65 20*0.0001 41.65 10*0.0001

10*0.0001 41.65 20*0.0001 41.65 20*0.0001 41.65 20*0.0001 41.65 20*0.0001 41.65 10*0.0001

10*0.0001 41.65 20*0.0001 41.65 20*0.0001 41.65 20*0.0001 41.65 20*0.0001 41.65 10*0.0001

10*0.0001 41.65 20*0.0001 41.65 20*0.0001 41.65 20*0.0001 41.65 20*0.0001 41.65 10*0.0001

10*0.0001 41.65 20*0.0001 41.65 20*0.0001 41.65 20*0.0001 41.65 20*0.0001 41.65 10*0.0001

10*0.0001 41.65 20*0.0001 41.65 20*0.0001 41.65 20*0.0001 41.65 20*0.0001 41.65 10*0.0001

10*0.0001 41.65 20*0.0001 41.65 20*0.0001 41.65 20*0.0001 41.65 20*0.0001 41.65 10*0.0001

10*0.0001 41.65 20*0.0001 41.65 20*0.0001 41.65 20*0.0001 41.65 20*0.0001 41.65 10*0.0001

10*0.0001 41.65 20*0.0001 41.65 20*0.0001 41.65 20*0.0001 41.65 20*0.0001 41.65 10*0.0001

10*0.0001 41.65 20*0.0001 41.65 20*0.0001 41.65 20*0.0001 41.65 20*0.0001 41.65 10*0.0001

10*0.0001 41.65 20*0.0001 41.65 20*0.0001 41.65 20*0.0001 41.65 20*0.0001 41.65 10*0.0001

10*0.0001 41.65 20*0.0001 41.65 20*0.0001 41.65 20*0.0001 41.65 20*0.0001 41.65 10*0.0001

10*0.0001 41.65 20*0.0001 41.65 20*0.0001 41.65 20*0.0001 41.65 20*0.0001 41.65 10*0.0001

10*0.0001 41.65 20*0.0001 41.65 20*0.0001 41.65 20*0.0001 41.65 20*0.0001 41.65 10*0.0001

10*0.0001 41.65 20*0.0001 41.65 20*0.0001 41.65 20*0.0001 41.65 20*0.0001 41.65 10*0.0001

10*0.0001 41.65 20*0.0001 41.65 20*0.0001 41.65 20*0.0001 41.65 20*0.0001 41.65 10*0.0001

10*0.0001 41.65 20*0.0001 41.65 20*0.0001 41.65 20*0.0001 41.65 20*0.0001 41.65 10*0.0001

10*0.0001 41.65 20*0.0001 41.65 20*0.0001 41.65 20*0.0001 41.65 20*0.0001 41.65 10*0.0001

10*0.0001 41.65 20*0.0001 41.65 20*0.0001 41.65 20*0.0001 41.65 20*0.0001 41.65 10*0.0001

10*0.0001 41.65 20*0.0001 41.65 20*0.0001 41.65 20*0.0001 41.65 20*0.0001 41.65 10*0.0001

10*0.0001 41.65 20*0.0001 41.65 20*0.0001 41.65 20*0.0001 41.65 20*0.0001 41.65 10*0.0001

10*0.0001 41.65 20*0.0001 41.65 20*0.0001 41.65 20*0.0001 41.65 20*0.0001 41.65 10*0.0001

10*0.0001 41.65 20*0.0001 41.65 20*0.0001 41.65 20*0.0001 41.65 20*0.0001 41.65 10*0.0001

10*0.0001 41.65 20*0.0001 41.65 20*0.0001 41.65 20*0.0001 41.65 20*0.0001 41.65 10*0.0001

10*0.0001 41.65 20*0.0001 41.65 20*0.0001 41.65 20*0.0001 41.65 20*0.0001 41.65 10*0.0001

10*0.0001 41.65 20*0.0001 41.65 20*0.0001 41.65 20*0.0001 41.65 20*0.0001 41.65 10*0.0001

10*0.0001 41.65 20*0.0001 41.65 20*0.0001 41.65 20*0.0001 41.65 20*0.0001 41.65 10*0.0001

10*0.0001 41.65 20*0.0001 41.65 20*0.0001 41.65 20*0.0001 41.65 20*0.0001 41.65 10*0.0001

10*0.0001 41.65 20*0.0001 41.65 20*0.0001 41.65 20*0.0001 41.65 20*0.0001 41.65 10*0.0001

10*0.0001 41.65 20*0.0001 41.65 20*0.0001 41.65 20*0.0001 41.65 20*0.0001 41.65 10*0.0001

10*0.0001 41.65 20*0.0001 41.65 20*0.0001 41.65 20*0.0001 41.65 20*0.0001 41.65 10*0.0001

10*0.0001 41.65 20*0.0001 41.65 20*0.0001 41.65 20*0.0001 41.65 20*0.0001 41.65 10*0.0001

10*0.0001 41.65 20*0.0001 41.65 20*0.0001 41.65 20*0.0001 41.65 20*0.0001 41.65 10*0.0001

10*0.0001 41.65 20*0.0001 41.65 20*0.0001 41.65 20*0.0001 41.65 20*0.0001 41.65 10*0.0001

10*0.0001 41.65 20*0.0001 41.65 20*0.0001 41.65 20*0.0001 41.65 20*0.0001 41.65 10*0.0001

10*0.0001 41.65 20*0.0001 41.65 20*0.0001 41.65 20*0.0001 41.65 20*0.0001 41.65 10*0.0001

10*0.0001 41.65 20*0.0001 41.65 20*0.0001 41.65 20*0.0001 41.65 20*0.0001 41.65 10*0.0001

10*0.0001 41.65 20*0.0001 41.65 20*0.0001 41.65 20*0.0001 41.65 20*0.0001 41.65 10*0.0001

10*0.0001 41.65 20*0.0001 41.65 20*0.0001 41.65 20*0.0001 41.65 20*0.0001 41.65 10*0.0001

10*0.0001 41.65 20*0.0001 41.65 20*0.0001 41.65 20*0.0001 41.65 20*0.0001 41.65 10*0.0001

10*0.0001 41.65 20*0.0001 41.65 20*0.0001 41.65 20*0.0001 41.65 20*0.0001 41.65 10*0.0001

10*0.0001 41.65 20*0.0001 41.65 20*0.0001 41.65 20*0.0001 41.65 20*0.0001 41.65 10*0.0001

10*0.0001 41.65 20*0.0001 41.65 20*0.0001 41.65 20*0.0001 41.65 20*0.0001 41.65 10*0.0001

10*0.0001 41.65 20*0.0001 41.65 20*0.0001 41.65 20*0.0001 41.65 20*0.0001 41.65 10*0.0001

10*0.0001 41.65 20*0.0001 41.65 20*0.0001 41.65 20*0.0001 41.65 20*0.0001 41.65 10*0.0001

10*0.0001 41.65 20*0.0001 41.65 20*0.0001 41.65 20*0.0001 41.65 20*0.0001 41.65 10*0.0001

10*0.0001 41.65 20*0.0001 41.65 20*0.0001 41.65 20*0.0001 41.65 20*0.0001 41.65 10*0.0001

10*0.0001 41.65 20*0.0001 41.65 20*0.0001 41.65 20*0.0001 41.65 20*0.0001 41.65 10*0.0001

10*0.0001 41.65 20*0.0001 41.65 20*0.0001 41.65 20*0.0001 41.65 20*0.0001 41.65 10*0.0001

10*0.0001 41.65 20*0.0001 41.65 20*0.0001 41.65 20*0.0001 41.65 20*0.0001 41.65 10*0.0001

10*0.0001 41.65 20*0.0001 41.65 20*0.0001 41.65 20*0.0001 41.65 20*0.0001 41.65 10*0.0001

10*0.0001 41.65 20*0.0001 41.65 20*0.0001 41.65 20*0.0001 41.65 20*0.0001 41.65 10*0.0001

10*0.0001 41.65 20*0.0001 41.65 20*0.0001 41.65 20*0.0001 41.65 20*0.0001 41.65 10*0.0001

10*0.0001 41.65 20*0.0001 41.65 20*0.0001 41.65 20*0.0001 41.65 20*0.0001 41.65 10*0.0001

10*0.0001 41.65 20*0.0001 41.65 20*0.0001 41.65 20*0.0001 41.65 20*0.0001 41.65 10*0.0001

10*0.0001 41.65 20*0.0001 41.65 20*0.0001 41.65 20*0.0001 41.65 20*0.0001 41.65 10*0.0001

10*0.0001 41.65 20*0.0001 41.65 20*0.0001 41.65 20*0.0001 41.65 20*0.0001 41.65 10*0.0001

10*0.0001 41.65 20*0.0001 41.65 20*0.0001 41.65 20*0.0001 41.65 20*0.0001 41.65 10*0.0001

10*0.0001 41.65 20*0.0001 41.65 20*0.0001 41.65 20*0.0001 41.65 20*0.0001 41.65 10*0.0001

10*0.0001 41.65 20*0.0001 41.65 20*0.0001 41.65 20*0.0001 41.65 20*0.0001 41.65 10*0.0001

10*0.0001 41.65 20*0.0001 41.65 20*0.0001 41.65 20*0.0001 41.65 20*0.0001 41.65 10*0.0001

10*0.0001 41.65 20*0.0001 41.65 20*0.0001 41.65 20*0.0001 41.65 20*0.0001 41.65 10*0.0001

10*0.0001 41.65 20*0.0001 41.65 20*0.0001 41.65 20*0.0001 41.65 20*0.0001 41.65 10*0.0001

10*0.0001 41.65 20*0.0001 41.65 20*0.0001 41.65 20*0.0001 41.65 20*0.0001 41.65 10*0.0001

10*0.0001 41.65 20*0.0001 41.65 20*0.0001 41.65 20*0.0001 41.65 20*0.0001 41.65 10*0.0001

10*0.0001 41.65 20*0.0001 41.65 20*0.0001 41.65 20*0.0001 41.65 20*0.0001 41.65 10*0.0001

10*0.0001 41.65 20*0.0001 41.65 20*0.0001 41.65 20*0.0001 41.65 20*0.0001 41.65 10*0.0001

10*0.0001 41.65 20*0.0001 41.65 20*0.0001 41.65 20*0.0001 41.65 20*0.0001 41.65 10*0.0001

10*0.0001 41.65 20*0.0001 41.65 20*0.0001 41.65 20*0.0001 41.65 20*0.0001 41.65 10*0.0001

10*0.0001 41.65 20*0.0001 41.65 20*0.0001 41.65 20*0.0001 41.65 20*0.0001 41.65 10*0.0001

10*0.0001 41.65 20*0.0001 41.65 20*0.0001 41.65 20*0.0001 41.65 20*0.0001 41.65 10*0.0001

10*0.0001 41.65 20*0.0001 41.65 20*0.0001 41.65 20*0.0001 41.65 20*0.0001 41.65 10*0.0001

10*0.0001 41.65 20*0.0001 41.65 20*0.0001 41.65 20*0.0001 41.65 20*0.0001 41.65 10*0.0001

NULL CON 1

POR CON 0.06

PERMJ EQUALSI

PERMK EQUALSI * 0.1

**$ 0 = pinched block, 1 = active block

PINCHOUTARRAY CON 1

PRPOR 5000

CPOR 5e-6

*MODEL *MISNCG ** Use the pseudomiscible option with

  ** no chase gas.

****

** Component Property section

****

TRES 255

PVT EG 1

***P	Rs	Bo	EgVisoVisg		
14.696	4.68138	1.09917	4.10159	0.902644	0.013601
173.583	32.1923	1.11173	49.1225	0.803844	0.013724
332.47	65.2796	1.12711	95.3676	0.719427	0.013905
491.357	101.621	1.1443	142.801	0.651788	0.014127

650.244	140.36	1.16295	191.364	0.59727	0.014385
809.131	181.027	1.18287	240.971	0.552597	0.014677
968.018	223.32	1.20393	291.506	0.515357	0.015001
1126.9	267.027	1.22604	342.824	0.483819	0.015357
1285.79	311.989	1.24913	394.75	0.45674	0.015745
1444.68	358.084	1.27314	447.084	0.433209	0.016164
1603.57	405.212	1.29803	499.604	0.412545	0.016612
1762.45	453.293	1.32376	552.077	0.394234	0.017088
1921.34	502.257	1.3503	604.264	0.377877	0.01759
2080.23	552.048	1.3776	655.935	0.363163	0.018116
2239.11	602.616	1.40566	706.874	0.349843	0.018664
2398	653.915	1.43443	756.888	0.337718	0.019232
3218.4	929.142	1.59372	995.379	0.288941	0.022371
4038.8	1219.15	1.76935	1195.74	0.255067	0.025643
4859.2	1521.47	1.95964	1360.49	0.229917	0.028854
5679.6	1834.43	2.16332	1496.29	0.21036	0.031914
6500	2193.143	2.37939	1609.67	0.19463	0.034795

*PVTS ** PVT table for solvent

*** P rssEsVissOmg_s

14.696	0	4.10159	0.013601	0
173.583	0	49.1225	0.013724	0
332.47	0	95.3676	0.013905	0
491.357	0	142.801	0.014127	0
650.244	0	191.364	0.014385	0
809.131	0	240.971	0.014677	0
968.018	0	291.506	0.015001	0
1126.9	0	342.824	0.015357	0
1285.79	0	394.75	0.015745	0

1444.68	0	447.084	0.016164	0
1603.57	0	499.604	0.016612	0
1762.45	0	552.077	0.017088	0
1921.34	0	604.264	0.01759	0
2080.23	0	655.935	0.018116	0
2239.11	0	706.874	0.018664	0
2398	0	756.888	0.019232	0.74
3218.4	0	995.379	0.022371	0.74
4038.8	0	1195.74	0.025643	0.74
4859.2	0	1360.49	0.028854	0.74
5679.6	0	1496.29	0.031914	0.74
6500	0	1609.67	0.034795	0.74

GRAVITY GAS 0.8

REFPW 14.696

DENSITY WATER 62.4

DENSITY SOLVENT 0.06248

BWI 1.06212

CW 3.72431e-006

VWI 0.23268

CVW 0.0

**$ Property: PVT Type Max: 1 Min: 1

PTYPE CON 1

DENSITY OIL 50.863

CO 1e-5

OMEGASG 0.77 ** Gas and solvent mixing parameter

```
MINSS   0.2                 ** Minimum solvent saturation

ROCKFLUID

  ********************************************************************

  ** Rock-Fluid Properties

  ********************************************************************

RPT 1

**$SwKrwKrowPcow

SWT

      0.2         0         1         5
     0.25    0.0004    0.6027         4
      0.3    0.0024     0.449         3
     0.31    0.0033    0.4165       2.8
     0.35    0.0075    0.3242       2.5
      0.4    0.0167    0.2253         2
     0.45     0.031    0.1492       1.8
      0.5    0.0515    0.0927       1.6
      0.6    0.1146    0.0265       1.4
      0.7    0.2133    0.0031       1.2
      0.8    0.3542         0         1
      0.9    0.5438         0       0.5
        1    0.7885         0         0


**$ SlKrgKrogPcog

SLT

      0.3    0.6345         0      1.92
      0.4    0.5036   0.00002      1.15
      0.5    0.3815   0.00096      0.77
```

0.6	0.2695	0.00844	0.5
0.7	0.1692	0.03939	0.32
0.8	0.0835	0.1301	0.22
0.85	0.0477	0.2167	0.18
0.9	0.0183	0.3454	0.15
0.95	0	0.5302	0.12
1	0	1	0.1

RPT 2 **********Rock Type 2**********

SWT

0	0	1
0.05	0.05	0.95
0.25	0.25	0.75
0.5	0.5	0.5
0.75	0.75	0.25
0.95	0.95	0.05
1	1	0

**$ Slkrgkrog

SLT

0	1	0
0.05	0.95	0.05
0.25	0.75	0.25
0.5	0.5	0.5
0.75	0.25	0.75
0.95	0.05	0.95
1	0	1

**********Assign different permeability curve to the shale matrix and fracture*******

RTYPE ALL

10*1 2 20*1 2 20*1 2 20*1 2 20*1 2 20*1 2 20*1 2 20*1 2 20*1 2 20*1

2 20*1 2 20*1 2 20*1 2 20*1 2 20*1 2 20*1 2 20*1 2 20*1 2 20*1 2 20*1

2 20*1 2 20*1 2 20*1 2 20*1 2 20*1 2 20*1 2 20*1 2 20*1 2 20*1 2 20*1

2 20*1 2 20*1 2 20*1 2 20*1 2 20*1 2 20*1 2 20*1 2 20*1 2 20*1 2 20*1

2 20*1 2 20*1 2 20*1 2 20*1 2 20*1 2 20*1 2 20*1 2 20*1 2 20*1 2 20*1

2 20*1 2 20*1 2 20*1 2 20*1 2 20*1 2 20*1 2 20*1 2 20*1 2 20*1 2 20*1

2 20*1 2 20*1 2 20*1 2 20*1 2 20*1 2 20*1 2 20*1 2 20*1 2 20*1 2 20*1

2 20*1 2 20*1 2 20*1 2 20*1 2 20*1 2 20*1 2 20*1 2 20*1 2 20*1 2 20*1

2 20*1 2 20*1 2 20*1 2 20*1 2 20*1 2 20*1 2 20*1 2 20*1 2 20*1 2 20*1

2 20*1 2 20*1 2 20*1 2 20*1 2 20*1 2 20*1 2 20*1 2 20*1 2 20*1 2 20*1

2 20*1 2 20*1 2 20*1 2 20*1 2 20*1 2 20*1 2 20*1 2 20*1 2 20*1 2 20*1

2 20*1 2 20*1 2 20*1 2 20*1 2 20*1 2 20*1 2 20*1 2 20*1 2 20*1 2 20*1

2 20*1 2 20*1 2 20*1 2 20*1 2 20*1 2 20*1 2 20*1 2 20*1 2 20*1 2 20*1

2 20*1 2 20*1 2 20*1 2 20*1 2 20*1 2 20*1 2 20*1 2 20*1 2 20*1 2 20*1

2 20*1 2 20*1 2 20*1 2 20*1 2 20*1 2 20*1 2 20*1 2 20*1 2 20*1 2 20*1

2 20*1 2 20*1 2 20*1 2 20*1 2 20*1 2 20*1 2 20*1 2 20*1 2 20*1 2 20*1

2 20*1 2 20*1 2 20*1 2 20*1 2 20*1 2 20*1 2 20*1 2 20*1 2 20*1 2 20*1

2 20*1 2 20*1 2 20*1 2 20*1 2 20*1 2 20*1 2 20*1 2 20*1 2 20*1 2 20*1

2 20*1 2 20*1 2 20*1 2 20*1 2 20*1 2 20*1 2 20*1 2 20*1 2 20*1 2 20*1

2 20*1 2 20*1 2 20*1 2 20*1 2 20*1 2 20*1 2 20*1 2 20*1 2 20*1 2 20*1

2 20*1 2 20*1 2 20*1 2 20*1 2 20*1 2 20*1 2 20*1 2 20*1 2 20*1 2 20*1

2 20*1 2 20*1 2 20*1 2 20*1 2 20*1 2 20*1 2 20*1 2 20*1 2 20*1 2 20*1

2 20*1 2 20*1 2 20*1 2 20*1 2 20*1 2 20*1 2 20*1 2 20*1 2 20*1 2 20*1

2 20*1 2 20*1 2 20*1 2 20*1 2 20*1 2 20*1 2 20*1 2 20*1 2 20*1 2 20*1

2 20*1 2 20*1 2 20*1 2 20*1 2 20*1 2 20*1 2 20*1 2 20*1 2 20*1 2 20*1

2 20*1 2 20*1 2 20*1 2 20*1 2 20*1 2 20*1 2 20*1 2 20*1 2 20*1 2 20*1

2 20*1 2 20*1 2 20*1 2 20*1 2 20*1 2 20*1 2 20*1 2 20*1 2 20*1 2 20*1

2 20*1 2 20*1 2 20*1 2 20*1 2 20*1 2 20*1 2 20*1 2 20*1 2 20*1 2 20*1

2 20*1 2 20*1 2 20*1 2 20*1 2 20*1 2 20*1 2 20*1 2 20*1 2 20*1 2 20*1

2 20*1 2 20*1 2 20*1 2 20*1 2 20*1 2 20*1 2 20*1 2 20*1 2 20*1 2 20*1

2 20*1 2 20*1 2 20*1 2 20*1 2 20*1 2 20*1 2 20*1 2 20*1 2 20*1 2 20*1

2 20*1 2 20*1 2 20*1 2 20*1 2 20*1 2 20*1 2 20*1 2 20*1 2 20*1 2 20*1

2 20*1 2 20*1 2 20*1 2 20*1 2 20*1 2 20*1 2 20*1 2 20*1 2 20*1 2 20*1

2 20*1 2 20*1 2 20*1 2 20*1 2 20*1 2 20*1 2 20*1 2 20*1 2 20*1 2 20*1

2 20*1 2 20*1 2 20*1 2 20*1 2 20*1 2 20*1 2 20*1 2 20*1 2 20*1 2 20*1

2 20*1 2 20*1 2 20*1 2 20*1 2 20*1 2 20*1 2 20*1 2 20*1 2 20*1 2 20*1

2 20*1 2 20*1 2 20*1 2 20*1 2 20*1 2 20*1 2 20*1 2 20*1 2 20*1 2 20*1

2 20*1 2 20*1 2 20*1 2 20*1 2 20*1 2 20*1 2 20*1 2 20*1 2 20*1 2 20*1

2 20*1 2 20*1 2 20*1 2 20*1 2 20*1 2 10*1

*INITIAL

****

** Initial Conditions Section

****

```
VERTICAL DEPTH_AVE WATER_OIL EQUIL

REFDEPTH 9984

REFPRES 6425

DWOC 15000


PB CON 2398

PBS CON 2398


  *NUMERICAL

  ************************************************************************

  ** Numerical Methods Control Section

  ************************************************************************


DTMIN 1e-9

NORTH 40

ITERMAX 100

RUN

DATE 2010 1 1

DTWELL 1e-008

**$

WELL  'Inj'

**$ wdepthwlengthrel_roughwhtempbhtempwradius
```

```
INJECTOR MOBWEIGHT 'Inj'

IWELLBORE  MODEL

**$ wdepthwlengthrel_roughwhtempbhtempwradius

   9987.  200.  0.0001  60.  255.  0.25

INCOMP  SOLVENT  GLOBAL  0.77  0.  0.2  0.  0.  0.  0.  0.03  0.          ********Injected solvent
composition******

OPERATE  MAX  BHP  7000.  CONT

OPERATE  MAX  STS  800000.  CONT

**$          rad  geofacwfrac  skin

GEOMETRY  K  0.25  0.37  1.  0.

PERF  GEOA  'Inj'

**$ UBA      ff  Status  Connection

7 28 7   1.  OPEN    FLOW-FROM  'SURFACE'

8 28 7   1.  OPEN    FLOW-FROM  1

9 28 7   1.  OPEN    FLOW-FROM  2

   10 28 7  1.  OPEN    FLOW-FROM  3

   11 28 7  1.  OPEN    FLOW-FROM  4  REFLAYER

   12 28 7  1.  OPEN    FLOW-FROM  5

   13 28 7  1.  OPEN    FLOW-FROM  6

   14 28 7  1.  OPEN    FLOW-FROM  7

   15 28 7  1.  OPEN    FLOW-FROM  8

SHUTIN 'Inj'

**$
```

```
**$

WELL  'Prod'

PRODUCER 'Prod'

OPERATE  MIN  BHP  2500.  CONT

**$ UBA ff Status Connection

**$ rad geofacwfrac skin

**$ UBA ff Status Connection

**$ UBA             ff  Status  Connection

**$         rad  geofacwfrac  skin

GEOMETRY  J  0.25  0.37  1.  0.

PERF  GEOA  'Prod'

**$ UBA      ff  Status  Connection

7 28 7   1.  OPEN    FLOW-TO  'SURFACE'

8 28 7   1.  OPEN    FLOW-TO  1

9 28 7   1.  OPEN    FLOW-TO  2

   10 28 7  1.  OPEN    FLOW-TO  3

   11 28 7  1.  OPEN    FLOW-TO  4  REFLAYER

   12 28 7  1.  OPEN    FLOW-TO  5

   13 28 7  1.  OPEN    FLOW-TO  6

   14 28 7  1.  OPEN    FLOW-TO  7

   15 28 7  1.  OPEN    FLOW-TO  8


OPEN 'Prod'
```

```
  *AIMSET *CON 0

  *AIMWELL *WELLN

WSRF GRID TNEXT

**********Primary depletion********

TIME 7200

SHUTIN 'Prod'

OPEN 'Inj'

*AIMSET *CON 0

AIMWELL WELLN

*******Cyclic gas injection process began************************

*Time  7300

SHUTIN 'Inj'

OPEN 'Prod'

AIMSET CON 0

AIMWELL WELLN

*Time  7400

SHUTIN 'Prod'

OPEN 'Inj'

AIMSET CON 0

AIMWELL WELLN

*Time  7500

SHUTIN 'Inj'

OPEN 'Prod'
```

```
AIMSET CON 0

AIMWELL WELLN

*Time  7600

SHUTIN 'Prod'

OPEN 'Inj'

AIMSET CON 0

AIMWELL WELLN

*Time  7700

SHUTIN 'Inj'

OPEN 'Prod'

AIMSET CON 0

AIMWELL WELLN

*Time  7800

SHUTIN 'Prod'

OPEN 'Inj'

AIMSET CON 0

AIMWELL WELLN

*Time  7900

SHUTIN 'Inj'

OPEN 'Prod'

AIMSET CON 0

AIMWELL WELLN

*Time  8000
```

SHUTIN 'Prod'

OPEN 'Inj'

AIMSET CON 0

AIMWELL WELLN

*Time 8100

SHUTIN 'Inj'

OPEN 'Prod'

AIMSET CON 0

AIMWELL WELLN

*Time 8200

SHUTIN 'Prod'

OPEN 'Inj'

AIMSET CON 0

AIMWELL WELLN

*Time 8300

SHUTIN 'Inj'

OPEN 'Prod'

AIMSET CON 0

AIMWELL WELLN

*Time 8400

SHUTIN 'Prod'

OPEN 'Inj'

AIMSET CON 0

```
AIMWELL WELLN

*Time  8500

SHUTIN 'Inj'

OPEN 'Prod'

AIMSET CON 0

AIMWELL WELLN

*Time  8600

SHUTIN 'Prod'

OPEN 'Inj'

AIMSET CON 0

AIMWELL WELLN

*Time  8700

SHUTIN 'Inj'

OPEN 'Prod'

AIMSET CON 0

AIMWELL WELLN

*Time  8800

SHUTIN 'Prod'

OPEN 'Inj'

AIMSET CON 0

AIMWELL WELLN

*Time  8900

SHUTIN 'Inj'
```

```
OPEN 'Prod'

AIMSET CON 0

AIMWELL WELLN

*Time  9000

SHUTIN 'Prod'

OPEN 'Inj'

AIMSET CON 0

AIMWELL WELLN

*Time  9100

SHUTIN 'Inj'

OPEN 'Prod'

AIMSET CON 0

AIMWELL WELLN

*Time  9200

SHUTIN 'Prod'

OPEN 'Inj'

AIMSET CON 0

AIMWELL WELLN

*Time  9300

SHUTIN 'Inj'

OPEN 'Prod'

AIMSET CON 0

AIMWELL WELLN
```

```
*Time  9400

SHUTIN 'Prod'

OPEN 'Inj'

AIMSET CON 0

AIMWELL WELLN

*Time  9500

SHUTIN 'Inj'

OPEN 'Prod'

AIMSET CON 0

AIMWELL WELLN

*Time  9600

SHUTIN 'Prod'

OPEN 'Inj'

AIMSET CON 0

AIMWELL WELLN

*Time  9700

SHUTIN 'Inj'

OPEN 'Prod'

AIMSET CON 0

AIMWELL WELLN

*Time  9800

SHUTIN 'Prod'

OPEN 'Inj'
```

```
AIMSET CON 0

AIMWELL WELLN

*Time  9900

SHUTIN 'Inj'

OPEN 'Prod'

AIMSET CON 0

AIMWELL WELLN

*Time 10000

SHUTIN 'Prod'

OPEN 'Inj'

AIMSET CON 0

AIMWELL WELLN

*Time 10100

SHUTIN 'Inj'

OPEN 'Prod'

AIMSET CON 0

AIMWELL WELLN

*Time 10200

SHUTIN 'Prod'

OPEN 'Inj'

AIMSET CON 0

AIMWELL WELLN

*Time 10300
```

SHUTIN 'Inj'

OPEN 'Prod'

AIMSET CON 0

AIMWELL WELLN

*Time 10400

SHUTIN 'Prod'

OPEN 'Inj'

AIMSET CON 0

AIMWELL WELLN

*Time 10500

SHUTIN 'Inj'

OPEN 'Prod'

AIMSET CON 0

AIMWELL WELLN

*Time 10600

SHUTIN 'Prod'

OPEN 'Inj'

AIMSET CON 0

AIMWELL WELLN

*Time 10700

SHUTIN 'Inj'

OPEN 'Prod'

AIMSET CON 0

```
AIMWELL WELLN

*Time 10800

SHUTIN 'Prod'

OPEN 'Inj'

AIMSET CON 0

AIMWELL WELLN

*Time 10900

SHUTIN 'Inj'

OPEN 'Prod'

AIMSET CON 0

AIMWELL WELLN

*Time 11000

SHUTIN 'Prod'

OPEN 'Inj'

AIMSET CON 0

AIMWELL WELLN

*Time 11100

SHUTIN 'Inj'

OPEN 'Prod'

AIMSET CON 0

AIMWELL WELLN

*Time 11200

SHUTIN 'Prod'
```

```
OPEN 'Inj'

AIMSET CON 0

AIMWELL WELLN

*Time 11300

SHUTIN 'Inj'

OPEN 'Prod'

AIMSET CON 0

AIMWELL WELLN

*Time 11400

SHUTIN 'Prod'

OPEN 'Inj'

AIMSET CON 0

AIMWELL WELLN

*Time 11500

SHUTIN 'Inj'

OPEN 'Prod'

AIMSET CON 0

AIMWELL WELLN

*Time 11600

SHUTIN 'Prod'

OPEN 'Inj'

AIMSET CON 0

AIMWELL WELLN
```

*Time 11700

SHUTIN 'Inj'

OPEN 'Prod'

AIMSET CON 0

AIMWELL WELLN

*Time 11800

SHUTIN 'Prod'

OPEN 'Inj'

AIMSET CON 0

AIMWELL WELLN

*Time 11900

SHUTIN 'Inj'

OPEN 'Prod'

AIMSET CON 0

AIMWELL WELLN

*Time 12000

SHUTIN 'Prod'

OPEN 'Inj'

AIMSET CON 0

AIMWELL WELLN

*Time 12100

SHUTIN 'Inj'

OPEN 'Prod'

AIMSET CON 0

AIMWELL WELLN

*Time 12200

SHUTIN 'Prod'

OPEN 'Inj'

AIMSET CON 0

AIMWELL WELLN

*Time 12300

SHUTIN 'Inj'

OPEN 'Prod'

AIMSET CON 0

AIMWELL WELLN

*Time 12400

SHUTIN 'Prod'

OPEN 'Inj'

AIMSET CON 0

AIMWELL WELLN

*Time 12500

SHUTIN 'Inj'

OPEN 'Prod'

AIMSET CON 0

AIMWELL WELLN

*Time 12600

SHUTIN 'Prod'

OPEN 'Inj'

AIMSET CON 0

AIMWELL WELLN

*Time 12700

SHUTIN 'Inj'

OPEN 'Prod'

AIMSET CON 0

AIMWELL WELLN

*Time 12800

SHUTIN 'Prod'

OPEN 'Inj'

AIMSET CON 0

AIMWELL WELLN

*Time 12900

SHUTIN 'Inj'

OPEN 'Prod'

AIMSET CON 0

AIMWELL WELLN

*Time 13000

SHUTIN 'Prod'

OPEN 'Inj'

AIMSET CON 0

```
AIMWELL WELLN

*Time 13100

SHUTIN 'Inj'

OPEN 'Prod'

AIMSET CON 0

AIMWELL WELLN

*Time 13200

SHUTIN 'Prod'

OPEN 'Inj'

AIMSET CON 0

AIMWELL WELLN

*Time 13300

SHUTIN 'Inj'

OPEN 'Prod'

AIMSET CON 0

AIMWELL WELLN

*Time 13400

SHUTIN 'Prod'

OPEN 'Inj'

AIMSET CON 0

AIMWELL WELLN

*Time 13500

SHUTIN 'Inj'
```

```
OPEN 'Prod'

AIMSET CON 0

AIMWELL WELLN

*Time 13600

SHUTIN 'Prod'

OPEN 'Inj'

AIMSET CON 0

AIMWELL WELLN

*Time 13700

SHUTIN 'Inj'

OPEN 'Prod'

AIMSET CON 0

AIMWELL WELLN

*Time 13800

SHUTIN 'Prod'

OPEN 'Inj'

AIMSET CON 0

AIMWELL WELLN

*Time 13900

SHUTIN 'Inj'

OPEN 'Prod'

AIMSET CON 0

AIMWELL WELLN
```

*Time 14000

SHUTIN 'Prod'

OPEN 'Inj'

AIMSET CON 0

AIMWELL WELLN

*Time 14100

SHUTIN 'Inj'

OPEN 'Prod'

AIMSET CON 0

AIMWELL WELLN

*Time 14200

SHUTIN 'Prod'

OPEN 'Inj'

AIMSET CON 0

AIMWELL WELLN

*Time 14300

SHUTIN 'Inj'

OPEN 'Prod'

AIMSET CON 0

AIMWELL WELLN

*Time 14400

SHUTIN 'Prod'

OPEN 'Inj'

AIMSET CON 0

AIMWELL WELLN

*Time 14500

SHUTIN 'Inj'

OPEN 'Prod'

AIMSET CON 0

AIMWELL WELLN

*Time 14600

SHUTIN 'Prod'

OPEN 'Inj'

AIMSET CON 0

AIMWELL WELLN

*Time 14700

SHUTIN 'Inj'

OPEN 'Prod'

AIMSET CON 0

AIMWELL WELLN

*Time 14800

SHUTIN 'Prod'

OPEN 'Inj'

AIMSET CON 0

AIMWELL WELLN

*Time 14900

SHUTIN 'Inj'

OPEN 'Prod'

AIMSET CON 0

AIMWELL WELLN

*Time 15000

SHUTIN 'Prod'

OPEN 'Inj'

AIMSET CON 0

AIMWELL WELLN

*Time 15100

SHUTIN 'Inj'

OPEN 'Prod'

AIMSET CON 0

AIMWELL WELLN

*Time 15200

SHUTIN 'Prod'

OPEN 'Inj'

AIMSET CON 0

AIMWELL WELLN

*Time 15300

SHUTIN 'Inj'

OPEN 'Prod'

AIMSET CON 0

```
AIMWELL WELLN

*Time 15400

SHUTIN 'Prod'

OPEN 'Inj'

AIMSET CON 0

AIMWELL WELLN

*Time 15500

SHUTIN 'Inj'

OPEN 'Prod'

AIMSET CON 0

AIMWELL WELLN

*Time 15600

SHUTIN 'Prod'

OPEN 'Inj'

AIMSET CON 0

AIMWELL WELLN

*Time 15700

SHUTIN 'Inj'

OPEN 'Prod'

AIMSET CON 0

AIMWELL WELLN

*Time 15800

SHUTIN 'Prod'
```

```
OPEN 'Inj'

AIMSET CON 0

AIMWELL WELLN

*Time 15900

SHUTIN 'Inj'

OPEN 'Prod'

AIMSET CON 0

AIMWELL WELLN

*Time 16000

SHUTIN 'Prod'

OPEN 'Inj'

AIMSET CON 0

AIMWELL WELLN

*Time 16100

SHUTIN 'Inj'

OPEN 'Prod'

AIMSET CON 0

AIMWELL WELLN

*Time 16200

SHUTIN 'Prod'

OPEN 'Inj'

AIMSET CON 0

AIMWELL WELLN
```

*Time 16300

SHUTIN 'Inj'

OPEN 'Prod'

AIMSET CON 0

AIMWELL WELLN

*Time 16400

SHUTIN 'Prod'

OPEN 'Inj'

AIMSET CON 0

AIMWELL WELLN

*Time 16500

SHUTIN 'Inj'

OPEN 'Prod'

AIMSET CON 0

AIMWELL WELLN

*Time 16600

SHUTIN 'Prod'

OPEN 'Inj'

AIMSET CON 0

AIMWELL WELLN

*Time 16700

SHUTIN 'Inj'

OPEN 'Prod'

```
AIMSET CON 0

AIMWELL WELLN

*Time 16800

SHUTIN 'Prod'

OPEN 'Inj'

AIMSET CON 0

AIMWELL WELLN

*Time 16900

SHUTIN 'Inj'

OPEN 'Prod'

AIMSET CON 0

AIMWELL WELLN

*Time 17000

SHUTIN 'Prod'

OPEN 'Inj'

AIMSET CON 0

AIMWELL WELLN

*Time 17100

SHUTIN 'Inj'

OPEN 'Prod'

AIMSET CON 0

AIMWELL WELLN

*Time 17200
```

SHUTIN 'Prod'

OPEN 'Inj'

AIMSET CON 0

AIMWELL WELLN

*Time 17300

SHUTIN 'Inj'

OPEN 'Prod'

AIMSET CON 0

AIMWELL WELLN

*Time 17400

SHUTIN 'Prod'

OPEN 'Inj'

AIMSET CON 0

AIMWELL WELLN

*Time 17500

SHUTIN 'Inj'

OPEN 'Prod'

AIMSET CON 0

AIMWELL WELLN

*Time 17600

SHUTIN 'Prod'

OPEN 'Inj'

AIMSET CON 0

```
AIMWELL WELLN

*Time 17700

SHUTIN 'Inj'

OPEN 'Prod'

AIMSET CON 0

AIMWELL WELLN

*Time 17800

SHUTIN 'Prod'

OPEN 'Inj'

AIMSET CON 0

AIMWELL WELLN

*Time 17900

SHUTIN 'Inj'

OPEN 'Prod'

AIMSET CON 0

AIMWELL WELLN

*Time 18000

SHUTIN 'Prod'

OPEN 'Inj'

AIMSET CON 0

AIMWELL WELLN

*Time 18100

SHUTIN 'Inj'
```

```
OPEN 'Prod'

AIMSET CON 0

AIMWELL WELLN

*Time 18200

SHUTIN 'Prod'

OPEN 'Inj'

AIMSET CON 0

AIMWELL WELLN

*Time 18300

SHUTIN 'Inj'

OPEN 'Prod'

AIMSET CON 0

AIMWELL WELLN

*Time 18400

SHUTIN 'Prod'

OPEN 'Inj'

AIMSET CON 0

AIMWELL WELLN

*Time 18500

SHUTIN 'Inj'

OPEN 'Prod'

AIMSET CON 0

AIMWELL WELLN
```

```
*Time 18600

SHUTIN 'Prod'

OPEN 'Inj'

AIMSET CON 0

AIMWELL WELLN

*Time 18700

SHUTIN 'Inj'

OPEN 'Prod'

AIMSET CON 0

AIMWELL WELLN

*Time 18800

SHUTIN 'Prod'

OPEN 'Inj'

AIMSET CON 0

AIMWELL WELLN

*Time 18900

SHUTIN 'Inj'

OPEN 'Prod'

AIMSET CON 0

AIMWELL WELLN

*Time 19000

SHUTIN 'Prod'

OPEN 'Inj'
```

```
AIMSET CON 0

AIMWELL WELLN

*Time 19100

SHUTIN 'Inj'

OPEN 'Prod'

AIMSET CON 0

AIMWELL WELLN

WSRF GRID TIME

*Time 19200

SHUTIN 'Prod'

OPEN 'Inj'

AIMSET CON 0

AIMWELL WELLN

**************************

STOP

**********The End**********************************************************************
```

Appendix C

MATLAB Code for Manipulating Well Schedules Input

```
clear;
clc;
k=zeros(1,200);
%%%%%Each cycle for 100 days injection, and 100 days production, last
10 cycles
k(1)=7200;
fori=1:20
    x=mod(i,2);
if(x==0)
k(i+1)=k(i)+100;
fprintf('*Time %5.0f\n', k(i+1))
disp('SHUTIN ''Prod''')
disp('OPEN ''Inj''')
disp('AIMSET CON 0')
disp('AIMWELL WELLN ')
elseif (x==1)
k(i+1)=k(i)+100;
fprintf('*Time %5.0f\n', k(i+1))
disp('SHUTIN ''Inj''')
disp('OPEN ''Prod''')
disp('AIMSET CON 0 ')
disp('AIMWELL WELLN ')
end
end
end
%%%%%1000 days gas injection for Pr increase
disp('*****1000 days gas injection for Pr increase')
k(22)=k(21)+1000;
fprintf('*Time %5.0f\n', k(22))
disp('SHUTIN ''Inj''')
disp('OPEN ''Prod''')
disp('AIMSET CON 0 ')
```

```
disp('AIMWELL WELLN ')

%%%%%%%%200 days production, 50 days injection
j=zeros(0,120);
j(1)=k(22);
for m=0:11
    y=mod(m,2);
if (y==0)

disp('*****200 days production, 50 days injection****')
for ii=1:12

    x=mod(ii,2);
if(x==1)
j(ii+12*m+1)=j(ii+12*m)+200;
fprintf('*Time %5.0f\n', j(ii+12*m+1))
disp('SHUTIN ''Prod''')
disp('OPEN ''Inj''')
disp('AIMSET CON 0')
disp('AIMWELL WELLN ')
elseif (x==0)
j(ii+12*m+1)=j(ii+12*m)+50;
fprintf('*Time %5.0f\n', j(ii+12*m+1))
disp('SHUTIN ''Inj''')
disp('OPEN ''Prod''')
disp('AIMSET CON 0 ')
disp('AIMWELL WELLN ')
end
end
end

else
disp('*****50 days production, 100 days injection****')


for ii=1:12
```

```
    x=mod(ii,2);
if(x==1)
j(ii+12*m+1)=j(ii+12*m)+50;
fprintf('*Time %5.0f\n', j(ii+12*m+1))
disp('SHUTIN ''Prod''')
disp('OPEN ''Inj''')
disp('AIMSET CON 0')
disp('AIMWELL WELLN ')
elseif (x==0)
j(ii+12*m+1)=j(ii+12*m)+100;
fprintf('*Time %5.0f\n', j(ii+12*m+1))
disp('SHUTIN ''Inj''')
disp('OPEN ''Prod''')
disp('AIMSET CON 0 ')
disp('AIMWELL WELLN ')
end
end
end
end
end
```

%%%%%%%%%%%The end %%%%%%%%%%%%%%%%%%%%%%%%%%%%%%%%%%%%%

Simple Economic analysis :

Appendix D

Economic Analysis

Assuming the inlet gas pressure is 200 psi and intercoolers cool the gas to 80 ^{o}F. We want to calculate the adiabatic horsepower required to compress 1 MMcfd of a 0.8 gravity natural gas to 7000 psi;

Overall compression ratio: $ratio = \frac{7000}{200} = 35$. Since this is greater than 6, more than one-stage compression is required. We use 3 stages of compression, $r = \left(\frac{7000}{200}\right)^{1/3} = 3.27$

We use the analytic method to get the horsepower for each stage:

$$-w\left(\frac{Hp}{MMcfd}\right) = \frac{k}{k-1}\frac{3.027p_b}{T_b}T_1\left[\left(\frac{p_2}{p_1}\right)^{z_1(k-1)/k} - 1\right]$$

Where T_b=540 ^{o}R, P_b=14.7 psi, k=1.28, P_1 is the inlet pressure and P_2 is the outlet pressure.

The first stage w1=59 hp; The second stage w2=52.6 hp; The third stage w3=40 hp;

So the total horsepower required to compress 1 MMcfd to 7000 psi is 152 hp.